Acta Universitatis Szegediensis

Acta Biologica Szegediensis

Volume 54, Number 1, 2010

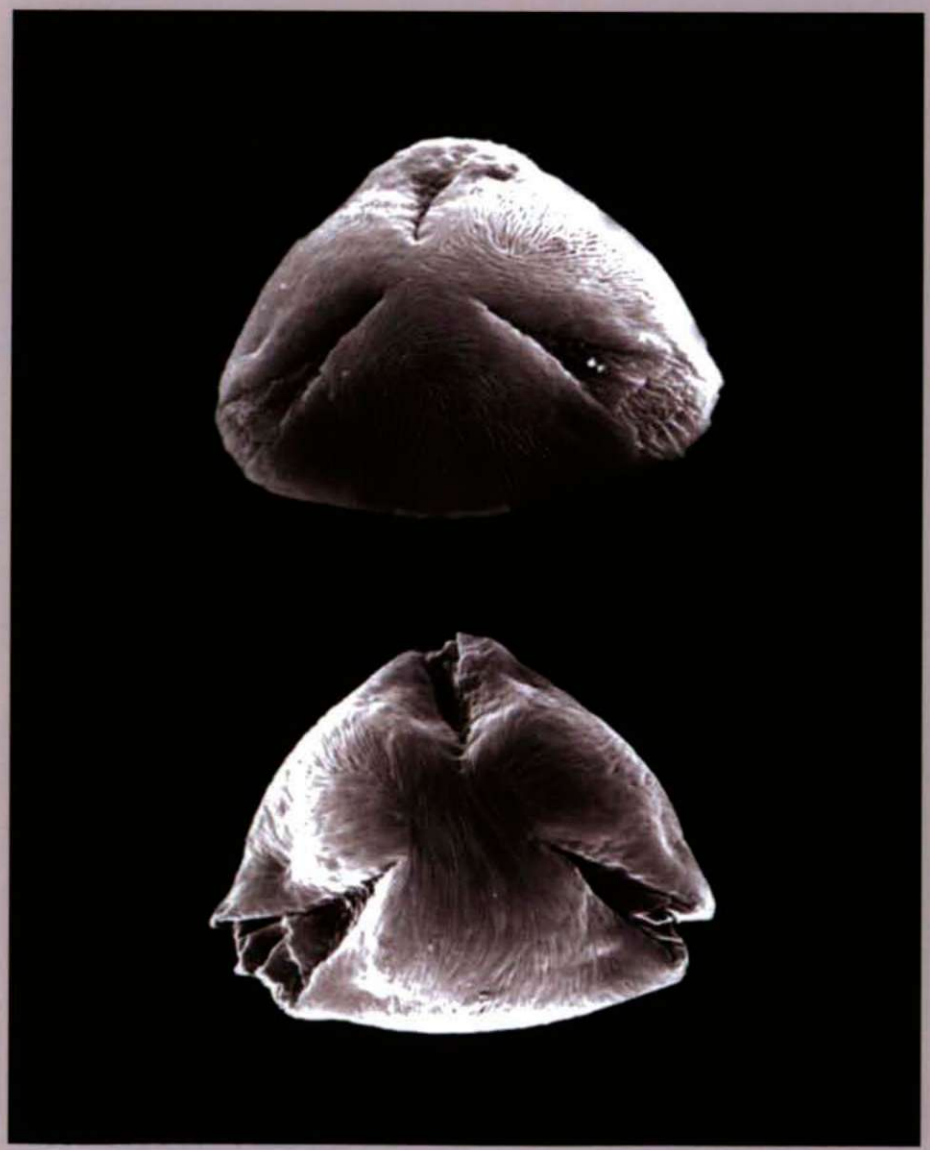

University of Szeged, Szeged, Hungary

Acta Biologica Szegediensis

Acta Biologica Szegediensis (ISSN 1588-385X print form; ISSN 1588-4082 online form), a member of the Acta Universitatis Szegediensis family of scientific journals (ISSN 0563-0592), is published yearly by the University of Szeged. Acta Biologica Szegediensis covers the growth areas of modern biology and publishes original research articles and reviews, involving, but not restricted to, the fields of anatomy, embryology and histology, anthropology, biochemistry, biophysics, biotechnology, botany and plant physiology, all areas of clinical sciences, conservation biology, ecology, genetics, microbiology, molecular biology, neurosciences, paleontology, pharmacology, physiology and pathophysiology, and zoology. Occasionally, Acta Biologica Szegediensis will publish symposium materials. Acta Biologica Szegediensis particularly encourages young investigators and clinicians to submit novel results of interest.

Submission of manuscripts

Manuscripts should be prepared in accordance with the Instructions to Authors published in each issue, also available at http://www.sci.u-szeged.hu/ABS, and submitted to:

Károly Gulya
Acta Biologica Szegediensis, Editorial Office
Department of Cell Biology and Molecular Medicine
University of Szeged
4 Somogyi u., H-6720 Szeged, Hungary
Phone: 36 (62) 544-570, fax: 36 (62) 544-569
E-mail: gulyak@bio.u-szeged.hu

Correspondence relating to the status of the manuscripts, proofs, publication, reprints and advertising should be sent to:

Tamás Mikola
Acta Biologica Szegediensis, Editorial Office
Department of Cell Biology and Molecular Medicine
University of Szeged
4 Somogyi u., H-6720 Szeged, Hungary
Phone: 36 (62) 544-569, fax: 36 (62) 544-569
E-mail: zool@bio.u-szeged.hu

Subscriptions

Acta Biologica Szegediensis is published yearly in two issues per volume. All subscriptions relate to the calendar year and must be pre-paid. The annual subscription rate is currently 100 USD and includes air mail delivery and handling.

Acta Biologica Szegediensis is indexed in BIOSIS Database, EMBASE, Excerpta Medica, Elsevier BIOBASE (Current Awareness in Biological Sciences) and Zoological Record.

The Table of Contents for the current issue and those for previous issues can be found at http://www.sci.u-szeged.hu/ABS.

ACTA BIOLOGICA SZEGEDIENSIS VOLUME 54(1), 2010

Table of Contents

Review article

Deepak Ganjewala, Shiv Kumar, Asha Devi S, Kumari Ambika
Advances in cyanogenic glycosides biosynthesis and analyses in plants: A review 1

Articles

László Bankó, László Erdei, Mónika Ördög, Erzsébet Mihalik
Histological comparison of the rhizome, leafy culm and aerial rhizome of the common reed (*Phragmites australis*) 15

Jolán Csiszár, Adrienn Guóth, Zsuzsanna Kolbert, Ágnes Gallé, Irma Tari, Sorin Ciulca, Emilian Madosa, László Erdei
Starch to protein ratio and α-amylase activities in grains of different wheat cultivars 19

Masoud Sheidai, Abbas Gholipour, Zahra Noormohammadi
Species relationship in the genus *Silene* L. Section *Auriculatae* (Caryophyllaceae) based on morphology and RAPD analyses 25

Ildikó Nyilasi, Sándor Kocsubé, László Galgóczy, Tamás Papp, Miklós Pesti, Csaba Vágvölgyi
Effect of different statins on the antifungal activity of polyene antimycotics 33

Ghader Habibi, Roghieh Hajiboland, Gholamreza Dehghan
Contrastive response of *Phlomis tuberosa* to salinity and UV radiation stresses 37

Lilla Ördögh, László Galgóczy, Judit Krisch, Tamás Papp, Csaba Vágvölgyi
Antioxidant and antimicrobial activities of fruit juices and pomace extracts against acne-inducing bacteria 45

Zamani A, Attar F, Maroofi H
Pollen morphology of the genus Pyrus (*Rosaceae*) in Iran 51

Obituary
Dr. György Bodrogközi (1924-2010) 57

Dissertation Summaries 59

On the cover: Pollen grains (genus Pyrus) under scanning electron microscope. (See in this issue Zamani et al.)

Volume 54(1):1-14, 2010
Acta Biologica Szegediensis
http://www.sci.u-szeged.hu/ABS

REVIEW

Advances in cyanogenic glycosides biosynthesis and analyses in plants: A review

Deepak Ganjewala[1,2] *, Shiv Kumar[1,3], Asha Devi S.[1], Kumari Ambika[1]

[1]School of Biosciences and Technology, Vellore Institute of Technology University, Vellore, Tamil Nadu, India, [2]Amity Institute of Biotechnology, Amity University Campus, Noida, Uttar Pradesh, India, [3]Central Drug Standard Control Organization, East Zone, Kolkata, Ministry of Health and Family Welfare, Government of India, India

ABSTRACT A number of species of plants produce repertoire of cyanogenic glycosides *via* a common biosynthetic scheme. Cyanogenic glycosides play pivotal roles in organization of chemical defense system in plants and in plant–insect interactions. Several commercial crop plants such as sorghum (*Sorghum bicolor*), cassava (*Manihot esculenta*) and barley (*Hordium vulgare*) are cyanogenic and accumulate significant amounts of cyanogenic glycosides. The study of biosynthesis of dhurrin in sorghum has underpinned several early breakthroughs in cyanogenic glycoside researches. Despite great deal of structural diversity in cyanogenic glycosides, almost all of them are believed to be derived from only six different amino acids L-valine, L-isoleucine, L-leucine, L-phenylalanine, or L-tyrosine and cyclopentenyl-glycine (a non protein amino acid). Our knowledge about biosynthesis of cyanogenic glycosides and molecular regulatory processes underlying their biosynthesis has been increased impressively in the past few years. The rapid identification, characterization and cloning of genes encoding enzymes of the cyanogenic glycoside biosynthetic and catabolic pathways from several plants has greatly facilitated our understanding of cyanogenic glycosides biosynthesis and regulation. Today it is known that enzymes of cyanogenic glycoside biosynthetic pathway in sorghum are organized as metabolon most likely to those of other secondary metabolic pathways. Knowledge of state of art of biosynthesis and regulation of cyanogenic glycosides made possible the metabolic engineering of these pathways resulting in development of transgenics of cassava, tobacco, lotus and Arabidopsis with manipulated cyanogenic glycosides content. Simultaneously, many new developments have been witnessed in methods/techniques/ procedures for detection of cyanogenic glycosides in plant samples, foods and foodstuffs. The present review sequentially discusses all of these issues with updated information gathered from the published reports on cyanogenic glycosides.

Acta Biol Szeged 54(1):1-14 (2010)

KEY WORDS

Arabidopsis
chromatography
cyanogenic glycosides
cytochrome P450s
dhurrin
metabolon
metabolic engineering
transgenics

More than 2,600 plant species produce myriad of cyanogenic glycosides (CGs), one of the biggest and extensively studied class of plant secondary metabolites (Moller and Conn 1980; Poulton 1990; Conn 1991; Fleming 1999; Moller and Seigler 1999; Vetter 2000; Zagrobelny et al. 2004). Chemically, CGs are defined as glycosides of α-hydroxynitriles; plants store these compounds in vacuoles (Fleming 1999; Vetter 2000). Most of the plant families producing CGs are belong to the Angyospermatophyta and remaining to the Dicotyledonopsida and Monocotyledonopsida (Vetter et al. 2000). Several important crop plants *viz.*, sorghum (*Sorghum bicolor*) (Moller and Conn 1980; Halkier and Moller 1989; 1990), cassava (*Manihot esculenta*) (Andersen et al. 2000), barley (*Hordium vulgare*; Forslund and Johnson 1997; Nielsen et al. 2002) are among others which essentially biosynthesize and accumulate CGs. Several bacteria and a number of animals particularly those feed on cyanogenic plants also contain CGs. [See review by Vetter (2000) for distribution, functions, biosynthesis and analysis of CGs in plants]. Cyanogenic glycosides have great impact on insect biology as well. Zagrobelny et al. (2004) have elaborately discussed biosynthesis and degradation of CGS in insects emphasizing their roles in plant-insect interactions.

Regarding to the biosynthesis of CGs, they are derived from only six amino acids namely L-valine, L-isoleucine, L-leucine, L-phenylalanine, or L-tyrosine and from a non protein amino acid cyclopentenyl-glycine. Cyanogenic glycoside biosynthesis has been broadly studied in many important plants, sorghum (*Sorghum bicolor*; Moller and Conn 1980; Halikar and Moller 1989; 1990; Sibbesen et al. 1994; 1995; Koch et al. 1995; Jones et al. 1999), cassava (*Manihot esculenta*) (Andersen et al. 2000), seaside arrow grass (*Triglochin maritimum*; Nielsen and Moller 1999; 2000) and barley (*Hordeum vulgare*; Nielsen et al. 2002). However, biosynthesis of dhurrin a tyrosine derived CGs found in sor-

Accepted June 1, 2010
*Corresponding author. E-mail: deepakganjawala73@yahoo.com

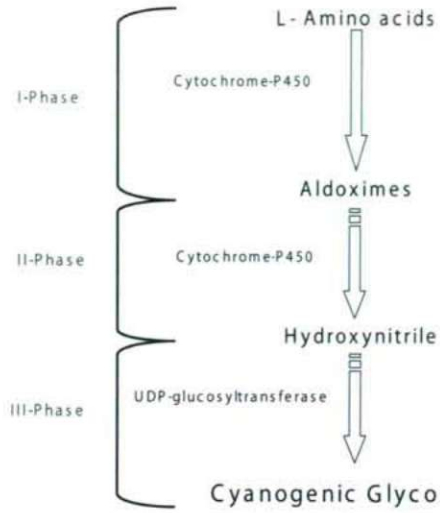

Figure 1. General scheme of the biosynthesis of cyanogenic glycosides in plants.

ghum has been comparatively most elaborately studied among others. Today the knowledge we have about biosynthesis and regulation of CGs in plants has largely gathered from the studies carried out in sorghum. In plants, CGs biosynthetic pathway can be unanimously treated in three steps (Fig. 1). Step- I: A precursor amino acid is converted to aldoxime through two successive N-hydroxylation of amino group of parent amino acid by an enzyme of cytochrome-P450 family. Step- II: aldoxime in turn is converted to cyanohydrin. This reaction is catalyzed by another cytochrome-P450 enzyme. Step- III: cyanohydrins get glycosylated by a soluble enzyme UDP-glucosyltransferase.

In sorghum, two cytochrome enzymes, CYP79A1 and CYP71E1, rcatalyze first and second steps respectively and a UDP-glucosyltransferase catalyzes the final step leading to dhurrin biosynthesis. A recent study has suggested that the above three enzymes are organized as metabolon thereby insuring an efficient channeling of precursors/substrates and intermediates required for biosynthesis of dhurrin in sorghum (Nielsen et al. 2008). Previously, organization of enzymes as metabolon and metabolic channeling has been well documented in biosynthesis of other plant natural products (Jorgensen et al. 2005). In plants and insects, CGs undergoes catabolic processes eventually leading to hydrogen cyanide. Enzymes, β-glucosidases and α-hydroxynitrilases are reported to catalyze catabolism of CGs in plants and insects (Vetter 2000; Zagrobelny et al. 2004).

In recent years, tremendous progress has been made on every aspects of CGs researches, particularly on identification and characterization of genes encoding enzymes of CGs biosynthetic and catabolic pathways rapidly identified and characterized from many cyanogenic plants in past few years (Koch et al. 1995; Hughes et al. 1994; Hasslacher et al. 1996; Trummler and Wajant 1997; Bak et al. 1998; Andersen et al. 2000; Nielsen and Moller 2000; Wang et al. 2004; see Table 2). With these cloned genes, metabolic engineering of pathways leading to CGs has become easier; by using these cDNA, transgenic plants with depleted or enhanced level of CGs have been developed (Bak et al. 2000; Tattersall et al. 2001; Morant et al. 2003, 2007; Siritunga and Sayre 2004a, b; Moller and Bak 2005; Kristensen et al. 2005). Transgenic cyanogens free cassava plant using RNAi technique has been developed (Siritunga and Sayre 2004b). Previously, transgenic cassava plant with negligible cyanogens was developed by selective inhibition of CGs biosynthesis in leaves and roots by antisense expression of CYP79D1/D2 gene fragments (Siritunga and Sayre 2004). Arabidopsis and lotus plants have been successfully engineered by introducing in them an entire dhurrin biosynthetic pathway from sorghum to produce dhurrin (Tattersall et al. 2001; Morant et al. 2003, 2007; Kristensen et al. 2005).

However, a range of articles on almost every aspect of CGs researches are available, information on cloned genes of CGs biosynthesis and catabolism is yet scattered and not available at one place. The main objective of the present article is to provide information on cloned genes of CGs biosynthesis and catabolism. In addition, other aspects of CGs including their occurrence, functions and biosynthesis of CGs derived from six parent amino acids with given emphasis to enzymes, cytochromes P450s and glucosyl transferase have been discussed briefly. Finally, we have included information on technical advancement in the methods of analysis/ detection of CGs.

Functions of CGs in plants

Large numbers of CGs are produced in plants to mediate both general and specialized functions. In fact, the primary role of CGs is in organization of chemical defense system in plants and in plant–insect interactions (Zagrobelnya et al. 2004). See review by Zagrobelnya et al. (2004) for detailed description on roles of CGs in plant-insect interactions. CGs have also been described as nitrogen storage compounds (Forslund and Jonsson 1997; Busk and Moller 2002). Moreover, they offer promises as being chemo-taxonomical candidates (Vetter, 2000). For herbivores that are specialists on plants containing CNGs, they serve as phagostimulants (Gleadow and Woodrow 2002). Even, degradation products of CGs such as β-cyanoalanine are reported to serve to deter predators. β-cyanoalanine which possess potent neurotoxin activity is a catabolic product of CGs in some plants (Ressler et al. 1969). These datasets demonstrate that attempts to assign a specific biological role to cyanogenic glucosides may not be meaningful. The function varies dependent on plant species, ecosystem, and abiotic and biotic stress factors. Accordingly, only careful and extensive field trials can decide on

the overall fitness of acyanogenic cassava plants (Jorgensen et al. 2005).

Biosynthesis of CGs

Biosynthesis of CGs have been studied in a number of plants including sorghum (*Sorghum bicolor*), cassava (*Manihot esculenta*), seaside arrow grass (*Triglochin maritimum*), and barley (*Hordeum vulgare*; Koch et al. 1995; Jones et al. 1999; Nielsen and Moller, 1999; Andersen et al. 2000; Nielsen et al. 2002; Forslund et al. 2004). Based on these reports all CGs are believed to be biosynthesized from one of the six amino acids, L-valine (L-Val), L-isoleucine (L-Ile), L-leucine (L-Leu), L-phenylalanine (L-Phe) or L-tyrosine (L-Tyr) and cyclopentenyl-glycine (cyclopentenyl-Gly). Several previous studies using labeled amino acids precursors in a number of plants have revealed the tight integration of amino acids with CGs biosynthesis in plants (Vetter 2000). The most elaborately studied CGs is the dhurrin, which is biosynthesized in sorghum plant. Today, all the details surrounding the dhurrin biosynthesis and regulation in sorghum are available including, cloned and characterized genes, intermediates and enzymes involved in its biosynthesis. Two cytochromes-P450s enzymes, CYP79A1 and CYP71E1 and an UDP-glucosyltransferase (UGT85B1) involved in the biosynthesis of the dhurrin in sorghum have been isolated and characterized. Concomitantly with CGs, plants also produce nitrile glucosides but their biosynthesis in plants is poorly understood.

Roles of cytochrome P450senzymes in CGs biosynthesis

Cytochrome-P450s are very well characterized enzymes, ubiquitously appears in many plant and animal species and plays important roles in many biochemical pathways. They have the ability to catalyze a range of biochemical reactions *via* C-hydroxylation and epoxidation, N-and S-oxidations, dehydrations, and O-, N- and S-de-alkylation (Zagrobelny et al. 2004). Many cytochrome-P450s associated with the biosynthesis of terpenoids, volatile phenylpropenes, volatile derived fatty acids, plant hormones (gibberellins), brassinosteroids, ecdysteroids are known (Dudereva et al. 2004; Fischbach and Clardy 2007). Till to date around 800 cytochrome-P450s sequences comprising 53 families are known from plants.

At least two cytochrome P450s enzymes catalyze the first two dedicated steps of CGs biosynthesis. The first committed step of conversion of parent amino acids to aldoximes is catalyzed by cytochrome-P450-I. In the next dedicated step aldoximes are converted into cyanohydrin by action of cytochrome-P450-II. Several cytochrome-P450s enzymes from plants associated with distinct CGs biosynthesis have been isolated and characterized (Koch et al. 1995; Kahn et al. 1997; Bak et al. 1998; Nielsen and Moller, 1999; 2000; Zhang et al. 2003; Andersen et al. 2000; Forslund et al. 2004). One of the first cytochrome-P450s characterized and sequenced was cytochrome-P450tyr from sorghum that catalyzes the conversion of L-tyrosine into Z-p-hydroxy-phenylacetaldoxime the first committed step of the dhurrin biosynthetic pathway. Cytochrome-P450tyr was recognized as the first member of a new family of cytochrome-P450 and given the name CYP79 and now CYP79A1 (Koch et al. 1995; Sibbesen et al. 1995). Also, cytochrome-P450tyr was the first membrane bound multifunctional enzyme isolated from plants. A membrane-bound cytochrome-P450 *N*-hydroxylases type however was known from animals and yeast which had broad substrate specificity catalyzing the hydroxylation of a wide range of xenobiotics. In contrast to cytochrome-P450s *N*-hydroxylases type, cytochrome P450tyr is substrate specific enzyme which hydroxylates only single endogenous substrate, tyrosine (Koch et al. 1995; Sibbesen et al. 1995).

Today several cytochromeP450s are known, two CYP79D1 and CYP79D2 from cassava (Zhang et al. 2003; Andersen et al. 2000) other two CYP79D3 and CYP79D4 from lotus (Forslund et al. 2004) and one CYP79B1 from *Sinapis alba*. The cytochromeP450s, CYP79D1 and CYP79D2 catalyzes the first two committed step in the biosynthesis of linamarin in cassava while CYP79D3 and CYP79D4 are key enzymes in the biosynthesis of cyanogenic glucosides (lotaustralin and linamarin) and glucoside nitrile (rhodenosydes A and D) in lotus plant. The above cytochrome-P450s from sorghum, cassava and lotus are similar in their structure and function. Sequence alignment analysis has revealed homology between lotus's CYP79D3 and CYP79A1 of sorghum and in between CYP79D4 of lotus and CYP73E1 of sorghum (Szczyglowski et al. 1997; Forslund et al. 2004). However, cassava's CYP79D1 and CYP79D2 displayed 54% sequence similarity with CYP79A1 of sorghum. Similarly, CYP79B1 of *S. alba* also showed 54% sequence similarity (with 73% scored similarity) to CYP79A1 of sorghum but CYP79B1 showed 95% sequence similarity to CYP79B2 of Arabidopsis (Bak et al. 1998).

Also, cytochrome-P450s are highly substrate specific and use only one amino acid as a substrate. In a given CGs biosynthetic pathway, the cytochrome P450-I, one, which catalyzes the first committed step comparatively has higher substrate specificity than cytochrome P450-II which has broader substrate specificity. For example, in sorghum the CYP79A1 involved in dhurrin biosynthesis strongly prefers tyrosine as a substrate while the CYP71E1 has broader substrate specificity. The CYP71E1 can broadly hydroxylate the aldoximes derived from phenylalanine, valine and/or isoleucine in addition to those derived from tyrosine (Celenza et al. 2001). The CYP79 of barley, however, is identical to CYP79A1 and CYP79E1 of sorghum but prefers leucine as a substrate and not the tyrosine. An analog of CYP71E1 present in *T. maritima* showed less interest in aldoximes as substrates if derived

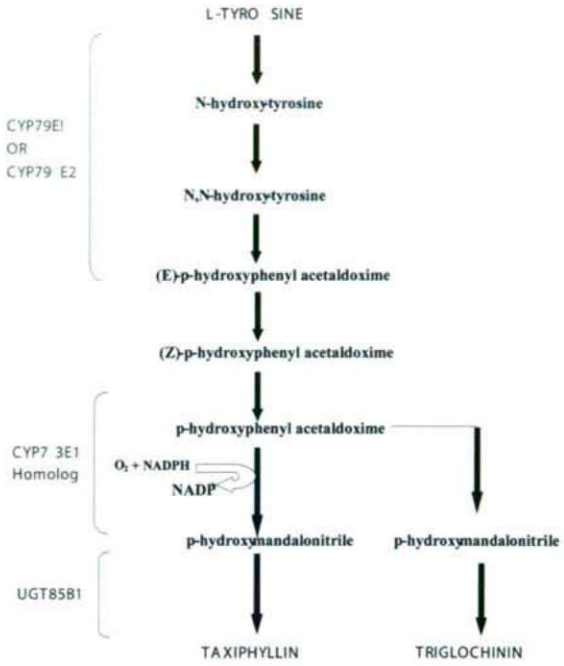

Figure. 2a. Scheme of the biosynthesis of L-tyrosine derived cyanogenic glycoside, dhurrin in *Sorghum bicolor*.

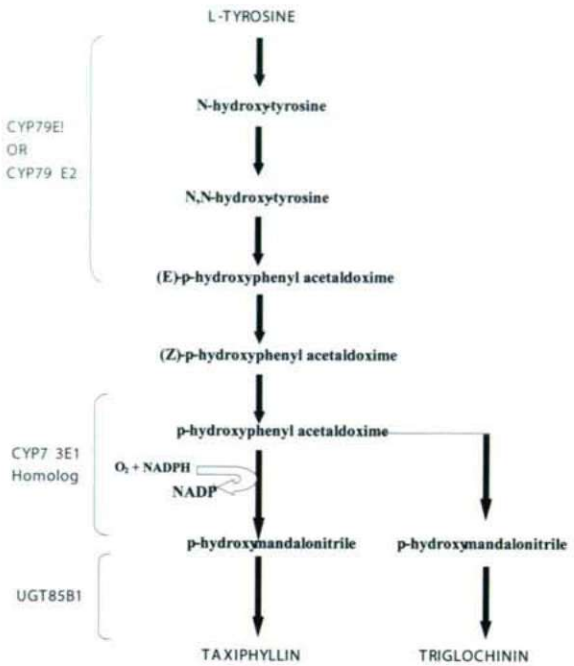

Figure 2b. Scheme of the biosynthesis of L-tyrosine derived cyanogenic glycosides, taxiphyllin and triglochinin in *Triglochin maritime*.

from phenylalanine (*p*-hydroxy-phenylacetonitrile). In *Lotus japonicum*, two cytochrome P450s, CYP79D3 and CYP79D4 almost identical (95%) have shown different choices for the amino acids as substrates, CYP79D3 for L-isoleucine and CYP79D4 for L-valine. In cassava, CYP79D1 preferably chooses L-valine as a substrate and not L-isoleucine a substrate of choice for CYP79D3 of lotus. Several other substrate specific cytochrome-P450s acting upon valine, leucine and tyrosine have been reported from seaside arrow grass (*Triglochin maritima*) and cassava (*Manihot esculenta*; Nielsen and Moller 1999; Andersen et al. 2000).

The huge diversity in CGs structure in plants has been attributed both to the substrate specificity of the first cytochrome-P450s as well as broader substrate specificity of the second cytochrome-P450s. Perhaps, the second step catalyzed by cytochromeP450-II is thought to be a source of diversity in CGs structures. For example cytochrome CYP79A1 in sorghum carried out three consecutive N-hydroxylations of the amino acid tyrosine (Moller and Seigler 1999). However, in barley, hydroxylations of 3-methylbutyro-nitrile intermediate, is carried out by cytochrome CYP71E resulting in hydroxynitiriles corresponding to five different cyano glucosides (Moller and Seigler 1999). The multiple and flexible binding positions of 3-methylbutyro-nitrile in the active site of the CYP71 monooxygenases enables the enzyme to carry out additional hydroxylations at the neighboring carbon atoms as well as to carry out successive hydroxylations at two or three other carbon atoms in followed by dehydration reactions (Nielsen et al. 2002). Recently, Watanabe et al. (2007) have explained the chemo- and regioselectivity of the monooxygenases after investigation of the oxidation of several acyclic monoterpenes by P450 in BM-3 and its mutants. Fischbach and Clardy (2007) have also favoured oxidative modifications catalyzed by four cytochrome P450 monooxygenases for structural diversity of gibberellins. It is plausible that cyanogenic plants might have adopted a similar strategy of diversification through post-aldoxime hydroxylation by cytochromes-P450s resulting in structural diversity in CGs.

Roles of UDP-Glc glucosyltransferase in CGs biosynthesis

UDP-Glc glucosyltransferases catalyzes the third step of the CGs biosynthesis. They are highly regarded enzymes owing to their roles in the biosynthesis of a wide range of primary and secondary metabolites in plants (Vogt and Jones 2000). The basic reaction catalyzed by these enzymes is the transfer of sugar moieties from activated donor molecules to specific acceptor molecules, forming glycosidic bonds. The CAZy database (Carbohydrates Active Enzymes) provide the continuously updated classification of glycosyltransferases using nucleotide diphospho-sugar, nucleotide monophospho-sugars and sugar phosphates (EC 2.4.1.x) and related proteins into distinct sequence-based families. In cyanogenic plants, glucosyltransferase performs glucosylation of cyanohydrin (final step in the biosynthesis of CGs) to produce distinct CG. A

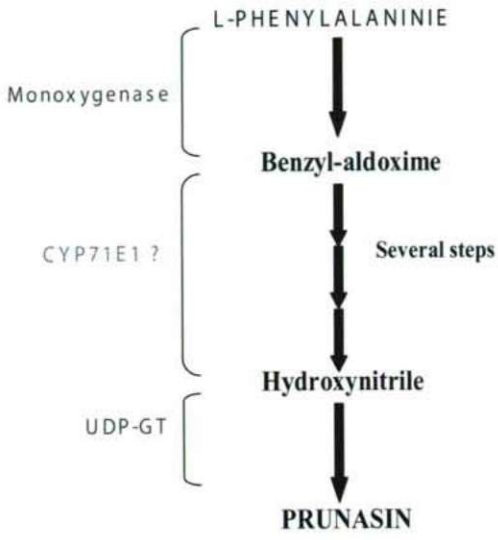

Figure 3. Scheme of biosynthesis of L-phenylalanine derived cyanogenic glycoside, prunasin in *Carica papaya*.

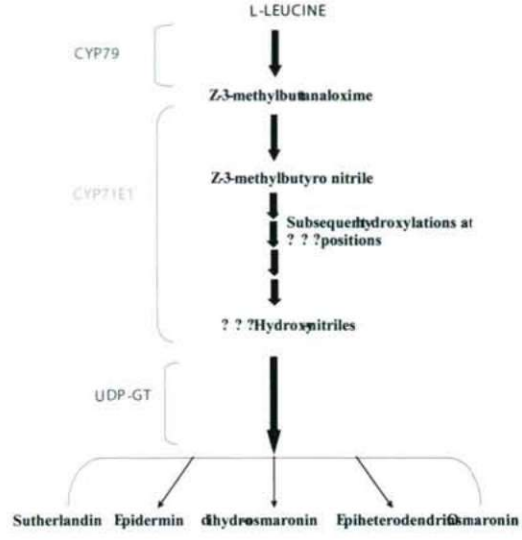

Figure 4. Scheme of the biosynthesis of L-leucine derived cyanogenic glucosides in *Hordium vulgare*.

soluble UDP-Glc-glucosyltransferase (UGT85B1) catalyzing glucosylation of p-hydroxy-mandelonitrile in the final step of dhurrin biosynthesis in sorghum has been isolated and characterized (Jones et al. 1999; Kahn et al. 1999; Thorsoe et al. 2005).

Tyrosine derived CGs

Several CGs *viz.*, dhurrin, triglochinin, taxiphyllin, holocalin and vicianin are derived from L-tyrosine. Study of biosynthesis of dhurrin (p-hydroxy-(S)-mandelonitrile-l-D-glucoside) in *Sorghum bicolor* has provided deeper insight into tyrosine derived CGs (Koch et al. 1995; Sibbesen et al. 1995; Kahn et al. 1997; Bak et al. 1998; Neilsen et al. 2007). A pathway (Fig. 2a) leading to dhurrin biosynthesis in sorghum has been completely elucidated (Sibbesen et al. 1994; 1995; Koch et al. 1995). Biosynthesis of dhurrin starts with the conversion of L-tyrosine into Z-p-hydroxyphenyl acetaldoxime catalyzed by the enzyme CYP79A1. The next enzyme CYP71E1 then catalyzes the conversion of Z-p-hydroxyphenyl acetaldoxime into cyanohydrin, p-hydroxy-mandelonitrile (Koch et al. 1995; Sibbesen et al. 1995; Kahn et al. 1997; Bak et al. 1998). However, a number of unusual and labile intermediates such as N-hydroxyamino acid, an N,N-dihydroxyamino acid, E- and Z-oximes and a cyanohydrin are also produced during dhurrin biosynthesis. These intermediates, except Z-oxime are efficiently channeled for the formation of dhurrin hence could not be trapped (Moller and Conn 1980; Sibbesen et al. 1995; Kahn et al. 1997; Kristensen et al. 2005). Both CYP79A1 and CYP71E1 are membrane bound multi-functional cytochrome P450s and performs six of seven steps in dhurrin synthesis with (Z)-p-hydroxyphenylacetaldoxime as the inter-enzymatic intermediate (Morant et al. 2003). In the final step of the pathway, the labile p-hydroxy-mandelonitrile is stabilized by glucosylation *via* a soluble UDP-glucosyltransferase UGT85B1 to produce dhurrin (Jones et al. 1999; Kahn et al. 1999; Thorsoe et al. 2005; Fig. 2a).

A similar pathway with changed cytochrome-P450s is used by all other plants for the biosynthesis of other tyrosine derived CGs, such as triglochinin and taxiphyllin (Fig. 2b). The pathway branches off from the point of formation of *p*-hydroxy-phenylacetonitrile. The branch point intermediate *p*-hydroxy-phenylacetonitrile leads to taxiphylin and triglinin in *T. maritime*, linustatin and neolinustatin in *Linum usitatissimum*, linamarin and lotaustralin in *Trifolium repens* L. (Nielsen and Moller 1999) and linamarin in *Manihot esculenta* Crantz (Nielsen and Moller 1999; Koch et al. 1992).

Phenylalanne derived CGs

Phenylalanine beside the progenitor of many CGs, also serve as precursor for biosynthesis of secondary metabolites such as flavonoids (Celenza, 2001; Bennett, et al. 1997). Some of the important CGs derived from L-phenylalanine includes prunasin (an aromatic cyanogenic glycoside), acacipetalin, proacacipetalin, 3-hydroxyheterodendrin, sambunigrin, amygdalin, (R)-vicianin, zierin, epilucumin and zierinxylosides. However, only little is known about biosynthesis and regulation of phenylalanine derived CGs in plants except the prunasin biosynthesis in *Carica papya*. *Carica papaya* concomitantly biosynthesizes glucosinolates (benzylglucosinolate) and cyanogenic glucosides (prunasin) using a

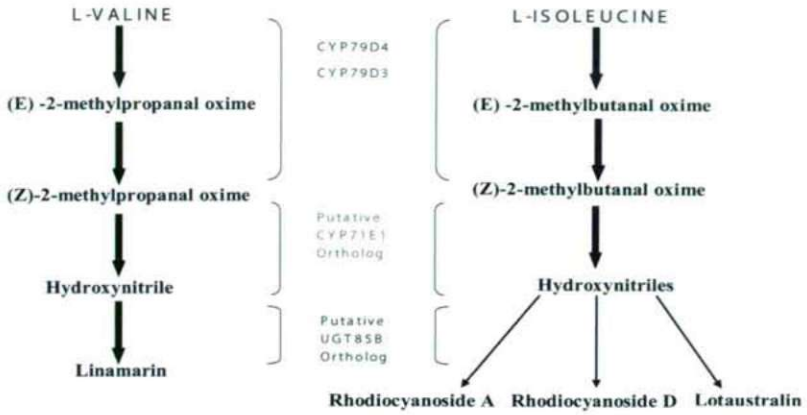

Figure 5. Scheme of the biosynthesis of L-valine and L-isoleucine derived cyanogenic glucosides, linamarin and lotaustralin and the nitrile glucosides, rhodiocyanoside A and D in *Lotus japonicus*.

common biochemical pathway. In *C. papaya*, the cytochrome-P450 (monoxygenase) catalyzes the first dedicated step of conversion of L-phenylalanine into benzylaldoxime in the biosynthesis of prunasin (Bennett et al. 1997; Fig. 3). The cytochrome-P450 monoxygenase is one of the three distinct enzymes (flavoprotein, cytochrome P450 MOs, and peroxidases) involved in the formation of aldoximes from amino acids in plants. Beside *C. papaya*, *Brassica* species have been reported to produce glucosinaolates, similar to those of *C. papaya*. However, our knowledge regarding to the biosynthesis of glucosinolates in plants is very poor but it has become clear that in nitrile glucosides, the hydroxyl and nitrile groups are not linked to the same carbon atom of the aglycone. Also, hydrolysis of nitrile glucosides by β-glucosidases does not result in HCN release (Forslund et al. 2004).

Leucine derived CGs

Leucine derived CGs, sutherlandin, epidermin, osmaronin, dihydro-osmaronin and epiheterodendrin have been reported from the barley (*H. vulgare*) seedlings (Nielsen et al. 2002). In barley, CGs biosynthesis is highly compartmentalized, in one compartment (tissue type) biosynthesis of CGs proceeds; CGs thus produced are accumulated in other compartment and they undergo catabolism in another compartment where the enzyme β-glucosidase start degradation of CGs (Fig. 4). As per the common scheme of CGs biosynthesis, in barley also, the first dedicated step is catalyzed by a CYP79 homolog as a result of which L-leucine is converted into Z-3-methylbutanaloxime. The resultant intermediate, Z-3-methylbutanaloxime then in two consecutive reactions catalyzed by a CYP71E homolog converted to a cyanohydrin *via* a nitrile compound as an intermediate (Nielsen et al. 2002). In the final step, nitrile is glycosylated by UDP-glucosyl transferase which later produces CGs (Fig. 4). It is reported that in barley CYP71E homolog hydroxylates the 3-methylbutyro-nitrile intermediate at the α-carbon atom.

The multiple and flexible binding positions of 3-methylbutyro-nitrile in the active site of the CYP71 monooxygenase enables the enzyme to carry out additional hydroxylations at the neighboring carbon atoms as well as at two or three other carbon atoms. Hydroxylation together with dehydration reactions provides a mechanism to explain the concomitant generation of hydroxynitiriles corresponding to five different CGs in barley seedlings (Nelsen et al. 2002).

Valine and isoleucine derived CGs

Cyanogenic glycosides, linamarin and lotaustralin found in Lotus species are believed to be biosynthesized from valine and isoleucine (Moller and Seigler 1999; Fig. 5). In most of the species of Lotus, linamarin and lotaustralin are biosynthesized together with nitrile glucosides, such as rhodiocyanoside A, and rhodiocyanoside D (Gebrehiwot and Beuselinck 2001; Andersen et al. 2000). Previous studies with radio labeled valine in Lotus species have revealed that petioles, midrib of the leaf, and the shoot apex are most active in synthesis of linamarin (Bediako et al. 1981). Further studies with radio labeled substrates L-isoleucine and L-valine have indicated that linamarin is derived from L-valine while lotaustralin and nitrile glucosides rhodiocyanoside A, and rhodiocyanoside D are derived from L-isoleucine (Forslund et al. 2004).

Most likely, *Lotus* species also use the common biochemical pathway for the biosynthesis of above CGs and nitrile glucosides. In Lotus species, the first two committed step of conversion of L-valine and L-isoleucine to their corresponding oximes is catalyzed by two cytochrome-P450s enzymes CYP79D3 and CYP79D4, respectively (Forslund et al. 2004; Fig. 5). Unlike others, *Lotus* species use two separate and independent biochemical pathways located in roots and aerial parts for the biosynthesis of CGs. The two pathways has separate CYP79 enzymes which express differentially in roots and aerial parts, CYP79D3 exclusively expressed in aerial parts while CYP79D4 in roots (Forslund et al. 2004).

Also these enzymes differ in catalytic properties that determine the cyanogenic glycosides profiles in lotus. Sequence analysis of amino acids indicated 94% similarity between CYP79D3 and CYP79D4 however little similarity between them was observed in promoter region (Forslund et al. 2004). Despite high degree of sequence similarities, CYP79D3 and CYP79D4 have shown substrate specificity. The CYP79D3 in *L. japonicus* has shown strong affinity for L-isoleucine as substrate while the CYP79D4 preferred L-valine as substrate for biosynthesis of linamarin.

In few cases like in *Lotus* and *Brassica* species in addition to CGs, nitrile glucosides are biosynthesized using a common precursor and a pathway of CGs (Lechtenberg et al. 1996; Nielsen et al. 2002; Forslund et al. 2004). In lotus species, nitrile glucosides namely rhodiocyanoside A and D are derived from the precursor L-isoleucine which is also a precursor for CGs, however, the biosynthesis of this class of compounds is still uncertain. In recent years, biosynthesis of CGs and nitrile glycosides in *L. japonicus* has been extensively studied with an objective to develop it as a model system to understand concomitant biosynthesis of CGs and nitrile glycosides in plants (Handberg and Stougaard, 1992; Asamizu et al. 2000; Nakamura et al. 2002; Perry et al. 2003). Currently, cDNA and genomic sequencing in *L. japonicus* is underway at the Kazusa DNA Research Institute (http://www.kazusa.or.jp/en/database.html) and will be available soon. The genome sequencing may underpin some early breakthrough in CGs and nitrile glucoside biosynthesis and regulation in plants.

Molecular biology and metabolic engineering of CGs biosynthesis

The genes encoding enzymes of CGs biosynthesis and degradation have been rapidly isolated cloned and characterized in the past few years (Table 2). In case of sorghum, all the genes encoding enzymes of dhurrin biosynthesis have been isolated, cloned and characterized (Nielson et al. 2008.). Beside, the list included genes for cytochrome-P450s, UDP-glucosyltransferases, cyanoalanine synthase, hydroxynitrile layases, glucosidases, rhodenases and vicianin hydrolase. The cloned genes (cDNA) are excellent tools in molecular biology and used to gain an understanding of the molecular regulatory processes underlying biosynthetic pathways leading to a variety of products. The whole deep knowledge of regulatory mechanisms is essential for metabolic engineering of the concerned biosynthetic pathway. In a similar way, cDNAs have greatly facilitated our understanding of molecular regulation of CGs biosynthesis as well as the metabolic engineering of the CGs biosynthetic pathways in acyanogenic plants.

Metabolic engineering of biochemical pathways of valuable plant products is rapidly growing for example the modification of flower colors, enhancement of lignin synthesis by down- regulation and production of pharmaceutically useful secondary metabolites. There are reports available on successful metabolic engineering of CGs and development of transgenic plants. The availability of cloned genes (cDNAs) of CGs pathway and deeper knowledge of regulatory process has been indispensable in the metabolic engineering of CGs biosynthesis in commercially valuable plants. In recent years, using metabolic engineering of cytochrome-P450 enzyme, transgenic cassava with depleted CGs, *Arabidopsis thaliana* producing CGs, and *L. japonicus* with altered cyanogenic, cyanoalkenyl or glucosinolate contents have been successfully developed (Tattersall et al. 2001; Morant et al. 2003, 2007; Kristensen et al. 2005).

The major objectives of the metabolic engineering of CGs biosynthesis are to produce CGs free varieties of plants and transgenic plants such as *Arabidopsis* with altered or enhanced production of CGs. With the above objectives, CGs content in cassava, sorghum, barley, lotus, tobacco and Arabidopsis have been manipulated using metabolic engineering (Tattersall et al. 2001; Morant et al. 2003, 2007; Kristensen et al. 2005). Based on the reports on genetic engineering of the CGs, mainly two strategies have been used for engineering of CGs pathways. According to the first strategy, a gene encoding enzyme of CGs pathway along with a promoter is introduced into non-cyanogenic plants. Second strategy utilizes RNAi technique for development of transgenic plants with altered or enhanced levels of cyanogenic glycosides. Jorgensen et al. (2005) have used RNAi technique for developing transgenic cyanogen free cassava plants (*Manihot esculenta* Crantz, cv MCol22). The RNAi was used to block expression of CYP79D1 and CYP79D2 the two key genes encoding the first committed enzymes in linamarin and lotaustralin synthesis. On the other hand, Siritunga and Sayre (2004b) generated transgenic cassava by selective inhibition of CGs biosynthesis in leaves and roots by antisense expression of CYP79D1/D2 gene fragments. Selectively inhibition of these genes in leaves resulted in transgenic plants with largely reduced (60- 94% reduction) linamarin content while the inhibition of same set of genes in roots has drastically reduced (99%) linamarin content in resultant transgenic plants. Previously, transgenic cassava plants were generated by over-expression (13-fold) of hydroxynitrile lyase (HNL) using a double 35S CaMV promoter (Siritunga et al. 2004a). This strategy was based on the fact that over expression of hydroxynitrile lyase (HNL) will accelerate cyanogenesis and cyanide volatilization during food processing thereby reducing cyanogen toxicity in cassava foods. HNL catalyze the conversion of acetone cyanohydrin to cyanide. Unlike previous transgenic cyanogen free cassava, transgenic plants over-expressing HNL in roots retain the herbivore deterrence of cyanogens while providing a safer food product.

Arabidopsis plants are promising in metabolic engineering of CGs. The first transgenic Arabidopsis producing p-hydroxybenzylglucosinolate was developed by introducing

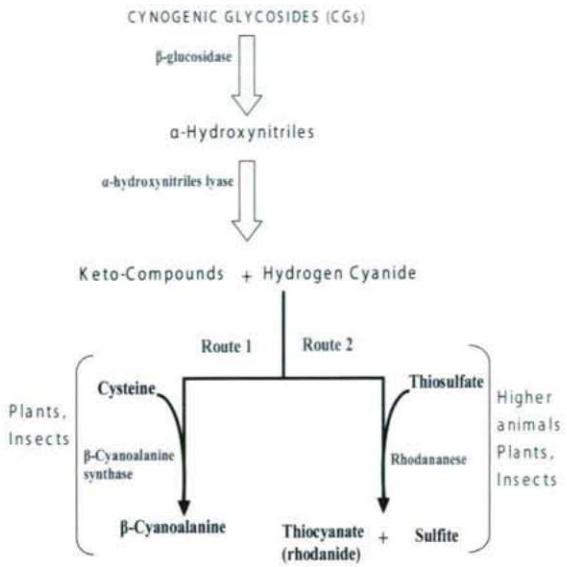

Figure 6. Schematic pathway of catabolism of cyanogenic glycosides.

CYP79A1 from *Sorghum bicolor* (Bak et al. 1999). The ability of CYP79A1 to integrate itself in to cyanogenic glycoside pathway is important for its implications in genetic engineering of CGs (Bak et al. 1999). Later, Bak and associates (2000) have developed transgenic tobacco and Arabidopsis plants expressing two multifunctional cytochrome-P450s, CYP79A1 and CYP71E1 of sorghum. These transformed plants were cyanogenic accumulating metabolites derived from intermediates in dhurrin biosynthesis. As a most recent development in transgenics CGs plants, two transgenic plants *A. thaliana* and *L. japonicus* have been developed by introducing entire dhurrin biosynthetic pathway from sorghum (Morant et al. 2003, 2007; Kristensen et al. 2005). In transgenic *A. thaliana* plant dhurrin content was recorded 4% (w/w) of leaf dry-weight. Ectopic expression of CYP79D2 from cassava (*Manihot esculenta* Crantz.) in *L. japonicus* has been resulted in a 5- to 20-fold increase of linamarin content, whereas the relative amounts of lotaustralin and rhodiocyanoside A/D remained unaltered (Forslund et al. 2004).

Catabolism of CGs

In plants, CGs undergoes catabolic pathways for their complete degradation into hydrogen cyanide (HCN). Enzymes β-glucosidases and α-hydroxynitrile lyases are the most important enzymes of catabolic pathways in plants (Conn 1980; Hosel and Conn 1982; Poulton 1990; Fig. 6). Enzyme β-glucosidase hydrolyzes CGs to the corresponding α-hydroxynitriles, which then dissociates spontaneously into a sugar, a keto- compound, and HCN if pH value is above 6. At lower pH, α-hydroxynitriles did not dissociate spontaneously but an enzyme α-hydroxynitrile lyase may catalyze its dissociation. Hydrogen cyanide, the final product of dissociation of α-hydroxynitriles then detoxified *via* two separate routes (Zagrobelny et al. 2004). The first route involves the formation of β-cyanoalanine from cysteine and is catalyzed by β-cyanoalanine-synthase (Fig. 6). Subsequently, β-cyanoalanine is converted into asparagine (Miller and Conn 1980). This route seems to be most common in plants and possibly in insects also. The second route proceeds by conversion of HCN into thiocyanate and is catalyzed by rhodanese (Bordo and Bork 2002; Fig. 6). Vertebrates predominantly utilizes thiocyanate route, however some plants and insects are also reported to use this route.

Genes encoding some of the enzymes of CGs catabolic-pathways have been cloned and characterized (Table 1). In plants, α-hydroxynitrile lyase are located in the tissues where β-glucosidases are present though their activity is observed in protein bodies (Swain et al. 1992), instead of in chloroplasts or apoplastic space as typically reported for β-glucosidases (Hickel et al. 1996). β-glucosidase and α-hydroxynitrile lyase that begins the cleavage of CNGs are localized in chloroplasts or apoplastic space in plants (Conn 1980; Hosel and Conn 1982; Poulton 1990). β-glucosidase has capability to recognize the aglycone moiety of CGs present within the plant species (Hosel et al. 1987; Hosel and Conn 1982; Nahrstedt 1985), on the other hand, α-hydroxynitrile lyases have shown the activity in protein bodies (Swain et al. 1992).

β-cyanoalanine synthase of mitochondria detoxifies HCN in pyridoxal phosphate (PLP) dependent reaction and produce β-cyanoalanine. The process is beneficial both ways as the detoxification of HCN prevents the mitochondrial degradation from the vulnerable attack of HCN, the resulted detoxification product β-cyanoalanine serve to deter predators (Ressler et al. 1969). Rhodanase is also proposed to be an enzyme involved in cyanide detoxification (Beesley et al. 1985) which is evidenced by high levels of rhodanase activity in 3-day-old etiolated *Sorghum bicolor* seedlings (Miller and Conn 1980). Rhodanese perhaps is not a common enzyme in plants but it is associated with sulfonation of proteins (Bordo and Bork 2002).

Detection of CGs

Several chromatographic procedures have been described for the qualitative and quantitative detection of CGs in plant samples, previously (Brimer et al. 1981; 1983; Brimer and Dalgaard 1984; Brimer and Molgaard 1986; Brimer 1988) (Table 3). Curtis et al. (2002) have described a new method to simultaneously detect cyanide and carbonyl compounds arising from CGs in plants. A portable gas chromatograph housing two detectors using a single carrier gas is employed to measure the carbonyl compound (photoionization detector) and cyanide as its cyanogen chloride derivative (electron capture detector) from the headspace of a plant sample. This method affords in-field, rapid screening of plants to determine

Table 1. Cloned genes encoding enzymes of cyanogenic glycoside biosynthesis and catabolism.

Enzyme	Plant	Accession No.	Size	Protein/Gene	References
Cytochrome P450ox	Sorghum bicolor	AAC39318	531	CYP71E1	Kahn et al. 1997
Cytochrome P450tyr	Sorghum bicolor	AAA85440	558	CYP79	Koch et al. 1995
		Q43135	558	CYP79A1	
Cytochrome P450	Manihot esculenta	AAP57704	511	C15	Zhang et al. 2003
		AF140614	541		Andersen et al. 2000
Putative Cytochrome P450	Lotus japonicus	AAB69644	490		Forslund et al. 2004
Cytochrome P450	*Triglochin maritima*	AAF66544	533	CYP79E2	Nielsen and Moller 2000;
		AAF66543	540	CYP79E1	Nielsen and Moller 1999
A-type cytochromes P450, CYP71E1, CYP98, and CYP99	*Sorghum bicolor*	AAC39318	531	CYP71E1	Bak et al. 1998
		AAC39317	519	CYP99A1	
		AAC39316	512	CYP98A1	
UDP-glucose:p-hydroxymandelonitrile-O-glucosyltransferase	*Sorghum bicolor*	AAF17077	492	UDPGT	Jones et al. 1999
A-hydroxynitrile lyase	*Manihot esculenta*	CAA82334	258	Abhydrolase_1	Hughes et al. 1994
		AAV52632	258	HNL	Wang et al. 2004
		CAA11219	258	HNL4	
		CAA11428	158	HNL 24	
(S)-hydroxynitrile lyase	*Hevea brasiliensis*	AAC49184	257	Hnl	Hasslacher et al. 1996
Hydoxynitrile lyase	*Prunus dulcis*	AAL11514	563	hnl1	Dreveny et al. 2001
		IJU2_B	536	hnl1	
(R)-(+)-mandelonitrile lyase	*Prunus serotina*	P52707	573	MDL3	Hu and Poulton 1999
Rhodanese	*Triticum aestivum*	AAK64575	307	TST	Niu et al. 2002
Rhodanese	*Arabidopsis thaliana*	CAB53639	318	RDH2	Hatzfeld and Saito 2000; Papenbrock and Schmidt 2000
		CAB64716	378	Mst1	
		CAB88023	366	Mst2	
Dhurrinase (β-glucosidase)	*Sorghum bicolor*	AAC49177	565	Glyco_hydro-1	Cicek and Esen 1998; Verdoucq et al. 2004
Dhurrinase (β-glucosidase)	*Zea mays*	AAD09850	563	Glu2	Bandaranayake and Esen1996; Czjzek et al. 2000
Dhurrinase (β-glucosidase)	*Secale cereale*	AAG00614	568	Glyco_hydro-1	Nikus et al. 2003
B-glucosidase	*Prunus avivum*	AAA91166	531	Glyco_hydro-1	Wiersma et al. 1996; Gerardi et al.2001
B-glucosidase (Amygdalin hydrolase)	*Prunus serotina*	AAA93234	553	AH1	Zheng and Poulton1995; Zhou et al. 2002
B-glucosidase	Manihot esculenta	CAA64442	551	Bgl1A	Liddle et al. 1998
B-glucosidase-DIMBOA	*Zea mays*	1E4N_B	512	Glyco_hydro-1	Cicek, and Esen 1999;
		1E4N_A	512	Glyco_hydro-1	Czjzek et al. 2000
B-(1)4-β-glucosidase	*Prevotella ruminicola Bacteria (gram –ve)*	AAA86753	785	cdxA	Wulff-Strobel and Wilson 1995
B-cyanoalanine synthase	*Solenum tuberosum*	BAB18760	351 aa	PCAS-1	Maruyama et al. 2001
		BAB20032	347 aa	PCAS-2	
B-cyanoalanine synthase	*Betula pendula*	AAN86822	352 aa	Beta-CAS	Vahala et al. 2003
Vicianin Hydrolase	*Vicia angustifolia*	ABD03937	509		Ahn et al. 2007
Cyanide hydratase	*Gloeocercospora sorghi*	AAA33353	368	Cht	Wang and Etten 1992
		P32964	368	CHT	
α-acetone cyanohydrin lyase	Linum usitertussimum	CAA70304	422		Trummler and Wajant1997
Prussanin β-glucosidase	*Prunus serotina*	P29265	15		Li et al1992
		P29264	16		
		P29263	14		

cyanogenicity. Simultaneous detection of both the cyanide and the carbonyl compounds allows for confirmation of the presence of CGs and eliminates the problem of false positives often seen in traditional cyanide test kits. This method could be useful for screening cyanogenic foodstuffs to determine suitability for consumption.

A cyanide-specific biosensor has been developed for the detection of CGs in the micro molar concentration in many medicinal and food plants (Keusgen et al. 2004). An immobilized cyanidase has been employed in this biosensor. Under this method, enzymatically formed ammonia is either detected by a potentiometric sensor based on an ammonia electrode or by a pH-sensitive electrolyte/insulator/semiconductor (EIS) layer structure made of Al/p-Si/SiO_2/Si_3N_4 (Keusgen et al. 2004). CGs were also studied using Raman spectroscopy (Thygesen et al. 2004). Surface-enhanced Raman Spectros-

Table 2. Methods for the detection of cyanogenic glycosides in plants.

Methods	Materials	Cyanogenic compounds	Detection limit	Reference
Pyridine-barbituric acid colorimetric procedure	Soybeans and soybean products	Cyanide (HCN)	Microgram	Honig et al. 1983
Direct determination method	Beans and bean paste products	Linamarin	Milligram	Kawamura et al. 1993
Picrate and acid hydrolysis methods	Flax seed and flax seed meal; Bamboo shoots; sorghum leaves	Total cyanide content	Ppm.	Haque and Beabdury 2002
Picrate paper kits	Cassava	Total cyanide content	Microgram	Hidayat et al. 2000
Barbituric acid pyridine, pyridine-pyrazolone and high performance liquid chromatography	Ax seed	Cyanogenic glycosides	Microgram	Kobaisy et al. 1996
Densitometric method	Cyanogenic plant	Small amounts of cyanogenic compounds	Nanogram	Brimer and Molgaard, 1986
Direct determination of cyanides by potentiometric biosensors	Several cyanogenic medicinal and food plants	Cyanogenic glycosides	Micromolar	Keusgen et al. 2004
Chromatographic determination using a porous graphitic carbon column	Almond tree roots	Prunasin and amygdalin		Berenguer Navarro et al. 2002
LC combined with tandem mass spectrometry (LC-MS/MS)	Vitis vinifera L.	Epimers of prunasin and sambunigrin		Franks et al. 2005
Gas chromatographic analysis	Linum usitatissimum L.	Linustatin and neolinustatin	Low- to sub-nanogram	Bacala and Barthet 2007
Gas chromatography-electron capture/photoionization detection	Foodstuffs	Simultaneous determination of cyanide and carbonyl compounds		Curtis et al. 2002
GC/EI-MS or GC/NCI-MS	Passiflora fruits	Mandelonitrile (Prunasin, amygdalin, mandelonitrile rhamnopyranosyl β-D-glucopyranosides, sambunigrin glycosides		Chassagne et al. 1996
Immunoassay using polyclonal antibodies	Pits of fruits and nuts	Amygdalin	Microgram-milligram	Cho et al. 2006

copy (SERS) has been demonstrated to be a more sensitive method for the determination of the cyanogenic potential of plant tissue. The SERS method was optimized by flow injection (FI) using a colloidal gold dispersion as effluent.

Very recently, Cho et al. (2006) have described an enzyme immunoassay method for the detection of high amygdalin content in various seeds and nuts. It utilizes an antiserum reactive to amygdalin for the detection of amygdalin. In fact, there are various other methods available to detect amygdalin in food extracts. Bacala and Barthet, (2007) reported gas chromatographic analysis of the cyanogenic glycosides linustatin and neolinustatin from flaxseed (*Linum usitatissimum* L.) using phenyl- β-D-glucopyranoside as an internal standard. Two quantitative methods direct (using linustatin and neolinustatin external standard curves) or indirect (by use of methyl-α-D-glucopyranoside as a surrogate external standard) were employed for the linustatin and neolinustatin. Limits of detection for all standards were in the low- to sub-nanogram level and were 10-100 times lower than the lower limit of quantification. Thus from the above discussion it is very clear that a broad-spectrum qualitative and quantitative methods are available for the detection of CGs. However, these methods have their own pros and cons, and have a limit of detection of CGs from nano- to milligram level. Furthermore, the principal underneath the detection, suitability and applicability of these methods is markedly varies.

Conclusion

Cyanogenic glycosides (CGs) are abundant in plant kingdom. They are amongst most important components of plant defense systems and mediate interactions of plants with insects. The study of the biosynthesis of CGs is desirable because several commercial and edible crop plants are cyanogenic, particularly sorghum, cassava and barley. Understanding of the CGs biosynthetic pathways and enzymatic steps as well as molecular regulatory process underlying therein is crucial for metabolic engineering of these pathway in order to develop cyanogen free crop plants. Already, transgenic cassava plants with no CGs have been successfully developed through metabolic engineering of key enzymes namely cytochromes-P450s. Similarly, transgenic Arabidopsis thaliana with ability to produce dhurrin, tobacco and Lotus japonicus with altered cyanogenic, cyanoalkenyl or glucosinolate profiles have been successfully generated.

With regard to CGs, genes encoding enzymes involved in their biosynthesis as well as degradation have also been cloned and characterized. Today cloned genes (cDNA) encoding enzymes of the dhurrin biosynthetic pathway from sorghum are available. Our knowledge, however is not limited to the characterization of enzymes but extended to many structural and organizational details including the concept of metabolon formation by the enzymes of cyanogenic glycoside biosynthesis has been uncovered. Also, some progress has been made towards understanding role of sub-cellular compartmentation in regulation of cyanogenic glycosides biosynthesis in plants. Existence of isoforms of cytochrome-P450 represents the compartmentalization of cyanogenic glycosides biosynthesis in plants. Several insect species are dependent on cyanogenic plants for cyanogenic glycoside as their food and live in association with such plants throughout their life cycle. By using the available cDNAs, transgenic plants can now be generated with an altered qualitative and quantitative content of cyanogenic glycosides and the plant-insect interaction could be shattered. Or cyanogenic plants can be made acyanogenic (with no detectable cyanogen glycosides) to deter insects dependent on such cyanogenic plants for cyanogenic glycosides as their food. Cyanogenic glycosides often have toxic effects in humans when consumed along with food and food products. In recent years, several efficient, highly sensitive and rapid method of detection of cyanogenic glycosides in foods and foodstuffs have been developed to determine suitability of these products for human consumptions.

Despite great progress made on every front, biosynthesis, molecular biology and metabolic engineering of cyanogenic glycosides, still we are short of detailed knowledge of the different regulatory mechanisms controlling biosynthesis of cyanogenic glycosides in plants. Also, extensive studies to be carried out to elucidate mechanisms or processes or enzyme characteristics particularly those which favors the formation of metabolon during biosynthesis of cyanogenic glycosides in plants. Another, unsolved but important issue related to cyanogenic glycosides biosynthesis in plants is the concomitant biosynthesis and accumulation of nitrile glucosides about which comparatively very little is known. However, it is expected that complete elucidation of Lotus japanicus genome sequence may provide some important clues to understand biosynthesis of the nitrile glucosides and their biosynthetic relationship with cyanogenic glycosides in plants. Simultaneously, current methods of detection of cyanogenic glycosides should be constantly evaluated to improve their efficiency and sensitivity and newer methods should be developed for detection of cyanogen glycosides in wide variety of plant samples, foods and foodstuffs.

Acknowledgments

Authors are grateful to Dr. G. Viswanathan, Chancellor, VIT University, Vellore and Dr. Ashok Chauhan, Founder President, Amity University, Uttar Pradesh for providing necessary support and facilities.

References

Ahn YO, Saino H, Mizutani M, Shimizu BI, Sakata K (2007) Vicianin hydrolase is a novel cyanogenic β-glycosidase specific to Ɒvicianoside (6-O-α-L-arabinopyranosyl-β-D-glucopyranoside) in seeds of *Vicia angustifolia*. Plant Cell Physiol 48:938-947.

Andersen MD, Busk PK, Svendsen I, Moller BL (2000) Cytochromes P-450 from cassava (*Manihot esculenta* Crantz) catalyzing the first steps in the biosynthesis of the cyanogenic glucosides linamarin and lotaustralin. Cloning, functional expression in *Pichia pastoris*. J Biol Chem 275:1966-1975.

Asamizu E, Nakamura Y, Sato S, Tabata S (2000) Generation of 7137 non redundant expressed sequence tags from a legume, *Lotus japonicus*. DNA Res 7:127-130

Bacala R, Barthet V (2007) Development of extraction and gas chromatography analytical methodology for cyanogenic glycosides in flaxseed (*Linum usitatissimum*). J AOAC Int 90:153-61

Bak S, Kahn RA, Nielsen HL, Moller BL, Halkier BA (1998) Cloning of three A-type cytochromes P450, CYP71E1, CYP98, and CYP99 from *Sorghum bicolor* (L.) Moench by a PCR approach and identification by expression in *Escherichia coli* of CYP71E1 as a multifunctional cytochrome P450 in the biosynthesis of the cyanogenic glucoside dhurrin. Plant Mol Biol 36:393-405.

Bak S, Olsen CE, Peterson BL, Moller BL, Halikier BA (1999) Metabolic engineering of p-hydroxybenzylglucosinolates in Arabidopsis by expression of the cyanogenic CYP79A1 from Sorghum bicolor. Plant J 20:663-672.

Bak S, Olsen CE, Halkier BA, Moller BL (2000) Transgenic tobacco and Arabidopsis plants expressing the two multifunctional sorghum cytochrome P450 enzymes, CYP79A1 and CYP71E1, are cyanogenic and accumulate metabolites derived from intermediates in dhurrin biosynthesis. Plant Physiol 123:1437-1448.

Bandaranayake H, Esen A (1996) Nucleotide sequence of a β-glucosidase (glu2) cDNA from maize. (Accession No. U44087) (PGR96-009). Plant Physiol 110:1048-1052.

Bediako MKM, Tapper BA, Pritchard GG (1981) Metabolism, synthetic site and translocation of cyanogenic glycosides in cassava. In *Tropical Crops* Terry ER, Oduro KO, Cavenees F, ed., Proceedings of the First Triennial Symposium of the International Society for Tropical Root Crops. African Branch. International Development Research Centre, Ottawa, pp. 143-148.

Beesley SG, Compton SG, Jones DA (1985) Rhodanese in insects. J Chem Ecol 11:45-50.

Bennett RN, Kiddle G, Wallsgrov RM (1997) Biosynthesis of benzylglucosinolate, cyanogenic glucosides and phenylpropanoids in *Carica papaya*. Phytochemistry 45:59-66.

Berenguer Navarro V, Giner Galvan RM, rane Teruel N, Arrazalo Paternina G (2002) Chromatographic determination of cyanogenglycosides prunasin and amygdalin in plant extracts using a porous graphitic carbon column. J Agric Food Chem 50:6960-6963.

Bordo D, Bork P (2002) The rhodanese/Cdc25 phosphatase superfamily sequence structure function relations. EMBO Rep 3:741-746.

Brimer L, Brogger Christensen S, Jaroszewski Jerzy W, Nartey F (1981) Structural elucidation and partial synthesis of 3-hydroxyheterodendrin, a cyanogenic glucoside from *Acacia sieberiana* var. woodii. Phytochemistry 20:2221-2223.

Brimer L, Dalgaard L (1984) Cyanogenic glycosides and cyanohydrins in plant tissues. Qualitative and quantitative determination by enzymatic post-column cleavage and electrochemical detection, after separation by high-performance liquid chromatography. J Chromatogr 303:77-88.

Brimer L, Christensen SB, Molgaard P, Nartey F (1983) Determination of cyanogenic compounds by thin-layer chromatography. 1. A densito-

metric method for quantification of cyanogenic glycosides, employing enzyme preparations (β-glucuronidase) from *Helix promatia* and picrate-impregnated ion-exchange sheers. J Agric Food Chem 31:789-793.

Brimer L, Molgaard P (1986) Simple densitometric method for estimation of cyanogenic glycosides and cyanohydrins under field conditions. Biochem Syst Ecol 14:97-103.

Brimer L (1988) Determination of cyanide and cyanogenic compounds in biological systems. Ciba Foundation symposium 140:177-200.

Busk PK, Moller BL (2002) Dhurrin synthesis in sorghum is regulated at the transcriptional level and induced by nitrogen fertilization in older plants. Plant Physiol 129:1222-1231.

Celenza JL (2001) Metabolism of tyrosine and tryptophan-new genes for old pathways. Curr Opin Plant Biol 4:234-240.

Chassagne D, Crouzet JC, Bayonove CL, Baumes RL (1996) Identification and quantification of passion fruit cyanogenic glucosides. J Agric Food Chem 44:3817-3820.

Cho AY, Yi KS, Rhim JH, Kim KI, Park JY, Keum EH, Chung J, Oh S (2006) Detection of abnormally high amygdalin content in food by an enzyme immunoassay. Mol. Cells 21:308-313.

Cicek M, Esen A (1998) Structure and expression of a dhurrinase (β-glucosidase) from sorghum. Plant Physiol 116:1469-1478.

Cicek M, Esen A (1999) Expression of soluble and catalytically active plant (monocot) beta-glucosidases in *E. coli*. Biotechnol Bioeng 20:392-400.

Conn EE (1980) Cyanogenic compounds. Annu Rev Plant Physiol 31:433-451.

Conn EE (1991) Metabolism of natural products: Lessons learned from cyanogenic glycosides. Planta Med 1:57-68.

Curtis AJ, Grayless CC, Fall R (2002) Simultaneous determination of cyanide and carbonyls in cyanogenic plants by gas chromatography-electron capture/photoionization detection. Analyst 127:1446-1449.

Czjzek M, Cicek M, Zamboni V, Bevan DR, Henrissat B, Esen A (2000) The mechanism of substrate (aglycone) specificity in β-glucosidases is revealed by crystal structures of mutant maize β-glucosidase-DIMBOA,-DIMBOAGlc, and -dhurrin complexes. Proc Natl Acad Sci USA 97:13555-13560.

Dreveny I, Gruber K, Glieder A, Thompson A, Kratky C (2001) The hydroxynitrile lyase from almond: a lyase that looks like an oxidoreductase. Structure 9:803-815.

Dudareva N (2004) Biochemistry of plant volatiles. Plant Physiol 135:1893-1902.

Fischbach MA, Clardy J (2007) One pathway many products. Nat Chem Biol 3:353-355.

Fleming FF (1999) Nitrile-containing natural products. Nat Prod Rep 16:597-606.

Forslund K, Jonsson L (1997) Cyanogenic glycosides and their metabolic enzymes in barley, in relation to nitrogen levels. Physiol Plant 101:367-372.

Forslund K, Morant M, Jorgensen B, Olsen CE, Asamizu E, Sato S, Tabata S, Bak S (2004) Biosynthesis of the nitrile glucosides rhodiocyanoside A and D and the cyanogenic glucosides lotaustralin and linamarin in *Lotus japonicus*. Plant Physiol 135:71-84.

Franks TK, Hayasaka Y, Choimes S, van Heeswijck R (2005) Cyanogenic glucosides in grapevine: polymorphism, identification and developmental pattern. Phytochemistry 66:615-173.

Gebrehiwot L, Beuselinck PR (2001) Seasonal variations in hydrogen cyanide concentration of three *Lotus* species. Agron J 93:603-608.

Gerardi C, Blando F, Santino A, Zacheo G (2001) Purification and characterisation of a beta-glucosidase abundantly expressed in ripe sweet cherry (*Prunus avium* L.) fruit. Plant Sci 160:795-805.

Gleadow RM, Woodrow IE (2002) Constraints on effectiveness of cyanogenic glycosides in herbivore defense. J Chem Ecol 28:1301-1313.

Halkier BA, Moller BL (1989) Biosynthesis of the cyanogenic glucoside dhurrin in seedlings of *Sorghum bicolor* (L.) Moench and partial purification of the enzyme system involved. Plant Physiol 90:1552-1559.

Halkier BA, Moller BL (1990) The biosynthesis of cyanogenic glucosides in higher plants. Identification of three hydroxylation steps in the biosynthesis of dhurrin in *Sorghum bicolor* (L.) Moench and the involvement of 1-ACI-nitro-2-(p-hydroxyphenyl) ethane as an intermediate. J Biol Chem 265:21114-21121.

Handberg K, Stougaard J (1992) *Lotus japonicus*, an autogamous, diploid legume species for classical and molecular-genetics. Plant J 2:487-496.

Haque RM, Beabdury JH (2002) Total cyanide determination of plants and foods using the picrate and acid hydrolysis methods. Food Chemi 77:107-114.

Hasslacher M, Schall M, Hayn M, Griengl H, Kohlwein SD, Schwab H (1996) Molecular cloning of the full-length cDNA of (S)-hydroxynitrile lyase from *Hevea brasiliensis*. Functional expression in *Escherichia coli* and *Saccharomyces cerevisiae* and identification of an active site residue. J Biol Chem 27:5884-5891.

Hatzfeld Y, Saito K (2000) Evidence for the existence of rhodanese (thiosulfate:cyanide sulfurtransferase) in plants: preliminary characterization of two rhodanese cDNAs from Arabidopsis thaliana. FEBS Lett 470:147-150.

Hickel A, Hasslacher M, Griengl H (1996) Hydroxynitrile lyases: functions and properties. Physiol Plant 98:891-898.

Hidayat A, Zuaraida N, Hanarida I, Damardjati DS (2000) Cyanogenic content of cassava root of 179 cultivars grown in Indonesia. J Food Compost Anal 13:71-82.

Honig DH, Hockridge ME, Gould RM, Rackis JJ (1983) Determination of cyanide in soybeans and soybean products. J Agric Food Chem 31:272-275.

Hosel W, Con EE (1982) The aglycone specificity of plant β-glucosidase. Trends Biochem Sci 7:219-221.

Hosel W, Tober I, Eklund SH, Conn EE (1987) Characterization of beta-glucosidases with high specificity for the cyanogenic glucoside dhurrin in *Sorghum bicolor* (L.) moench seedlings. Arch Biochem Biophys 252:152-62.

Hu Z, Poulton JE (1999) Molecular analysis of (R)-(+)-mandelonitrile lyase microheterogeneity in black cherry. Plant Physiol 119:1535-1546.

Hughes J, Carvalho FJ, Hughes MA (1994) Purification, characterization, and cloning of alpha-hydroxynitrile lyase from cassava (*Manihot esculenta* Crantz). Arch Biochem Biophys 311:496-502.

Jones PR, Moller BL, Hoj PB (1999) The UDP-glucose: p-hydroxymandelonitrile-O-glucosyltransferase that catalyzes the last step in synthesis of the cyanogenic glucoside dhurrin in *Sorghum bicolor*. J Biol Chem 274:35483-35491.

Jorgensen K, Rasmussen AV, Morant M, Nielsen AH, Bjarnholt N, Zagrobelny M, Bak S, Moller BL (2005) Metabolon formation and metabolic channeling in the biosynthesis of plant natural products. Curr Opin Plant Biol 8:280-291.

Kahn RA, Bak S, Svendsen I, Halkier BA, Moller BL (1997) Isolation and reconstitution of cytochrome P450ox and in vitro reconstitution of the entire biosynthetic pathway of the cyanogenic glucoside dhurrin from sorghum. Plant Physiol 115:1661-1670.

Kahn RA, Fahrendorf T, Halkier BA, Moller BL (1999) Substrate specificity of the cytochrome P450 enzymes CYP79A1 and CYP71E1 involved in the biosynthesis of the cyanogenic glucoside dhurrin in *Sorghum bicolor* (L.) Moench. Arch Biochem Biophys 363:9-18.

Kawamura Y, Hikidi S, Maruyama K, Uchiyama S, Saito Y (1993) Improvement of the direct determination method of linamarin in beans and bean paste products. J Food Hyg Soc Japan 34:74-79.

Keusgen M, Kloock JP, Knobbe DT, Junger M, Krest I, Goldbach M, Klein W, Schoning MJ (2004) Direct determination of cyanides by potentiometric biosensors. Sens Actuat B Chem 103:380-385.

Kobaisy M, Oomah BD, Mazza G (1996) Determinations of cyanogenic glycosides in ax seed by barbituric acid pyridine, pyridine-pyrazolone and high performance liquid chromatography methods. J Agric Food Chem 44:3178-3181.

Koch B, Nielson VS, Olsen CE, Moller BL (1992) The biosynthesis of cyanogenic glycosides in seedlings of cassava (Manihot esculents Crantz). Arch Biochem Biophys 292:141-150.

Koch BM, Sibbesen O, Halkier BA, Svendsen I, Moller BL (1995) The primary sequence of cytochrome P450tyr, the multifunctional N-

hydroxylase catalyzing the conversion of L-tyrosine to p-hydroxyphenyl acetaldehyde oxime in the biosynthesis of the cyanogenic glucoside dhurrin in *Sorghum bicolor* (L.) Moench. Arch Biochem Biophys 323:177-186.

Kristensen C, Morant M, Olsen CE, Ekstrom CT, Galbraith DW, Moller BL, Bak S (2005) Metabolic engineering of dhurrin in transgenic Arabidopsis plants with marginal inadvertent effects on the metabolome and transcriptome. Proc Natl Acad Sci USA 102:1779-1784.

Lechtenberg M, Nahrstedt A., Fronczek FR (1996) Leucine-derived nitrile glucosides in the rosaceae and their systematic significance. Phytochemistry 41:779-785.

Li CP, Swain E, Poulton JE (1992) *Prunus serotina* amygdalin hydrolase and prunasin hydrolase: Purification, N-terminal sequencing, and antibody production. Plant Physiol 100:282-290.

Liddle S, Keresztessy Z, Hughes J, Hughes MA (1998) A genomic cyanogenic beta-glucosidase gene from Cassava (Accession No. X94986). (PGR98-148). Plant Physiol 117:1526-1526.

Maruyama A, Saito K, Ishizawa K (2001) Beta-cyanoalanine synthase and cysteine synthase from potato: molecular cloning, biochemical characterization, and spatial and hormonal regulation. Plant Mol Biol 46:749-60.

Moller BL, Conn EE (1980) The biosynthesis of cyanogenic glucosides in higher plants. Channeling of intermediates in dhurrin biosynthesis by a microsomal system from *Sorghum bicolor* (Linn) Moench. J Biol Chem 255:3049-3056.

Moller BL, Seigler DS (1999) Biosynthesis of cyanogenic glucosides and related compounds. In *Plant Amino Acids*. Singh BK, ed., Marcel Dekker, New York, USA, pp. 563-609.

Moller BL, Bak S (2005) Metabolic engineering of dhurrin in transgenic Arabidopsis plants with marginal inadvertent effects on the metabolome and transcriptome. Proc Natl Acad Sci USA 102:1779-784.

Morant AV, Jorgensen K, Jorgensen B, Dam W, Olsen CE, Moller BL, Bak S (2007) Lessons learned from metabolic engineering of cyanogenic glucosides. Metabolomics 3:383-398.

Morant M, Bak S, Moller BL, Werck-Reichhart D (2003) Plant cytochromes P450: tools for pharmacology, plant protection and phytoremediation. Curr Opin Biotechnol 14:1-12.

Nahrstedt A (1985) Cyanogenic compounds as protecting agents for organisms. Plant Sys Evol 150:35-47.

Nakamura Y, Kaneko T, Asamizu E, Kato T, Sato S, Tabata S (2002) Structural analysis of a *Lotus japonicus* genome. II. Sequence features and mapping of sixty-five TAC clones which cover the 6.5-Mb regions of the genome. DNA Res 9:63-70.

Nielsen JS, Moller BL (1999) Biosynthesis of cyanogenic glucosides in *Triglochin maritima* and the involvement of cytochrome P450 enzymes. Arch Biochem Biophys 368:121-130.

Nielsen JS, Moller BL (2000) Cloning and expression of cytochrome P450 enzymes catalyzing the conversion of tyrosine to p-hydroxyphenylacetaldoxime in the biosynthesis of cyanogenic glucosides in *Triglochin maritima*. Plant Physiol 122:1311-1322.

Nielsen KA., Olsen CE, Pontoppidan K, Moller BL (2002) Leucine derived cyano-glucosides in barley. Plant Physiol 129:1066-1075.

Nielsen KA, Tattersall DB, Jones PR, Moller BL (2008) Metabolon formation in dhurrin biosynthesis. Phytochemistry 69:88-98.

Nikus J, Esen A, Jonsson LMV (2003) Cloning of a plastidic rye (Secale cereale) beta-glucosidase cDNA and its expression in *Escherichia coli*. Physiol Plant 118:337-345.

Niu JS, Yu L, Ma ZQ, Chen PD, Liu DJ (2002) Molecular cloning, characterization and mapping of a rhodanese like gene in wheat. Yi Chuan Xue Bao 29:266-272.

Papenbrock J, Schmidt A (2000) Characterization of a sulfurtransferase from *Arabidopsis thaliana*. Eur J Biochem 267:145-154.

Perry JA, Wang TL, Welham TJ, Gardner S, Pike JM, Yoshida S, Parniske M (2003) A TILLING reverse genetics tool and a web-accessible collection of mutants of the legume *Lotus japonicus*. Plant Physiol 131:866-871.

Poulton JE (1990) Cyanogenesis in plants. Plant Physiol 94:401-405.

Ressler C, Nigam S, Giza Y (1969) Toxic principle in vetch: isolation and identification of γ-L-glutamyl-l-β-cyanoalanine from common vetch seeds: distribution in some legumes. J Am Chem Soc 91:2758-2765.

Szczyglowski K, Hamburger D, Kapranov P, de Bruijn FJ (1997) Construction of a *Lotus japonicus* late nodulin expressed sequence tag library and identification of novel nodule-specific genes Plant Physiol 114:1335-1346.

Sibbesen O, Koch B, Halkier BA, Moller BL (1994) Isolation of the heme-thiolate enzyme cytochrome P-450TYR, which catalyses the committed step in the biosynthesis of the cyanogenic glucoside dhurrin in *Sorghum bicolor* (L.) Moench. Proc Natl Acad Sci USA 91:9740-9744.

Sibbesen O, Koch B, Halkier BA, Moller BL (1995) Cytochrome P-450TYR is a multifunctional heme-thiolate enzyme catalyzing the conversion of l-tyrosine to *p*-hydroxyphenylacetaldehyde oxime in the biosynthesis of the cyanogenic glucoside dhurrin in *Sorghum bicolor* (L.) Moench. J Biol Chem 270:3506-3511.

Siritunga D, Arias-Garzon D, White W, Sayre RT (2004a) Over-expression of hydroxynitrile lyase in transgenic cassava roots accelerates cyanogenesis and food detoxification. Plant Biotechnol J 2:37-43.

Siritunga D, Sayre R (2004b) Engineering cyanogen synthesis and turnover in cassava (*Manihot esculenta*). Plant Mol Biol 56:661-669.

Swain E, Li CP, Poulton JE (1992) Tissue and subcellular localization of enzymes catabolizing (R)-amygdalin in mature *Prunus serotina* seeds. Plant Physiol 100:291-300.

Tattersall DB, Bak S, Jones PR, Olsen CE, Nielsen JK, Hansen ML, Hoj PB, Moller BL (2001) Resistance to an herbivore through engineered cyanogenic glucoside synthesis. Science 293:1826-1828.

Thorsoe KS, Bak S, Olsen CE, Imberty A, Breton C, Moller BL (2005) Determination of catalytic key amino acids and UDP sugar donor specificity of the cyanohydrin glycosyltransferase UGT85B1 from *Sorghum bicolor*. Molecular modelling substantiated by site-specific mutagenesis and biochemical analyses. Plant Physiol 139:664-673.

Thygesen LG, Jorgensen K, Moller BL, Engelsen SB (2004) Raman spectroscopic analysis of cyanogenic glucosides in plants: development of a flow injection surface-enhanced Raman scatter (FI-SERS) method for determination of cyanide. Appl Spectrosc 58:212-217.

Trummler K, Wajant H (1997) Molecular cloning of acetone cyanohydrin lyase from flax (*Linum usitatissimum*). Definition of a novel class of hydroxynitrile lyases. J Biol Chem 272:4770-4774.

Vahala J, Ruonala R, Keinanen M, Tuominen H, Kangasjarvi J (2003) Ethylene insensitivity modulates ozone-induced cell death in birch. Plant Physiol 132:185-195.

Verdoucq L, Moriniere J, Bevan DR, Esen A, Vasella A, Henrissat B, Czjze M (2004) Structural determinants of substrate specificity in family 1 beta-glucosidases: novel insights from the crystal structure of sorghum dhurrinase-1, a plant beta-glucosidase with strict specificity, in complex with its natural substrate. J Biol Chem 279:31796-31803.

Vetter J (2000) Plant cyanogenic glycosides. Toxicon 38:11-36.

Vogt T, Jones D (2000) Glycosyltransferase in plant natural product synthesis. Characterization of supergene family. Trends Plant Sci 5:380-386.

Wang D, Li W, Wan J (2004) Cloning and preliminary expression of alpha-hydroxynitrile lyase gene from cassava. Chinese J Appl Environ Biol 10:428-431.

Wang P, Van Etten HD (1992) Cloning and properties of a cyanide hydratase gene from the phytopathogenic fungus *Gloeocercospora sorghi*. Biochem Biophys Res Commun 187:1048-1054.

Watanabe Y, Laschat S, Budde M, Affolter O, Shimadac Y, Urlacher VB (2007) Oxidation of acyclic monoterpenes by P450 BM-3 monooxygenase: influence of the substrate E/Z-isomerism on enzymechemo- and regioselectivity. Tetrahedron, 63:9413-9422.

Wiersma PA, Fils-Lycaon BR (1996) Molecular cloning and nucleotide sequence (Accession No. U39228) of a beta-glucosidase cDNA from ripening sweet cherry fruit (PGR95-127). Plant Physiol 110:337-337.

Wulff-Strobel CR, Wilson DB (1995) Cloning, sequencing, and characterization of a membrane-associated *Prevotella ruminicola* B(1)4 beta-glucosidase with cellodextrinase and cyanoglycosidase activities. J Bacteriol 177:5884-5890.

Zagrobelny M, Bak S, Rasmussen AV, Jorgensen B, Naumann CM, Lindberg

Moller BL (2004) Cyanogenic glucosides and plant-insect interactions. Phytochemistry 65:293-306.

Zhang P, Bohl-Zenger S, Puonti-Kaerlas J, Potrykus I, Gruissem W (2003) Two cassava promoters related to vascular expression and storage root formation. Planta 218:192-203.

Zheng L, Poulton JE (1995) Temporal and spatial expression of amygdalin hydrolase and (R)-(+)-mandelonitrile lyase in black cherry seeds. Plant Physiol 109:31-39.

Zhou J, Hartmann S, Shepherd BK, Poulton JE (2002) Investigation of the microheterogeneity and aglycone specificity-conferring residues of black cherry prunasin hydrolases. Plant Physiol 129:1252-1264.

Volume 54(1):15-18, 2010
Acta Biologica Szegediensis
http://www.sci.u-szeged.hu/ABS

ARTICLE

Histological comparison of the rhizome, leafy culm and aerial rhizome of the common reed (*Phragmites australis*)

László Bankó, László Erdei*, Mónika Ördög, Erzsébet Mihalik

Department of Plant Biology, University of Szeged, Szeged, Hungary

ABSTRACT In this study we focused on the morphology of an unusual organ, appeared on the culm of read (named as aerial rhizome), rhizome and leafy culm of the reed plant (*Phragmites australis* (Cav.) Trin. Ex Steudel). The aerial rhizome appeared on young reclined culms or at occasionally broken nodes of reed plants grown in a glasshouse, in perlite and nutrient solution. During the 5 years of cultivation, under greenhouse circumstances the plants remained small if their size is compared to that of the natural reed stands, but the segments developed into an interconnected, well-grown system of roots and leafy culms. According to the histological results, the structure of the aerial rhizome and rhizome revealed a great similarity. The resemblance is not only noticeable in the number of the cell-lines and size of the primary cortex and central cylinder but also in the existence of the lacunae and the central cavity. So far no information concerning the role of the aerial rhizome came to light in the literature; according to our best knowledge, similar structure has not even been mentioned. It is tempting to speculate that the structure's main role may be the vegetative reproduction, horizontal spread of the clone, since histologically greatly resembles to the rhizome. We hypothesize that the structure develops under extreme conditions, e.g. continuous stress such as growing the plants in spatial constrains which cannot be found in natural conditions. Consequently, the cause of the formation of the structure can originate from the extremism of the living-conditions.
Acta Biol Szeged 54(1):15-18 (2010)

KEY WORDS

aerial rhizome
culm type
reed
Phragmites australis

On the horizontal or in some cases broken reclining culms of reed plants, grown under greenhouse conditions in nutrient solution, at the nodes, certain organs named by us as aerial rhizomes, evolved. According to the best of our knowledge the literature did not even mention such an organ. In one of the studies of Haslam (Haslam 1968) in case of reed 4 fundamental culm types are described: the horizontal and vertical rhizome, the aboveground culm and the infrequent runner (*legehalme, long runner).*

In woody monocotyledonous species, e.g. in case of *Cordyline* the appearance of aerial rhizomes was observed (Bell 1991), which under certain circumstances could evolve into an independent plant.

The organs evolved on plants kept under artificial circumstances comprised of several nodes and internodes developing into leafy shoots exhibited negative geotropism. In our study we histologically compared the culm, rhizome and aerial rhizome. According to the results the structure of the aerial rhizome morphologically is highly similar to that of the rhizome. There is no primary cortex in the culm, the multicell-layered epidermis directly reaches the vessels. The aerial rhizome and rhizome are differentiated into a wide multicell-layered primary cortex and a central cylinder. In the parenchyma of the primary cortex lacunae, in the central cylinder three collateral closed vessels are found. The size of the bundles gradually decrease from inside to outward.

Materials and Methods

Morphological observations were carried out on the rhizome, aerial rhizome and culm of common reed (*Phragmites australis* (Cav.) Trin. ex Steudel). The rhizome segments were collected from a natural reed stand, Csukásér canal near Gátér (Csongrád County, Hungary). Two-bud rhizome segments were placed into plastic vessels filled up with perlite, supplied with complete Hoagland nutrient solution. From the initials during 5 years a full-grown rhizome network was developed with 10-15 ramets (Bankó et al. 2002). In the present experiment we worked with 3-3 samples coming from 3 plants. After de-aeration and dehydration we applied paraffin embedment instead of the carcinogenic xylol and benzol. Bioclear was used as an intermediate compound.

The samples placed in 100% ethyl alcohol were transferred in 70-30, 50-50 and 30-70 alcohol-Bioclear rate solution and this was transferred into the Bioclear compound. During the paraffin impregnation the samples were placed into a 35-40°C thermostat, since at a lower temperature the

Accepted November 20, 2009
*Corresponding author. E-mail: erdei@bio.u-szeged.hu

Figure 1. The „aerial rhizome", developed on an aerial stem of reed. Bar = 1 cm.

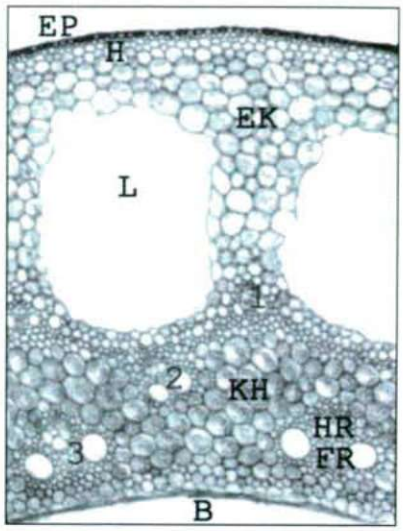

Figure 2. Microscopic photograph on the cross-section of rhizome. EP: epidermis, H: hypodermis, EK: primary cortex, L: aerenchyme, KH: central cylinder, HR: phloem, FR: xylem, B: central cavity. 1: The outer small; 2: the middle, 3: and the inner large-sized vascular bundle circles.

solution would have been become saturated soon. At 60°C the paraffin remained molten and continuously paraffin was added to the solution. The impregnation took 3 weeks then the volume of the paraffin was two-fold of that of the solution. Depending on the samples the evaporation of the Bioclear took 1 week and the material was ready for cutting sections. The samples were set in aluminium blocks, the blocks were filled up with paraffin. Before cutting the foil was removed, the paraffin was cut in the form of a dice then the dices were glued with few molten paraffin onto a wood base for fixing it to the platen.

The samples were cut with microtome equipped with steel blade in large quantity between 12 and 17 μm in thickness. The photograph of the CCD camera joined with the light microscope was digitalized with computer and were evaluated with Image Pro Plus software. The dataset made from the numerous photos were analyzed with Microsoft Excel.

Results and Discussion

The reed plants gorwn according to the above written circumstances had typical 3-15-noded structures ending in bud on their thin reclined culms (Fig. 1). These mostly resembled the horizontal, underground rhizomes (Fiala 1976). Although variations in soil conditions (Kudo and Ito 1997) sulphide levels (Fogli et al. 2002) or C/N metabolic malfunctions (Erdei et al. 2001) altered rhizome and shoot development, similar aerial organ shown by Figure 1, was not seen in the open nature.

As the histological results revealed, the structure of the rhizome and aerial rhizome showed a high degree of similarity. In both cases under the epidermis consisting of one cell-layer, the hypodermis's wall is slightly thickened. The primary cortex is thick, consisting of 14 and 8 cell-layers for the rhizome and aerial rhizome, respectively.

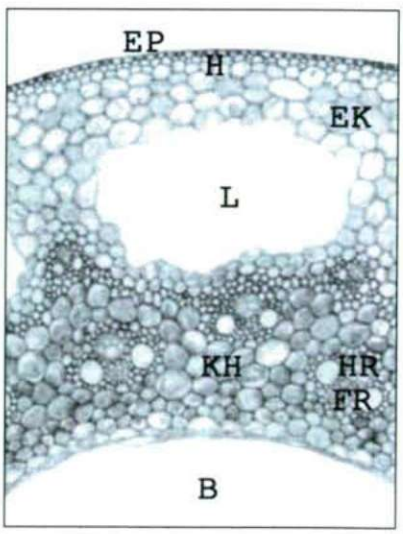

Figure 3. Microscopic photograph of the cross-section of aerial rhizome. The primary cortex and the central cylinder are formed of fewer cell-lines than those of the rhizome. In the structure of the aerenchyme further differences can be discovered; the cavities are flat, narrow, rather resembling an oblong form with rounded sides. EP: epidermis, H: hypodermis, EK: primary cortex, L: aerenchyme, KH: central cylinder, HR: phloem, FR: xylem, B: central cavity.

In the parenchyma substance of the primary cortex large-sized air passages evolved. Their function is oxygen-supply

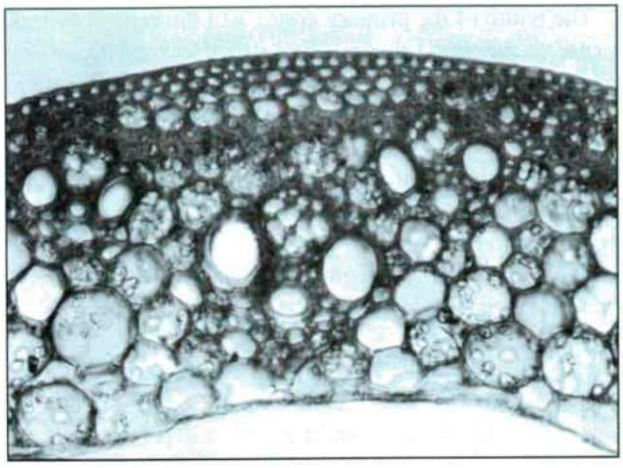

Figure 4. Cross-section of *Phragmites* stem (culm). Under the one-layered epidermis, hypodermis and the primary cortex's two cell-lines the three circles of vascular bundles are embedded in the tissue of the parenchyma of the central cylinder.

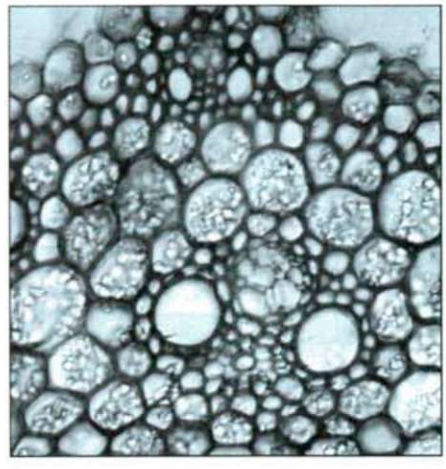

Figure 5. Leucoplasts were found in smallest quantity in the aerial rhizomes. As seen on the picture in rhizome and stem the parenchyma cells – which build up the central cylinder – abundantly contain leucoplasts.

for subterraneous organs under hypoxia. Between the air passages, on their inward sides, small-sized bundles were observed, occupying a place in the tissue of the central cylinder which wave-likely protrudes between the air passages. The collateral closed vessels form three circles. The outer smallest bundles are followed by a medium-sized, then a large-sized thin-walled bundle-circle. Both in case of the rhizome and the aerial rhizome large thin walled cells build up the central part of the cortex, whereas the cells adjutant to the cortex's outer and inner surface hardly reach half of the diameter of the former cells. The lacuna system has a well expressed sharp border. The lacunae are placed in the large parenchyma substance, in turn, along its inner wall facing the central cylinder small-sized, one cell-layer wide cortex parenchyma forms the boundary (Figs 2 and 3).

The parenchyma of the central cylinder exhibits a structure similar to the primary cortex. The cylinder's outer and inner walls are accompanied by cell-lines of smaller cells. The two inner bundles are placed in the large-diametered cell-substance in such a way that these small-sized cells shut them in. The outer smallest bundles are located between the small cells that are intruding wavely into the interspace among the lacunae. The circle of the bundle is separated by one cell-layer from outside from the cortex-parenchyma. The central cavity's border is sharp and due to intensive cell-elongation flat cells border.

Beside the significant morphological similarities between the rhizome and aerial rhizome the different structure of the lacunae is a great difference. The lacunae in case of the rhizome are nearly rounds with rounded sides whereas in

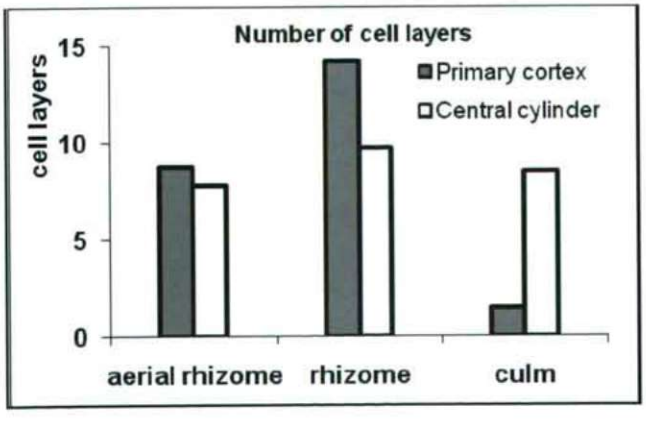

Figure 6. Numbers of cell-lines building up the primary cortex and central cylinder of reed aerial rhizome, rhizome and culm.

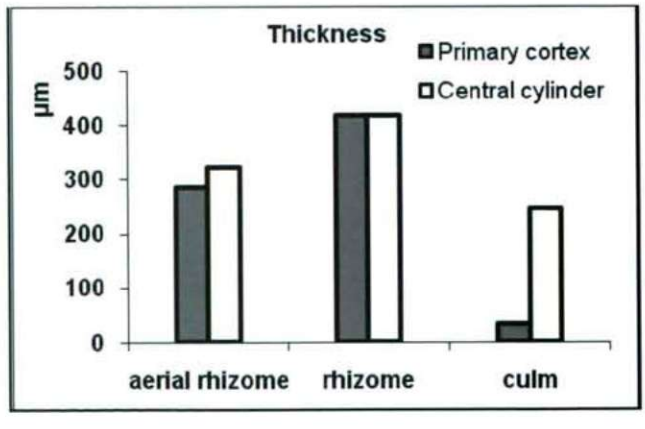

Figure 7. The thickness of the primary cortex and central cylinder of reed aerial rhizome, rhizome and culm.

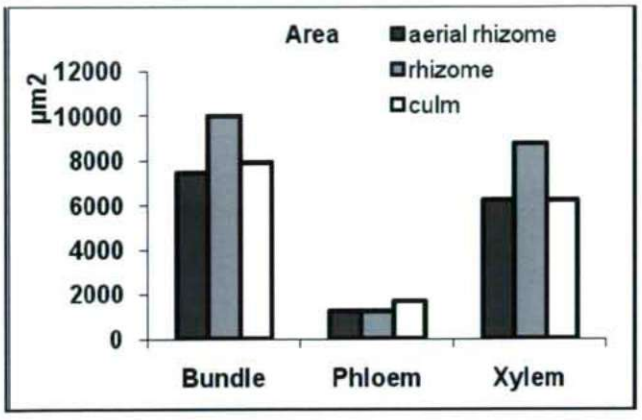

Figure 8. The area of the vascular bundles, xylem and phloem of reed aerial rhizome, rhizome and culm.

case of the aerial rhizome they are oblong-shaped with better expressed sides.

The mechanical strengthening of the culm is provided by sclerenchyma. The supporting tissue is localized in several places: thus under the hypodermis, between the vessels and along the central cylinder and the cortex. In the central cylinder of the leafy culm three bundle-circles evolved similarly to the underground shoot (Fig. 4).

Leucoplasts were found in the least amount in the aerial rhizomes. The parenchyma cells enclosing the vessels in the culm and the rhizome contained a great quantity of starchy granules (Fig. 5).

After evaluating statistically the dataset of the numerous sections, the similarity of the aerial rhizome and rhizome became obvious. The statistical analyses correlated with the results of the light microscopic observations. The primary cortex of the culm and the aerial rhizome are thick which in case of the aerial rhizome and the rhizome consist of 8 and 14 cell layer, respectively. Their central cylinder is also wide, 8 and 10 cell-layered. The cortex of the culm between the most exterior bundles is represented by a thin parenchyma of 1-2 cell layers, which are unobservable above the bundles, while the 9 cell-layered central cortex is comprised of several tissues (Fig. 6).

The width of the primary cortex and the central cylinder in case of the aerial rhizome and rhizome are 600 and 800 µm, respectively. This quite exceeds the shoot's value which is under 300 µm, although the central cylinder here is also thick, having a 250 µm average value (Fig. 7).

In the rhizome and aerial rhizome the phloem to vessel ratio is higher in the outer smallest vessel than in case of the two larger inner vessels. In the culm, the area of the phloem is slightly larger as compared to those of the rhizome and aerial rhizome (Fig. 8).

In conclusion it can be stated that in case of reed plant the characteristics of the aerial rhizome can be described as a new culm type. We only have vague assumptions concerning its function in nature – if it would be found in nature at all.

The aerial rhizome may contribute to the vegetative reproduction of the clone, similarly to the function of the rarely found runner. It is the future's task to elucidate the physiological and hormonal background of this formation. The results may contribute to a better understanding of the reproductive strategy of this clonal species.

Acknowledgements

This work was supported by the Hungarian Sientific Research Fund grant No. OTKA T 032524.

References

Bankó L, Ördög M, Erdei L (2002) The role of rhizome system in the distribution of cadmium load among ramets of *Phragmites australis*. Acta Biol Szeged 46(3-4):81-82.

Bell AD (1991) Plant Form: An illustrated guide to to flowering plant morphology. Oxford University Press, Oxford, ISBN 0-19-854279-8. p. 170.

Erdei L, Horváth F, Tari I, Pécsváradi A, Szegletes Zs, Dulai S (2001) Differences in photorespiration, glutamine synthetase and polyamines between fragmneted and closed stands of Phragmites australis. Aq Bot 69:165-176.

Fiala K (1976) Underground organs of *Phragmites communis*, their growth, biomass and net production. Folia Geobot Phytotax 11:225-259.

Fogli S, Marchesini R, Gerdol R (2002) Reed (*Phragmites australis*) decline in a brackish wetland in Italy. Marine Environ Res 53:465-479.

Haslam SM (1968) Stem types of *Phragmites communis* Trin Ann Bot 33:127-131.

Kudo G, Ito K (1988) Rhizome development of *Phragmites australis* in a reed community. Ecol Res 3:239-252.

Volume 54(1):19-23, 2010
Acta Biologica Szegediensis
http://www.sci.u-szeged.hu/ABS

ARTICLE

Starch to protein ratio and α-amylase activities in grains of different wheat cultivars

Jolán Csiszár[1]*, Adrienn Guóth[1], Zsuzsanna Kolbert[1], Ágnes Gallé[1], Irma Tari[1], Sorin Ciulca[2], Emilian Madosa[2], László Erdei[1]

[1]Department of Plant Biology, Faculty of Science and Informatics, University of Szeged, Szeged, Hungary, [2]Faculty of Horticulture and Sylviculture, Banat's University of Agricultural Sciences and Veterinary Medicine, Timisoara, Romania

ABSTRACT Starch and total protein contents, α-amylase activity of grains as well as falling number in the flour, an internationally accepted measure of α-amylase activity in the food industry, were compared in wheat (*Triticum aestivum* L.) genotypes which are widely used in the agriculture and breeding in Romania and Hungary. These cultivars were originated from Romania (20 cultivars), Hungary (cv. GK Élet, GK Öthalom and Mv Emese), France (cv. Cappelle Desprez), the USA (cv. Plainsman) and China (cv. Xiang). The starch contents of the grains were high in those cultivars, where the protein contents were relatively low. The highest starch content among the investigated wheat genotypes was found in the Romanian Gruia cultivar, which could be characterized also with low starch degrading α-amylase activity in the grain and with a high falling number. This wheat genotype can be a good candidate for utilization in starch industry. Other genotypes, which had relatively high starch contents and, a low α-amylase activity (or high falling number) were the Romanian Crina and Gloria, the Hungarian GK Öthalom, GK Élet, Mv Emese and the French Cappelle Desprez cultivars.
Acta Biol Szeged 54(1):19-23 (2010)

KEY WORDS

α-amylase activity,
falling number,
total protein content,
starch content,
wheat genotypes

The composition of wheat storage proteins and starch permit the production of wide range of food and industrial products from the processed grain. These storage products, proteins (albumins, globulins and the fractions of glutene, gliadins and glutenins) and starch accumulate in the endosperm and act as a nutrient source for the germinating seedling.

The protein content is an indicator of direct nutritional value and is a key specification for wheat and flour purchasers since the bread-making quality is to large extent determined by the quantity and composition, polymeric amount and size distribution of storage proteins. The genetic improvement of wheat has received considerable attention over the years from plant breeders with the purpose of increasing protein content and yield. In recent years however, there has been an increased interest in starch content and composition of wheat because of the growing industrial demand and the possible production of fuel alcohol from grain.

Starch is the most abundant storage polysaccharide in plants, and occurs as granules in the chloroplast of green leaves and the amyloplast of seeds, pulses and tubers. Starch, is a staple in the diet of much of the world's population, and is also widely used in the Western world in the food and beverage industries as a thickener and a sweetener, as well as having some manufacturing applications in the paper and textile industries. The more prevalent use of starch for industrial purposes will only become economically viable when its use as a raw material rivals those derived from petroleum-based products (Slattery et al. 2000). The use of starch as a renewable and biodegradable polymer is becoming increasingly attractive because of the environmental concerns about the industrial wastes generated from petroleum products and the growing awareness of the potential deleterious consequences of greenhouse gas emissions from these activities. Biofuels can be derived from any substance yielding fermentable sugars. Cereal grains are good feedstock because grains contain a high proportion of starch and can be stored dry for many months, allowing year round processing.

Starch is composed of two different glucan chains, amylose and amylopectin. These polymers have the same basic structure, but differ in their length and degree of branching. Amylose is an essentially linear chain of glucose residues linked via α-1,4 glucosidic linkages, whereas amylopectin is a branched α-1,4: α-1,6 D-glucan polymer, that is made up of a linear glucose backbone with occasional glucose side branches. The ratio of amylose to amylopectin in starch contributes to its physical properties and its functionality varies between species and varieties (Slattery et al. 2000). The percentage of amylose and amylopectin in wheat starches is ca. 25% and 75%, respectively.

Accepted July 6, 2010
*Corresponding author. E-mail: csiszar@bio.u-szeged.hu

Starch in grains is packed into granules which, based on size, may be classified into large (25-35 μm, A type) and small (2.0-8.0 μm, B type) granule starch. Brosnan et al. (1998) reported, that total starch content is more important for industrial purpose (e.g. alcohol yield) than the relative amounts of large and small granules. In the matter of using starch as feedstock, alcohol processing yield depends on (i) the amount of starch present, (ii) how much of this starch is converted to fermentable sugars, and (iii) the efficiency with which these sugars are fermented into alcohol. Increasing starch quantity directly impact yield in the industrial application.

Starch reserves may be degraded *in vitro* by the action of endogenous amylases. α-amylase is an endoamylolytic enzyme that hydrolyzes the α-1,4-glucosidic linkages of starch; the hydrolytic products have α-configuration. It is found in most reserve tissues during periods of starch mobilization. In germinating cereal seeds, α-amylase secreted from the aleurone cells initiates the degradation of starch granules in the non-living endosperm. It liberates soluble glucans that can be further degraded by other hydrolytic enzymes such as debranching enzymes and β-amylases.

Some α-amylase enzyme is present in the embryo or germ of sound wheat kernels, and α-amylase isoenzymes are exist also in immature wheat. During the development of wheat grains, the α-amylase activity increases and reaches a maximum value about 16 days after heading, then the amylase activity rapidly decreases and reaches a minimum value at the maturation stage. Interestingly, wheat kernel contains a number of albumin components that actively inhibit many α-amylases from sources other than wheat but are inactive with α-amylase of wheat (Pace et al. 1978). When germination begins, the embryo and layers surrounding the starchy endosperm produce α-amylase at an accelerating rate. A severely sprout-damaged kernel contains many thousands of times the amounts of enzyme present in kernels that are in the early stages of germination. Because of this, a wheat grain sample containing very low levels of severely sprouted kernels may exhibit significant amylase activity. α-amylase converts starch into sugars in the sprouting kernel, and similarly breaks down the starch granules in wheat flour when mixed with water to make bread dough.

A genetic defect, named Late Maturity α-amylase (LMA) or Prematurity α-amylase activity (PMAA), present in particular wheat genotypes, was reported by Gale et al. (1983). LMA may result in the accumulation of unacceptable levels of high amylase in grains in the absence of germination or weather damage and it has been inadvertently disseminated to wheat programmes around the world. Grain of these genotypes may develop high pI α-amylase activity either under normal growing conditions or, more commonly, as a result of cool temperature stress (Mrva et al. 2006).

For bakers, the α-amylase activity of the flour is important, because it has negative effects on the dough. Flour damaged by α-amylase holds less water when mixed and the dough absorbs less water during baking. The enzyme also affects gas retention, dough handling and bread texture. Too much α-amylase activity causes wet, sticky dough that is hard to handle in a commercial bakery. The loaf may have large, open holes and the crumb texture is gummy. Gummy bread is difficult to slice and builds up on slicer blades. Loaves are often deformed, hard to package and unattractive to customers. Because of these, the α-amylase activity of flour is a relevant information. In the food industry, falling number is the internationally accepted measure of α-amylase activity. It could be argued that low falling number samples may give more efficient starch conversion because of higher levels of endogenous amylase, but conversely poor quality, e.g. sprouted samples may have already lost starch, and therefore for example alcohol yields might be reduced.

In this work the starch and protein contents as well as α-amylase activities of 26 wheat cultivars mostly of Romanian and Hungarian origin were compared. The investigated genotypes are widely used by the agriculture and breeding in Romania and Hungary. Our aim was to investigate the variations present in these cultivars and find a correlation between the protein and starch content of grains.

Materials and Methods

Plant material

Wheat (*Triticum aestivum* L.) kernels were originated from Romania (20 cultivars), Hungary (cv. GK Élet, GK Öthalom and Mv Emese), France (cv. Cappelle Desprez), the USA (cv. Plainsman) and China (cv. Xiang) from the yield of 2007 year. The grains of Romanian cultivars were kindly provided by the Horticulture Faculty, Banat's University of Agricultural Sciences, Timisoara, Romania; Mv Emese was given by Agricultural Research Institute of the Hungarian Academy of Sciences, Martonvásár, Hungary (László Láng); the other plant material were kindly provided by László Cseuz, Cereal Research Non-Profit Company, Szeged, Hungary. Wheat grains were conditioned to equalize the moisture content (15.5%) of each sample.

Determination of starch and protein content

Starch content of the grains was measured by the polarimetric analytical method used in food industry (according to MSZ 6367/13-82, polarimetric Ewers method, in Institute of Food Engineering, Faculty of Engineering, University of Szeged, Hungary), and by the method of Lásztity and Törley (1987). The protein content of the samples was determined also by the method used in food industry (Ma et al. 2007).

Measurements of α-amylase activity

For determination of the α-amylase activities, 0.5 g of the whole grains was homogenized with 50 ml water. For mea-

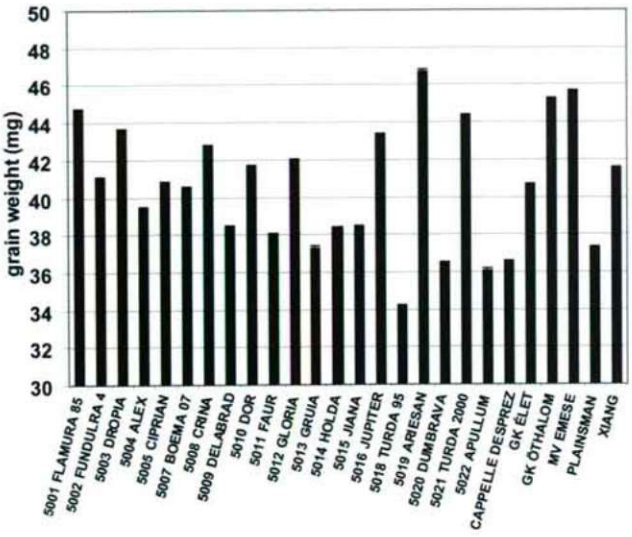

Figure 1. Dry weight of grains of different wheat cultivars.

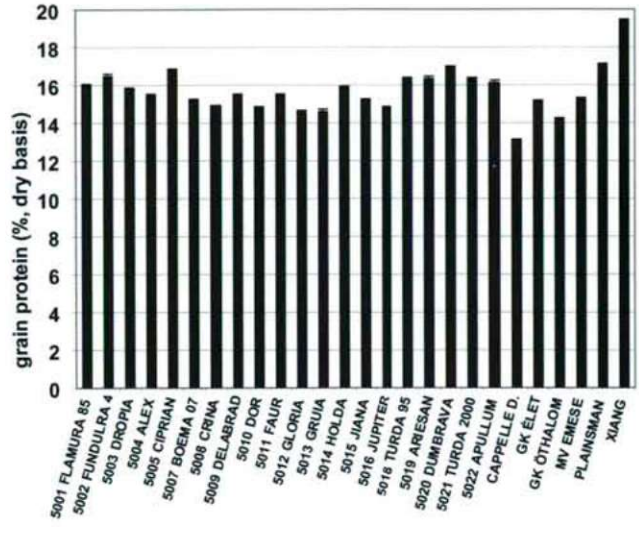

Figure 2. Protein content in % of the grain dry weight of different wheat cultivars.

suring the amount of starch degraded by α-amylase, 15 ml reaction mixture containing 13 mg ml^{-1} of starch and 5 ml of plant extract containing α-amylase activity was used. The reaction was performed at 30°C for 20 minutes. The starch content not degraded by the enzyme, was detected with KI/I_2 solution. For the quantification, calibration curve was made with diluted starch solution in the range of 1.3-13 mg ml^{-1} concentrations.

The α-amylase activity of the wheat flour was also examined by measuring the falling number. This method utilizes the gelatinization of starch polymers in suspension of water and flour. The principle of the falling number method is that the enzyme activity can be indirectly measured by the rheological properties of heated starch suspensions. The procedure involves the agitation by a stirring rod of a meal-water mixture within a precision test tube immersed in a boiling water bath. After 1 min, the stirring rod is released at the top of the tube and falls by its own weight through the viscous suspension. The time, in seconds, needed for the stirrer to travel through a fixed depth of suspension, plus 60 (from the agitation period) is the Hagberg Falling Number (FN). All the measurements were repeated at least three times, and the means ± SD were calculated.

Results and Discussion

The average dry weight of grains displayed a high variability among the investigated wheat cultivars from 34.21±0.019 (cv. Turda) to 46.73±0.136 mg (cv. Ariesan; Fig. 1). However, there were a much less difference in the protein and starch content of the different cultivars. The protein content of the grains on dry weight basis varied between 13.12±0.021 (cv. Cappelle Desprez) and 19.41±0.049% (cv. Xiang; Fig. 2). Determination of the starch content from grain samples by the polarimetric method revealed that the amount of the starch in the chosen varieties was between 60.14 and 66.93% (Fig. 3). According to our results, the Romanian cv. Gruia had the highest starch content, but similarly good level was measured in the Romanian Crina, Boema 07 and Gloria genotypes, or in the Hungarian GK Öthalom and in the French Cappelle Desprez wheat cultivars (their starch content varied between 65.85 and 66.93%). The Xiang genotype contained the less starch, but among the local genotypes, the Romanian Fundulra 4, Ciprian, Turda 95 and Dumbrava had ca. 62 % starch, these can be regarded as wheat cultivars with relative low starch levels (Fig. 3). Using wheat genotypes of different origin made the variability of these parameters greater.

Starch granules are embedded within a protein matrix within the endosperm. Comparing the starch content with the protein content of the grains revealed a strong negative correlation (R^2= 0.82). Due to inverse relation between starch and protein contents, increases in starch amount are correlated with decreases in grain protein content (Fig. 4).

The ratio of starch and various proteins like water soluble albumins and globulins or gluten (gliadins and glutenins) accumulating in wheat grains is determined by the genotype, but environmental factors are also important. Technological quality of wheat is determined by the quantity and quality of reserve proteins and the status of carbohydrate-amylase complex. This means that the degree of the damage to starch granules and the content and activity of α-amylase in the flour determines the flour quality. The extent of starch conversion can be assessed conventionally using the falling number (FN)

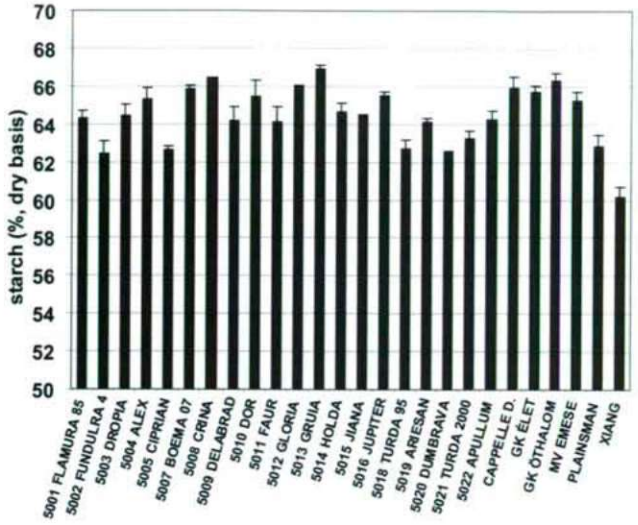

Figure 3. Starch content in % of the grain dry weight in the investigated wheat genotypes measured by polarimetric method.

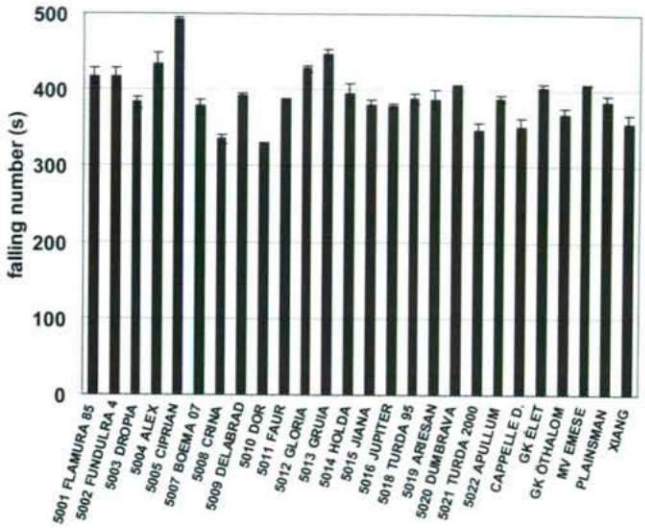

Figure 5. Falling number of the investigated wheat genotypes.

test, which was performed on flour samples. The FN values were between 330 and 492 s (Fig. 5). The Romanian cv. Cyprian had the highest falling number, but the Alex, Gloria and Gruia genotypes had also relatively high FN, which means relatively low amylase activity. Low falling number was measured in the flour of Dor, Crina, Turda 2000 and Cappelle Desprez wheat cultivars.

Many buyers place strict limits on falling number in the wheat they buy. It could be argued that low falling number samples may give more efficient starch conversion because of higher levels of endogenous amylase, but conversely poor quality, e.g. sprouted samples may have already lost starch, and therefore the industrial utilization of the grains might be reduced.

The falling number is a complex parameter, which depends on the α-amylase activity and the properties of starch in the grain. Therefore, we measured the α-amylase activities of the grains also by another method. Measuring the amount of the degraded starch in the samples originated from these wheat grains revealed approximately constant level of α-amylase activities (Fig. 6.). Relatively high activities was detected in the Romanian Flamur 85, Fundulra 4 and Ciprian genotypes,

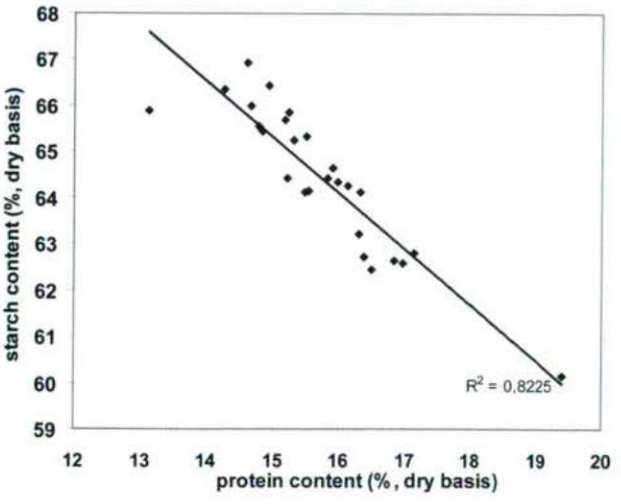

Figure 4. Starch content of grain samples from investigated wheat varieties against total protein content.

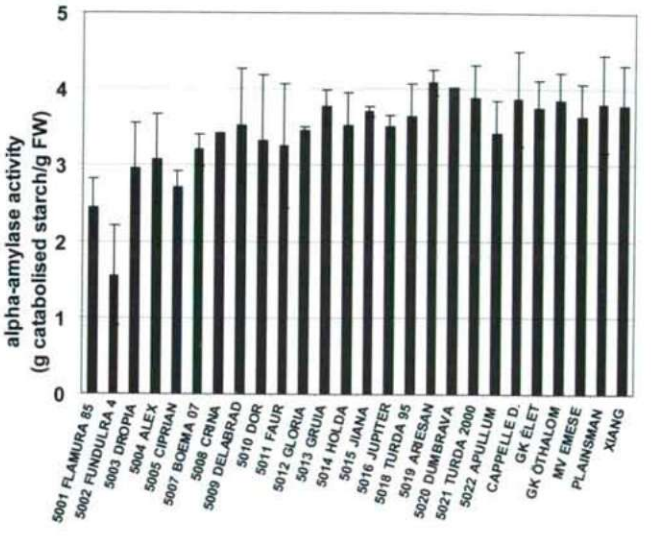

Figure 6. α-amylase activities of the investigated wheat genotypes measured according to the degraded starch by the grain extracts.

and low values were measured e.g. in the Romanian Gruia, Jiana, Ariesan, Dumbrava, Turda 2000 lines, in the Hungarian genotypes (Élet, Öthalom, Emese), in the French Cappelle Desprez and in the American Plainsman wheat.

High endogenous α–amylase activity (and low falling number) can be associated with the pre-harvest sprouting and economic losses of grain dry matter, but may also result in starch conversion to sugars without any visible sprouting damage. The genotypes characterised by high falling number and low starch degrading amylase activity in the grain can be submitted for industrial purpose. For example, cv. Gruia could be characterised by high FN and low α-amylase activities, as expected; so in this case the α -amylase activity correlated with the flour quality.

In summary, using wheat genotypes with different origin displayed high variability in protein and starch content. Generally, the starch content of the wheat grains was high in those varieties, where the protein contents were relatively low. Those genotypes, which had relatively high starch content and, according to our results, a low α-amylase activity (or high falling number) are the Romanian Crina and Gloria, the Hungarian GK Öthalom, GK Élet, Mv Emese and the French Cappelle Desprez cultivars.

The highest starch content among the investigated wheat genotypes was found in the Romanian Gruia genotype, which can be characterized also with a high falling number and low α-amylase activity. This wheat line can be good candidate for utilization in starch industry.

Acknowledgment

This work was supported by the HURO-06-02/006 project and by 2010TÁMOP 4.2.1.B.

References

Brosnan JM, Makari SLP, Cochrane MP (1998) What makes a good distilling wheat? In Campbell I, ed., Proceedings of the fifth Aviemore conference on malting, brewing and distilling. Institute of Brewing, London

Gale MD, Flintham JE, Arthur ED (1983) Alpha-amylase production in the late stages of grain development: an early sprouting damage risk? In Kruger EJ, LaBerge ED, eds., Third International symposium on preharvest sprouting in cereals. Boulder, Colorado: Westwiev Press, pp. 29-35.

Lásztity R, Törley D (1987) Keményítő (Starch) In Alkalmazott élelmiszeranalitika I. Mezőgazdasági Kiadó, Budapest, pp. 473-474. (Hungarian)

Ma W, Sutherland MW, Kammholz S, Banks P, Brennan P, Bovill W, Daggard G (2007) Wheat flour protein content and water absorption analysis in a doubled haploid population. J Cereal Sci 45:302-308.

Mrva K, Wallwork M, Mares DJ (2006) α-Amylase and programmed cell death in aleurone of ripening wheat grains. J Exp Bot 57:877-885.

Pace W, Parlamenti R, Rab UR, Silano V, Vittozzi L (1978) Protein α-amilase inhibitors from wheat flour. Cereal Chem 55:244-254.

Slattery CJ, Kavakli H, Okita TW (2000) Engineering starch for increased quantity and quality. Trends Plant Sci 5:291-298.

Smith TC, Kindred DR, Brosnan JM, Weightman RM, Shepherd M, Sylvester-Bradley R (2006) Wheat as a feedstock for alcohol production. HGCA Research Review 61:1-89.

Volume 54(1):25-31, 2010
Acta Biologica Szegediensis
http://www.sci.u-szeged.hu/ABS

ARTICLE

Species relationship in the genus *Silene* L. Section *Auriculatae* (Caryophyllaceae) based on morphology and RAPD analyses

Masoud Sheidai[1]*, Abbas Gholipour[2], Zahra Noormohammadi[3]

[1]Shahid Beheshti University, GC., Faculty of Biological Sciences, Tehran, Iran, [2]Payame-Noor University, Sari, Iran, [3]Biology Department, School of Basic sciences, Science and Research Branch, Islamic Azad University (SRBIAU), Poonak, Tehran, Iran

ABSTRACT Morphological and RAPD studies were performed on *Silene* species of the sect. *Auriculatae* growing in Iran for the first time using phenetic, parsimony and Bayesian analyses. Trees obtained differed in the species groupings although agreed in some parts. Parsimony and Bayesian analyses of morphological characters produced some clades which were not well supported by bootstrap and clade credibility values but UPGMA tree showed a high cophenetic correlation. Grouping based on morphological characters partly support the species affinity given in Flora Iranica. Out of 40 RAPD primers used 15 primer produced reproducible polymorphic bands. In total 347 bands were produced out of which 340 bands were polymorph and 7 bands were monomorph. Among the species studied *S. goniocaula* showed the highest number of RAPD bands (184), while *S. commelinifolia* var. *isophylla* showed the lowest number (123). Some of the species studied showed the presence of specific bands which may be use for species discrimination. NJ and Bayesian trees of RAPD data partly agree with morphological trees obtained.
Acta Biol Szeged 54(1):25-31 (2010)

KEY WORDS

Morphometry
Parsimony
Phenetic
RAPD
Silene

Silene L. is the largest genus of Caryophyllaceae with about 700 species distributed throughout the northern hemisphere; Europe, Asia and northern Africa (Greuter 1995). It includes several important weeds, very beautiful horticultural plants and some medicinal species (Swank 1932). About 110 *Silene* species grow in Iran out of which about 35 species are endemic with very limited geographical distribution (Melzheimer 1988). *Silene* species have been placed in 44 sections (Chowdhuri 1957), but recent molecular studies do not support such sectional classifications particularly for the endemic North American taxa (Oxelman and Lidén 1995; Oxelman and Berglund 1997; Oxelman and al. 2000; Burleigh and Holtsford 2003).

The basic chromosome number of *Silene* is $x = 10$ or 12 (Melzheimer 1978; 1988; Markova and al. 2006; Popp and Oxelman 2007), most of the species are diploid ($2n = 2x = 24$), some are tetraploid ($2n = 4x = 48$) and hexaploid ($2n = 6x = 72$). Few species show higher polyploidy levels for e.g. $2n = c.$ 96, 120 and 192 (Bari 1973), while $2n = 3x = 30$ is reported for *S. fortunei* (Heaslip 1951).

The section *Auriculatae* (Boiss.) Schischkin is the largest section of the genus containing about 35 species in Iran, out of which 21 species are endemic with very restricted distribution in mountainous areas such as Elburz, Zagros and Azarbayejan (Melzheimer 1988). The members of this section are caespitose plants with large flowers placed at the end of short stems. Their inflorescence is unifloral or dichasial. Calyx is cylindrical-clavate, pubescent or glandular-pubescent. The petals have conspicuous auricule at the end of claw.

Different molecular markers have been used in systematic studies. Random Amplified Polymorphic DNA is one of these molecular markers widely used to study genetic polymorphism in plants, identifying hybrid specie and to study the species relationships (Bogani et al. 1994; Sanz-Cortés 2001; Çelebi et al. 2008). For example RAPD markers were used to study the taxonomic status of 42 taxa of species of the genus *Fritillaria* (Çelebi et al. 2008) and based on RAPD, morphological and protein analyses, two species of *F. acmopetala* subsp. acmopetala and *F. sororum* were considered as synonyms. Similarly Badr et al. (2000) showed close affinity of *H. vulgare* to *H. spontaneum* by RAPD analysis. Saitou et al. (2007) studied the hybrid origin of the diploid grass *Calamagrostis longiseta* var. *longe-aristata*, morphometric and genetic analyses of this taxon and its putative parental taxa were performed. The morphometric analyses revealed that, in general, *C. longiseta* var. *longe-aristata* is morphologically intermediate between C. *longiseta* var. *longiseta* and *C. fauriei*. RAPD analyses showed that individuals of *C. longiseta* var. *longe-aristata* were placed in both of the clusters formed by each putative parental taxon.

Accepted May 13, 2010
*Corresponding author. E-mail: msheidai@yahoo.com
msheidai@sbu.ac.ir

Oxelman (1996) used morphological and molecular markers including Internal Transcribed Spacer DNA (ITS) and RAPD markers to study the species relationships in the genus *Silene* sect. *Sedoides* and concluded that RAPD markers separated the best the species studied compared to either morphological and ITS markers used. Moreover RAPD markers were useful in subsp. delimitation and also confirmed allopolyploid nature of *S. aegaea*.

Biosystematic studies of the genus *Silene* in Iran is confined to few cytological reports only (Sheidai et al. 2008; Gholipour and Sheidai 2010). The present study considers morphometry and RAPD analysis of species relationships in the genus *Silene*, sect. *Auriculatae* of Iran for the first time.

Materials and Methods

Plant materials

Morphological and molecular studies were performed in 32 *Silene* species, subspecies and varieties from the sect. *Auriculatae* L. growing in Iran. The species studied are: 1- *S. commelinifolia* Boiss. var. *commelinifolia*, 2- *S. commalinifolia* var. *isophylla* Bornm., 3- *S. commelinifolia* var. *ovatifolia* Melzh., 4- *S. aucheriana* Boiss., 5- *S. nizvana* Melzh., 6- *S. oligophylla* Melzh., 7- *S. meyeri* Fenzl ex Boiss. ssp. *persica*, 8- *S. meyeri* Fenzl ex Boiss. ssp. *meyeri*, 9- *S. rhynchocarpa* Boiss., 10- *S. persica* Boiss., 11- *S. gynodioica* Ghazanfar; 12- *S. lucida* Chowdhuri, 13- *S. erysimifolia* Stapf., 14- *S. hirticalyx* Boiss.& Hausskn., 15- *S. microphylla* Boiss., 16- *S. goniocaula* Boiss., 17- *S. albescens* Boiss., 18- *S. daenensis* Melzh., 19- *S. dschuparensis* Bornm., 20- *S. eriocalycina* Boiss., 21- *S. prilipkoana* Schischk., 22- *S. sojakii* Melzh., 23- *S. sisianica* Boiss. & Buhse, 24- *S. palinotricha* Fenzl. ex Boiss., 25- *S. gertraudiae* Melzh., 26- *S. pseudonurensis* Melzh., 27- *S. elymaitica* Bornm., 28- *S. persepolitana* Melzh., 29- *S. indeprensa* Schischk., 30- *S. crispans* Litw., 31- *S. renzii* Melzh., 32- *S. araratica* Schischk. Moreover, *S. parrowiana* Boiss & Hausskn., from the sect. *Lasiostemones* and *pungens* Boiss., from the sect. *Pinifoliae* were included as out-group species in the RAPD analysis. The voucher specimens are deposited in Herbarium of Shahid Beheshti University (HSBU).

Morphometry

In total 40 morphological characters were used for morphometry, including quantitative and qualitative characters taken from published materials on *Silene* (Oxelman 1996), species description given in Flora Iranica (Melzheimer 1980) and personal observations in the field. Quantitative morphological characters were randomly measured in at least 5 plants and the means were used in phenetic analyses. Qualitative characters were coded as binary or multistate characters accordingly.

In phenetic analyses, different clustering method including UPGMA (Unweighted Paired Group using Arithmetic Average) and Neighbor Joining (NJ) clustering as well as ordination plots based on Principal Components Analysis (PCA) and Principal Coordinate Analysis (PCO) were used for grouping of the species studied. Cophenetic correlation and bootstrapping was performed to check the fit of dendrograms obtained (Podani 2000). Factor analysis was used to identify the most variable morphological characters among the species. For clustering, morphological data were standardized (Mean = 0, variance = 1) and used to determine Taxonomic and Euclidean distances (Podani 2000). Similarly unrooted parsimony and Bayesian clustering was performed on morphological data and the results were compared with those of phenetic analyses.

RAPD analysis

Forty decamer RAPD primers of Operon technology (Alameda, Canada) belonging to OPA, OPH sets were used in molecular study of the wild *Silene*. DNA extraction was done by using the CTAB method (Murry and Tompson 1980) with modification described by De la Rosa et al. (2002). The PCR reaction mixture consisted of 1 ng template DNA, 1 x PCR buffer (10 mM Tris-HCL pH 8.8, 250 mM KCL), 200 µM dNTPs, 0.80 µM 10-base random primers and 1 unit of Taq polymerase, in a total volume of 25 µl. DNA amplification was performed on a palm cycler GP-001 (Corbet, Australia). Template DNA was initially denatured at 92°C for 3 min, followed by 35 cycles of PCR amplification under the following parameters: denaturation for 1 min at 92°C, primer annealing for 1 min at 36°C and primer extension for 2 min at 72°C. A final incubation for 10 min at 72°C was performed to ensure that the primer extension reaction proceeded to completion. The PCR amplified products were separated by electrophoresis on a 2% agarose gels using 0.5 X TBE buffer (44.5 Mm Tris/Borate, 0.5 Mm EDTA, pH 8.0) or 6% polyacrylamide gels. The gels were stained with ethidium bromide and visualized under UV light (Sambrook et al. 2001). A 100 bp DNA ladder (GeneRuler, Fermentas) was used as the molecular standard in order to confirm the appropriate RAPD markers. RAPD markers were named by primer origin, followed with the primer number and the size of amplified products in base pairs.

The reproducible RAPD bands were treated as binary characters and coded accordingly (presence =1, absence = 0). Jaccard similarity as well as Nei's genetic distance (Nei 1972) were determined among the species studied and used for clustering and ordination based on principal coordinate analysis (PCO; Podani 2000). The fit of dendrograms obtained were checked by cophenetic correlation.

Bayesian clustering using Markova chain Monte Carlo (MCMC) was performed on RAPD data and the results were compared with NJ and UPGMA dendrograms. Bootstrapping was performed by using 10000 replications. NTSYS Ver. 2.02 (1998) was used for clustering and PCO analyses and Bayes-

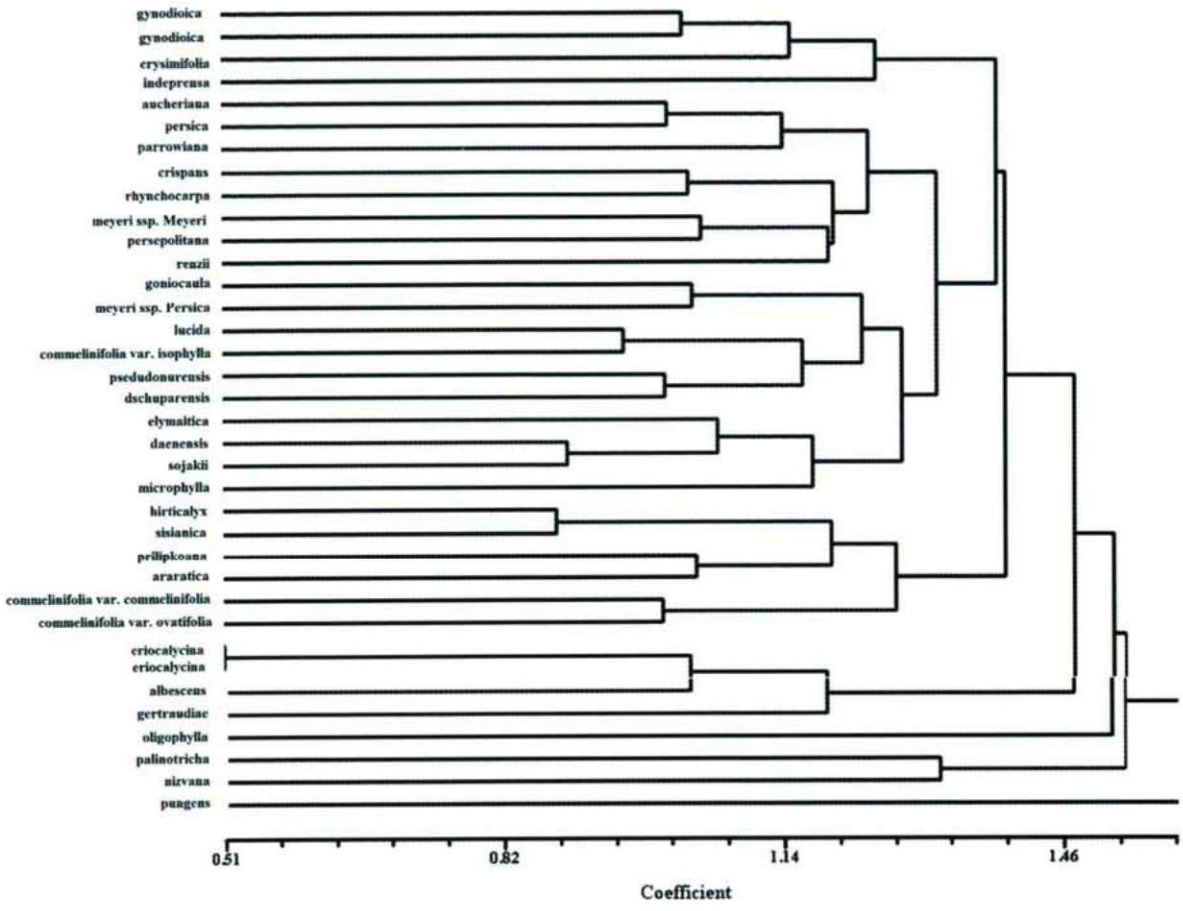

Figure 1. UPGMA dendrogram based on morphological characters.

ian clustering was done by Mr. Bayes ver. 3.1 (2005). The trees were obtained by Treeview ver. 1.6. 6 (2001).

Results and Discussion

Morphometry

UPGMA and NJ analyses of morphological data produced similar results and due to higher cophenetic correlation value of UPGMA dendrogram (r = 80) it is discussed bellow (Fig. 1). Two species of *S. pungens* and *S. parrowiana* were out-group taxa used in the analysis, out of which *S. pungens* is separated from the other species but *S. parrowiana* is placed with in-group species studied.

In general 5 major clusters are formed. The first major cluster is comprised of *S. indeprensa*, *S. erysimifolia* and *S. gynodioica*. These species share several morphological characteristics like cespitose-sufferutescent growth form, galandular indumentums, glandular calyx indumentums, absence of calyx inside indumentums, length of coronal scales longer than 1 mm, length of petal limb division longer than ½ limb, point of epipetal filament insertion shorter than 2 mm, capsule situation to calyx included in calyx, lack of testa cell projections and dentate testa cell margin. In Flora Iranica (Melzheimer 1988) these species are placed far from each other which is not supported by morphometric analysis.

The second major cluster is comprised of 2 sub-clusters. Three species of *S. aucheriana*, *S. pseudoaucheriana* and *S. persica* of the first sub-cluster grow in Alpine meadows habitat and share morphological characteristics of cauline leaf length shorter than 25 mm, lateral pedicel length shorter than 1 mm, clavate-cylindric calyx form, reticulate calyx veins, pink-rosea petal color, large conspicuous auricle size, length of alternate filament larger than Epipetal filament, elongate-ovate capsule form, capsule included in calyx, length of antophore 5-10 mm, antophore pubescent in the lower part. These species have been considered close to each other in Flora Iranica too.

The species of *S. crispans*, *S. rynocharpa*, *S. meyeri*, *S. renzi* and *S. persepolitana* also from the same sub-cluster, share morphological characteristics of cauline leaf width shorter than 2.5 mm, elongate-ovate capsule, capsule included in calyx, dentate testa cell margin. In Flora Iranica 3 species

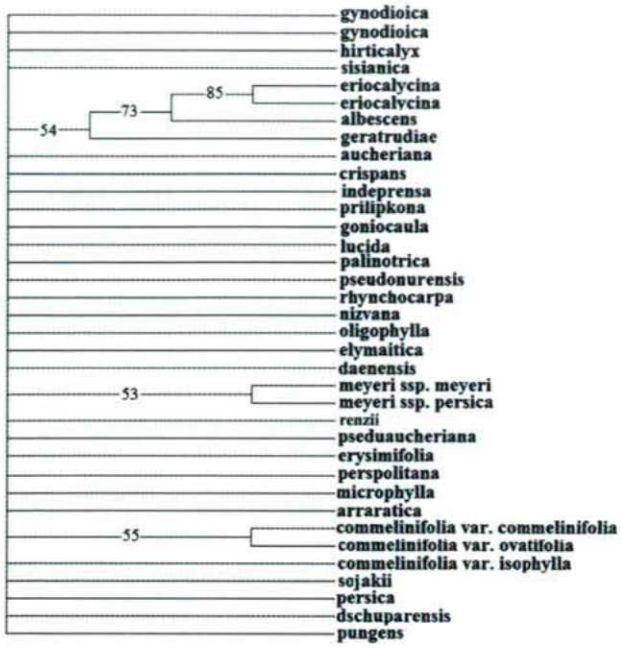

Figure 2. Parsimony tree based on morphological characters. (values at the base of clades are bootstrap values).

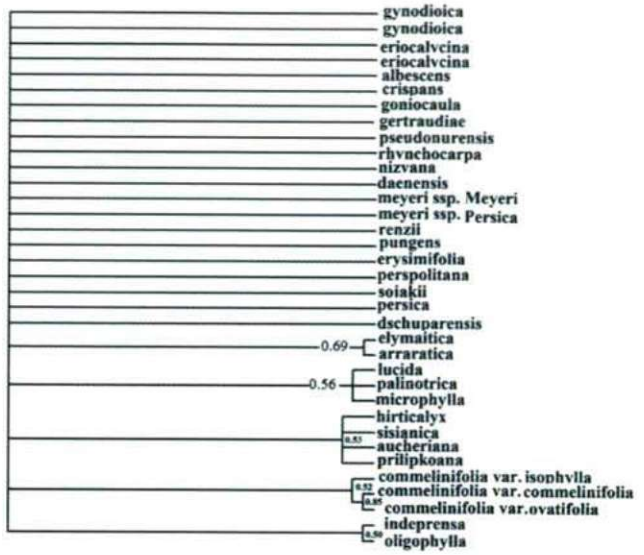

Figure 3. Bayesian tree based on morphological characters. (values at the base of clades are clade credibility values).

of *S. meyeri ssp. meyeri*, *S. renzi* and *S. persepolitana* are placed close to each other.

The species of *S. goniocaula*, *S. meyeri* ssp. *Persica*, *S. lucida*, *S. commelinifolia* var. *isophylla*, *S. dschuparensis* and *S. pseudonurensis* from the second sub-cluster share similar morphological characteristics of linear-lanceolate basal leaf form, basal leaf width shorter than 2.5 mm, strigose/lanate calyx indumentums, calyx length 21-32mm, petal limb length shorter than 5 mm, point of epipetal filament insertion shorter than 2 mm, lack of testa cell projections. In Flora Iranica two species of *S. goniocaula* and *S. lucida* have been considered close to each other but other species of this sub-cluster have been placed far from each other.

The species of *S. elymaitica*, *S. daenesis*, *S. sojakii* and *S. microphylla* also from the same sub-cluster share morphological characteristics like cauline leaf length shorter than 25 mm, clavate-cylindric calyx form, pink-rosea petal color, large conspicuous auricle, point of epipetal filament insertion shorter than 2 mm, capsule length longer than 10 mm, capsule included in calyx and dentate testa cell margin. In Flora Iranica two species of *S. elymaitica* and *S. daenesis* are placed close to each other.

The third major cluster is comprised of *S. hirticalyx*, *S. sisanica*, *S. prilipkoana*, *S. araratica*, *S. commelinifolia* var. *commelinifolia* and *S. commelinifolia* var. *ovatifolia* form the third major cluster and share morphological characters like reticulate calyx veins, large conspicuous auricle, claw placed in calyx. In Flora Iranica *S. hirticalyx*, *S. sisanica* and *S. prilipkoana* have been placed close to each other while the other species members of this cluster have been placed far from them. *S. araratica* has also been considered close to varieties of *S. commelinifolia*.

The fourth major cluster is formed by *S. eriocalycina*, *S. albescens* and *S. gertardiae* with the first two species showing more similarity. These species share similar morphological characteristics of cauline leaf length 25-35 mm, compound dichasium inflorescence, alar pedicel length 2-5 mm, lateral pedicel length shorter than 1 mm, clavate-cylindric calyx, internal side of calyx with no indumentums, calyx tooth length shorter than 2.5 mm, large conspicuous auricle, lack of style indumentums, petal claw length shorter than 10 mm, length of petal limb division longer than 1/2 limb, claw placed in calyx, elongate-ovate capsule, capsule length 7-10 mm, antophore with pubescent in the lower part and dentate testa cell margin. In Flora Iranica *S. eriocalycina* and *S. albescens* have been placed close to each other while *S. gertraudiae* is placed far from them.

The species of *S. oligophylla*, *S. palinotricha* and *S. nizvana* are placed far from the other species studied forming the fifth major cluster. These species also differ from each other in morphological characteristics as they join each other with great distance. Two species of *S. oligophylla* and *S. nizvans* have also been placed close to each other in Flora Iranica.

Factor analysis revealed that the first 7 components comprise about 60% of total variance in which, morphological characters like plant height, basal leaf form, basal leaf width, length/width ratio, cauline leaf width, calyx length, calyx tooth length, petal claw length and capsule form showed the highest positive/ negative correlation (>0.60/ <-0.60) and may

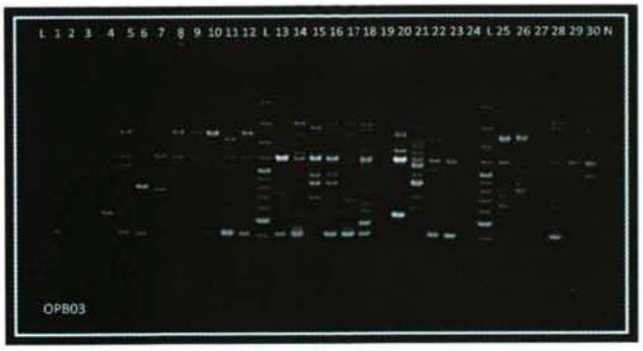

Figure 4. RAPD profile of primer OP8-03. Species No. are: 1- *commelinifolia* var. *ovatifolia*, 2- *S. commelinifolia* var. *commelinifolia*, 3- *S. commalinifolia* var. *isophylla*, 4- *S. lucida*, 5- *S. goniocaula*, 6- *S. gynodioica*, 7- *S. albescens*, 8- *S. daenensis*, 9- *S. dschuparensis*, 10- *S. hirticalyx*, 11- *S. eriocalycina*, 12- *S. erysimifolia*, 13- *S. meyeri* ssp. *Meyeri*, 14- *S. persica*, 15- *S. microphylla*, 16- *S. prilipkoana*, 17- *S. sojakii*, 18- *S. sisianica*, 19- *S. palinotricha*, 20- *S. gertraudiae*, 21- *S. nizvana*, 22- *S. rhynchocarpa*, 23- *S. oligophylla*, 24- *S. aucheriana*, 25- *S. pseudonurensis*, 26- *S. elymaitica*, 27- *S. persepolitana*, 28- *S. pungens*, 29- *S. meyeri* ssp. *Persica*, 30- *S. parrowiana*. L = Molecular ladder.

Figure 5. RAPD profile of primer OPB-12. Species No. as in Fig. 4.

be considered as the most variable morphological characters among the species studied.

Parsimony analysis

Cladogram obtained by major parsimony analysis after bootstrapping and using majority rule consensus tree is presented in Figure 2. In general the clades obtained are not well supported by bootstrapping and only one clade containing two species of *S. eriocalycina* and *S. albescens* show >70% bootstrap value and other clades formed, show <60% bootstrap values. The length of tree obtained is 608, with consistency index (CI) = 0.1102, homoplasy index (HI) = 0.8898 and retention index (RI) = 0.0339, indicating the presence of high homoplasy in morphological characters used in taxonomy of *Silene* as also revealed by other studies on other sections of this genus (Oxelman and Lidén 1995; Oxelman 1996; Oxelman and Berglund 1997; Oxelman et al. 2000).

Three distinct clades are present in this cladogram which agrees with our phenetic dendrogram discussed earlier. Three species *S. eriocalycina*, *S. albescens* and *S. gertraudiae* are placed in one clade, *S. meyeri* ssp. *meyeri*, *S. meyeri* ssp. *persica* and S. renzi show close affinity and form a separate clade and two varieties of *S. commelinifolia* var. *commelinifolia* and *S. commelinifolia* var. *ovatifolia* are placed close to each other. The other species studied show polytomy and are not differentiated in separate clades.

Bayesian analysis

In Bayesian tree (Fig. 3) also only 5 clades are recognized with 0.50-0.85 posterior probability (clade credibility). In the first clade *S. indeprensa* and *S. oligophylla* are placed together which does not agree with UPGMA and parsimony results. Three varieties of *S. commelinifolia* form a separate clade in agreement with parsimony analysis, four species of *S. hirticalyx*, *S. sisanica*, *S. aucheriana* and *S. prilipkoana* comprise a separate clade which partly agrees with UPGMA and parsimony results. Two species of *S. araratica* and *S. elymaitica* show close affinity and form another clade which is not supported by UPGMA and parsimony results.

Therefore it seems that in general morphological studies in *Silene* by different phenetic, cladistic and Bayesian approaches differ from each other and will not lead us to a clear cut grouping unable to show the species interrelationship in the sect. *Auriculatae*. Morphological characters used in the present study are taken from descriptions of *Silene* species provided in Flora Iranica (Melzheimer 1988) and previous taxonomy work on *Silene* (Oxelman 1996). Stevens (1991) states that morphological studies in a genus or among sections usually confront difficulties as clear cut qualitative characteristics separating closely related species are hard to find. Similarly Oxelman (1996) while studying morphological and molecular characteristics of *Silene* species from the sect. *Sedoides* revealed that morphological characters show high level of homoplasy and are not able to differentiate the species studied; however RAPD and ITS molecular characteristics were useful.

RAPD analysis

Out of 40 RAPD primers used 15 primer produced reproducible polymorphic bands (Table 2., Figs. 4 & 5). In total 347 bands were produced out of which 340 bands were polymorph and 7 bands were monomorph. Among primers used OPB12 produced the highest number of bands (28), while primers OPI12 produced the lowest number of bands (17). In total 11 unique bands were produced with the highest number of unique bands (3) produced by primer OPB05 while some of the primers like OPB12 and OPB20 produced no unique band at all.

Among the species studied *S. goniocaula* showed the highest number of RAPD bands (184), while *S. commelini-*

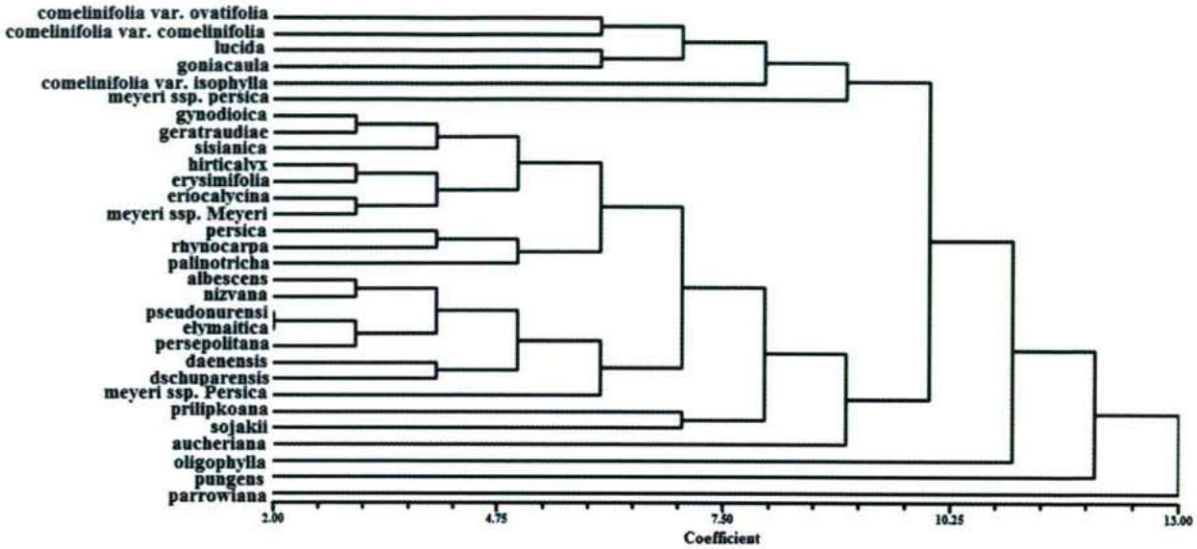

Figure 6. NJ dendrogram based on RAPD data.

folia var. *isophylla* showed the lowest number (123). Some of the species studied showed the presence of specific bands, for example band no. 14 (400 bp), of the primer OPB-03 was specific for *S. nizvana*, bands No. 2 and 17 (2700 & 470 bp respectively) of the primer OPB-05 was specific for *S. parrowiana* (one of the out-group species used), band No. 18 (450 bp) of the primer OPB-05 was specific for *S. persepolitana*, band No. 2 (2700 bp) of the primer OPC-01 was specific for *S. prilipkoana*, band No. 10 (930 bp) of the primer OPC-03 was specific for *S. pungens* and bands No. 15 and 19 (650 & 450 bp respectively) of the primer OPI-05 were specific for *S. meyei* ssp. *meyeri*.

NJ and Bayesian dendrograms of RAPD data are presented in Figures 6 & 7. In NJ tree, the out-group species i.e. *S. pungens* is almost placed far from the other species while in Bayesian tree it is not so. In both analyses all three varieties of *S. commelinifolia* var. *commelinifolia*, *S. commalinifolia* var. *isophylla*, *S. commelinifolia* var. *ovatifolia*, are placed close to

Table 2. RAPD primers producing bands, their sequences and bands produced.

Primer	Sequence	No. bands produced	Polymorphic bands	Monomorphic bands	Specific bands
OPB03	5′ CATCCCCCTG 3′	28	27	1	1
OPB05	5′ TGCGCCCTTC 3′	23	20	3	3
OPB07	5′ GGTGACGCAG 3′	21	21	0	1
OPB12	5′ CCTTGACGCA 3′	31	30	1	0
OPB20	5′ GGACCCTTAC 3′	28	27	1	0
OPC01	5′ TTCGAGCCAG 3′	25	25	0	1
OPC02	5′ GTGAGGCGTC 3′	18	18	0	0
OPC03	5′ GGGGGTCTTT 3′	25	25	0	0
OPC04	5′ CCGCATCTAC 3′	25	25	0	2
OPC06	5′ GAACGGACTC 3′	24	24	0	0
OPC09	5′ CTCACCGTCC 3′	20	20	0	0
OPC10	5′ TGTCTGGGTG 3′	18	18	0	0
OPI05	5′ TGTTCCACGG 3′	24	24	0	2
OPI12	5′ AGAGGGCACA 3′	17	16	01	1
OPI16	5′ TCTCCGCCCT 3′	20	20	0	0
Σ		347	340	7	11

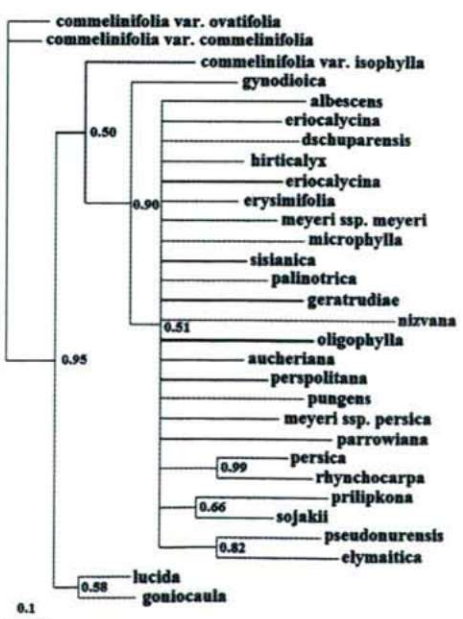

Figure 7. Bayesian dendrogram based on RAPD data.

each other along with *S. lucida* and *S. goniocaula* forming a separate cluster. However, two varieties of *S. commelinifolia* var. *commelinifolia* and var. *ovatifolia* show more affinity together and two species of *S. lucida* and *S. goniocaula* also show close relationship. Similarly both trees show close affinity of *S. pseudonurensis* and *S. elymaitica*, *S. prilipkoana* and *S. sojakii*, *S. rhynchocarpa* and *S. persica*. Both trees also show some affinity between *S. hirticalyx*, *S. erysimifolia*, *S. eriocalycina* and *S. meyeri* ssp. *meyeri* along with *S. gynodioica*, *S. gertraudiae* and *S. sisianica*.

Compairing RAPD tree with UPGMA tree of morphological data shows affinity between *S. lucida* and *S. goniocaula*, between *pseudonurensis* and *S. elymaitica*, between *S. prilipkoana* and *S. sojakii*, between *S. rhynchocarpa* and *S. persica*, and between *S. hirticalyx* and *S. sisianica*. Therefore it seems that both morphological and RAPD analyses are of limited application in showing *Silene* species relationships and further studies using other molecular markers may be performed.

References

Badr A, Muller K, Schafer-Pregl R, Rabey H, Effgen S, Ibrahim HH, Pozzi C, Rohde W, Salamini F (2000) On the origin and domestication history of barley (*Hordeum vulgare*). Mol Biol Evol 17:499-510.

Bari EA (1973) Cytological studies in the genus *Silene* L. New Phytol 72:833-838.

Bogani P, Cavalieri D, Petruccelli R, Roselli G (1994) Identification of olive tree cultivars by using Random Amplified Polymorphic DNA. Acta Hort 356:98-101.

Burleigh JG, Holtsford TP (2003) Molecular systematics of the eastern North American *Silene* (Caryophylaceae): Evidence from nuclear ITS and chloroplast *trn*L intron sequences. Rhodora 105:76-90.

Çelebi A, Tekşen M, Açİk L, Aytaç Z (2008) Taxonomic relationships in the *Fritillaria* (Liliaceae): Evidence from RAPD-PCR and SDS-PAGE of seed proteins. Acta Bot Hung 50:325-343.

Chowdhuri PK (1957) Studies in the genus *Silene*. Notes from the Royal Bot Garden Edinb 22:221-278.

De La Rosa R, James C, Tobutt KR (2002) Isolation and characterization of polymorphic microsatellite in olive (*Olea europaea* L.) and their transferability to other genera in the *Oleaceae*. Mol Ecol Notes 2: 265-267.

Gholipour A, Sheidai M (2010) Karyotype analysis and new chromosome number reports in *Silene* L. species (Sect. *Auriculatae*, Caryophyllaceae).Biologia 65(1):23-27.

Greuter W (1995) *Silene* (Caryophylaceae) in Greece: A subgeneric and sectional classification. Taxon 44:543-581.

Heaslip MB (1951) Some cytological aspects in the evolution of certain species of the plant genus *Silene*. Ohio J Sci 51:62-70.

Markova M, Martina L, Zluvova J, Janousek B, Vyskot B (2006) Karyological analysis of an interspecific hybrid between the diocious *Silene latifolia* and the hermaphroditic *Silene viscose*. Genome 42:373-379.

Melzheimer V (1978) Notes on cytology of several species of the genus *Silene* (Caryophyllaceae) from central Greece and from Crete. Plant Syst Evol 130:203-207.

Melzheimer V (1988) Caryophyllaceae In Flora Iranica, Rechinger KH ed., No.163. pp. 353-508. Akademische Druck-U. Verlagsanstalt, Graz, Austria.

Murry MG, Tompson WF (1980) Rapid isolation of high molecular weight plant DNA. Nucleic Acid Res 8:4321-4325.

Nei M (1972) Genetic distance between populations. Amer Naturalist 106:283-292.

Oxelman B (1996) RAPD patterns, nrDNA ITS sequences and morphological patterns in *Silene* section *Sedoideae* (*Caryophyllaceae*). Plant Syst Evol 201:93-116.

Oxelman B, Liden M, Berglund D (1997) Chloroplast *rps*16 intron phylogeny of the tribe Sileneae (Caryophyllaceae). Plant Syst Evol 206:411-420.

Oxelman B, Lidén M (1995) Generic boundaries in the tribe Sileneae (Caryophyllaceae) as inferred from nuclear rDNA sequences. Taxon 44:525-542.

Oxelman B, Lidén M, Rabeler RK, Popp M (2000) A revised generic classification of the tribe Sileneae (Caryophylaceae). Nord J Bot 20:743-748.

Podani J (2000) Introduction to the Exploration of Multivariate Data. English translation. Backhuyes Publishers, Leide, pp. 407.

Popp M, Oxelman B (2007) Origin and evolution of North American polyploidy *Silene* (Caryophyllaceae). Amer J Bot 94:330-349.

Sambrook J, Fritsch EJ, Maniatis T (2001) Molecular cloning: A laboratory manual.- Cold Spring Harbor Laboratory Press, Cold Spring Harbor-New York.

Saitou K, Fukuda T, Yokoyama J, Maki M (2007) Morphological and molecular (RAPD) analyses confirm the hybrid origin of the diploid grass *Calamagrostis longiseta* var. longe-aristata (Gramineae). Folia Geobot 42:63-76.

Sanz-Cortés F, Badenes ML, Paz S, Iniquez A, Llacer G (2001) Molecular characterization of olive cultivars using RAPD markers.- J. Amer Soci Hort Sci 126:7-12.

Sheidai M, Nikoo M, Gholipour A (2008) Cytogenetic variability and new chromosome number reports in *Silene* L. species (Sect. *Lasiostemones*, Caryophylaceae). Acta Biol Szeged 52:313-319.

Swank GR (1932) The Ethnobotany of the Acoma and Laguna Indians. MA Thesis, University of New Mexico.

Volume 54(1):33-36, 2010
Acta Biologica Szegediensis
http://www.sci.u-szeged.hu/ABS

ARTICLE

Effect of different statins on the antifungal activity of polyene antimycotics

Ildikó Nyilasi[1]*, Sándor Kocsubé[1], László Galgóczy[1], Tamás Papp[1], Miklós Pesti[2], Csaba Vágvölgyi[1]

[1]Department of Microbiology, Faculty of Science and Informatics, University of Szeged, Szeged, Hungary, [2]Department of General and Environmental Microbiology, Faculty of Sciences, University of Pécs, Hungary

ABSTRACT The antifungal activities of amphotericin B/statin and nystatin/statin combinations against some opportunistic pathogenic fungi (*Candida albicans, Candida glabrata, Paecilomyces variotii, Aspergillus fumigatus, Aspergillus flavus* and *Rhizopus oryzae*) were investigated. The *in vitro* interactions between polyene antifungal drugs and different statins were evaluated using a standard chequerboard broth microdilution method. Most of the detected interactions were additive, though in some cases synergism was also observed. In most cases, the extents of inhibition were higher when these compounds were applied together, and as a result the concentrations of amphotericin B and a given statin, needed to prevent fungal growth, generally could be decreased by some dilution steps. **Acta Biol Szeged 54(1):33-36 (2010)**

KEY WORDS

amphotericin B
drug interaction
microscopic fungi
nystatin
statins

The number of opportunistic fungal infections is continuously increasing which creates a substantial challenge for establishing new and more efficient antifungal therapies (Singh 2001; Groll 2009). One approach could be the application of combination therapy: co-administration of different antifungal compounds might improve the efficacy of the treatment. Reduced toxicity (due to the lower effective concentration of antifungal drugs) is also an important advantage (Baddley and Pappas 2005; Nosanchuk 2006; Vazquez 2007). More and more studies have focused on the antifungal activities of non-antifungal drugs, and on the development of antifungal combination therapies based on non-antifungal compounds (Afeltra and Verweij 2003).

Nystatin (NYS) and amphotericin B (AMB) belongs to the polyene antifungals: among them AMB and its lipid complexes (Tiphine et al. 1999; Moen et al. 2009) are one of the most efficient antimycotic agents. However, AMB is quite toxic and may have serious side effects (Gallagher et al. 2003). Combined application of AMB with other effective antifungal agents would be advantageous as a basis of a less toxic therapy. Therefore, there is a substantial interest for drugs, which can act additively or synergistically with AMB, and allow decreasing its therapeutic concentration.

Statins act by inhibiting 3-hydroxy-3-methylglutaryl-coenzyme A (HMG-CoA) reductase in the sterol biosynthesis pathway; therefore, they are used in human therapy to reduce the level of cholesterol in the blood. These compounds also have certain other (pleiotropic) effects, e.g. decreasing inflammation and improving the endothelial function (Liao and Laufs 2005). Recent reports described their inhibitory effect on the growth of different pathogenic fungi (Roze and Linz 1998; Lukács et al. 2004; Macreadie et al. 2006). Sun and Singh (2009) in their publication reported that statins directly attenuate the virulence of microorganisms: modulate regulatory pathways involved in the infection process. There are also sporadic new reports on the combined application of statins and different antimycotics (Lorenz and Parks 1990; Chin et al. 1997; Nash et al. 2002; Chamilos et al. 2006; Natesan et al. 2008; Nyilasi et al. 2010).

The aim of the present work was to investigate the *in vitro* antifungal activities of the most widely used polyene antimycotics (NYS and AMB), in combination with the most important, commercially available statins – lovastatin (LOV), pravastatin (PRA), simvastatin (SIM), fluvastatin (FLV), atorvastatin (ATO) and rosuvastatin (ROS) – against some opportunistic pathogenic yeast and filamentous fungi.

Materials and Methods

Fungal strains

The following fungal strains were used in this study: *Candida albicans* (*C. albicans*, American Type Culture Collection, USA; ATCC 90028), *Candida glabrata* (*C. glabrata*, Centraalbureau voor Schimmelcultures, Baarn, The Netherlands; CBS 138), *Aspergillus fumigatus* (*A. fumigatus*, Szeged Microbial Collection, Szeged, Hungary SZMC 2486), *Aspergillus flavus* (*A. flavus*, SZMC 2521), *Rhizopus oryzae* (*R. oryzae*, CBS 109939) and *Paecilomyces variotii* (*P. variotii*, ATCC 36257). All these strains were maintained on potato dextrose agar (PDA, Sigma-Aldrich, 0.4% potato starch, 2% glucose, 1.5% agar) slants at 4°C.

Accepted May 11, 2010
*Corresponding author. E-mail: nyilasiildi@gmail.com

Table 1. Examples of effective AMB/statin combinations.

Isolate / Combination [MIC alone (μg/ml)][a]	MIC (μg/ml) of AMB and MIC (μg/ml) of the different statins in combination [effect, IR][b]
C. albicans ATCC 90028	
AMB-ATO [1, 128]	0.5/0.391 [A, 1.13]
C. glabrata CBS 138	
AMB-ROS [1, 128]	0.5/0.391 [A, 1,02]
AMB-ATO [1, 32]	0.5/0.391 [A, 0.88]
P. variotii ATCC 36257	
AMB-SIM [0.125, 8]	0.031/1.563 [A, 0.77]
AMB-ATO [0.125, 32]	0.063/0.391 [A, 0.81]
A. fumigatus SZMC 2486	
AMB-FLV [4, 2]	2/1.563 [A, 0.57]
AMB-ATO [4, 64]	2/0.391 [A, 1.15]
A. flavus SZMC 2521	
AMB-FLV [8-16, 128]	4/12.5 [S, 1.62], 1/25 [A, 1.13]
R. oryzae CBS 109939	
AMB-SIM [2-4, 64]	0.25/25 [A, 0.79]
AMB-FLV [2-4, 2-3.125]	1/1.563 [A, 0.65]
AMB-ROS [2-4, >128]	2/25 [A, 0.91]
AMB-ATO [2-4, 32]	1/6.25 [A, 0.74], 0.5/12.5 [A, 1.20]

[a] In brackets, MICs of AMB and the given statin are presented, respectively. MICs for statins were determined earlier by Nyilasi et al. (2010).
[b] Effective drug combinations are presented as the lowest concentrations of the combined drugs that caused total growth inhibition together; the first number indicates the concentration of AMB, and the second is the concentration of the given statin. In brackets, the type of the interaction (A, additive; S, synergistic) and IR values are presented, respectively.

Antifungal drugs

AMB (Sigma-Aldrich) was purchased as a stock solution (250 μg/ml in deionised water). NYS (Sigma-Aldrich) was provided by the manufacturer as standard powder and dissolved in dimethyl sulfoxide at a concentration of 16 mg/ml. The statins used in this study were FLV (Lescol, Novartis), LOV (Mevacor, Merck Sharp & Dohme), SIM (Vasilip, Egis), ROS (Crestor, AstraZeneca) and ATO (Atorvox, Richter), which were of pharmaceutical grade and PRA (Sigma-Aldrich), which was provided as standard powder. Statins stocks (12.8 mg/ml) were prepared in methanol (except PRA, which was dissolved in distilled water). Stock solutions were stored at -70°C until needed. For drug tests, dilutions were performed in RPMI 1640 medium (Sigma-Aldrich) containing L-glutamine, but lacking sodium bicarbonate, buffered to pH 7.0 with 0.165 M 3-(N-morpholino)propanesulfonic acid (Sigma-Aldrich). LOV and SIM were activated freshly from their lactone pro-drug forms by hydrolysis in ethanolic NaOH [15% (v/v) ethanol, 0.25% (w/v) NaOH] at 60°C for 1 h as described by Lorenz and Parks (1990).

In vitro antifungal susceptibility testing

The antifungal activities of NYS, AMB and statins were determined using a broth microdilution method according to the CLSI guidelines (NCCLS 1997; NCCLS 2002). Assays were performed as described earlier (Galgóczy et al. 2009a; Nyilasi et al. 2010) in 96-well flat-bottomed microtitre plates by measuring the optical density of the fungal cultures at 620 nm after incubation for 48 h at 35°C. Final inocula (prepared in RPMI 1640) were 5×10^3 CFU/ml and 5×10^4 spores/ml, for yeasts and for filamentous fungi, respectively. In the wells, the final concentrations for each statin ranged from 0.25 to 128 μg/ml, and for AMB and NYS ranged from 0.0313 to 16 μg/ml. For calculation of the extents of inhibition the OD_{620} readings of the drug-free control cultures were referred to 100% growth. MICs for statins were determined earlier by Nyilasi et al. (2010). MICs for AMB and NYS were the lowest concentration of drugs that produced an optically clear well. All experiments were repeated 3 times.

Statin/polyene interactions were tested by chequerboard broth microdilution method using twofold dilutions from each drug. Fifty μl of each drug dilutions for both drugs were placed in the wells, and were mixed with 100 μl of yeast or sporangiospore suspension. The final concentrations of AMB and NYS were the same as described previously, while those of the various statins ranged from 0.391 to 25 μg/ml. Condition for chequerboard broth microdilution (inoculum preparation, initial inoculum, controls and the conditions of the incubation) were the same as described by Nyilasi et al. (2010).

Data analysis

Interaction ratio between the investigated drugs was calculated using the Abbott formula: $I_e = X+Y-(XY/100)$: I_e is the expected percentage inhibition for a given interaction, X and Y are the percent inhibitions given by each compound when used alone. If I_o is the observed percentage inhibition, the interaction ratio (IR) is given by $IR = I_o/I_e$, which corresponds to the type of the interaction between the compounds. The interaction is additive when IR is between 0.5 and 1.5, when IR>1.5 denotes synergism and when IR<0.5 denotes antagonism (Gisi 1996).

Results and discussion

Sensitivity to statins and polyene antifungals

The MICs of the involved statins and polyene antifungals against the tested fungal isolates are listed in Table 1 and 2. AMB was very effective against all of the investigated isolates in the administered concentration range. The most sensitive species were *P. variotii* (MIC: 0.125 μg/ml), *C. albicans* (MIC: 1 μg/ml) and *C. glabrata* (MIC: 1 μg/ml). Filamentous fungi were also sensitive to AMB in the range of 2-16 μg/ml (Table 1). NYS was also effective against *Candida* isolates and *P. variotii* in the range of 1-2 μg/ml. *A. fumigatus* and *A. flavus* was moderately sensitive to NYS (MICs: 8 and 16 μg/ml, respectively), whilst *R. oryzae* was not sensitive at all to NYS in the administered concentration range (Table 2).

Antifungal potentials of the involved statins were reported in a previous study (Nyilasi et al. 2010). Among the statins, FLV and SIM exhibited potent antifungal activities and frequently showed higher activity than the other statins. The natural statins (SIM and LOV) were inactive in their pro-drug forms, but their active metabolites obtained by hydrolysis of the lactone ring manifested pronounced antifungal effects.

Interactions between AMB and statins

The *in vitro* interactions between AMB and the different statins were studied using a standard chequerboard broth microdilution method. The interaction ratios between the compounds were calculated using the Abbott formula. Table 1 and Table 2 show data of the effective drug combinations for the fungi tested, which indicates the combined drugs in the lowest concentrations causing total growth inhibition.

Positive drug interactions were observed for every investigated strain. The majority of these interactions were found in the case of *R. oryzae*: when AMB was combined with SIM, FLV, ROS or ATO additive effects were observed, so the concentrations of AMB and the given statin needed to block fungal growth completely could be decreased by some dilution steps. AMB-FLV and AMB-ATO combinations were effective in the case of most isolates, moreover, AMB and FLV acted synergistically in inhibiting the growth of *A. flavus*. AMB and FLV inhibited the growth of this fungus at relatively high concentrations, (MICs: 8-16 µg/ml and 128 µg/ml, respectively), but in combination 4 µg/ml AMB and 12.5 µg/ml FLV or 1 µg/ml AMB and 25 µg/ml FLV already inhibited the fungal growth (IRs: 1.62 and 1.13, respectively). In contrast, AMB-LOV, AMB-SIM and AMB-ATO combinations were antagonistic in the case of *A. flavus* . However, antagonistic interactions were not observed at other fungal strains.

Interactions between NYS and statins

The *in vitro* interactions between NYS and the different statins were also studied, Table 2 shows data of the effective drug combinations. NYS-LOV and NYS-FLV combinations were effective in the case of several isolates. PRA did not inhibit the fungal growth alone, but NYS-PRA combination was effective at *A. flavus*, so the concentrations needed to block fungal growth could be reached with lower concentrations in combination. However, NYS-LOV, NYS-SIM and NYS-FLV combinations were also antagonistic in the case of *A. flavus*, whilst antagonistic interactions were not observed at any other fungal strains.

NYS and ATO acted additively (near to the synergistic values) in inhibiting the growth of *R. oryzae*: NYS did not inhibit the growth of this fungus in the administered concentration range, but in combination 4 µg/ml NYS and 12.5 µg/ml ATO or 1 µg/ml NYS and 25 µg/ml ATO already inhibited the fungal growth (IRs: 1.43 and 1.47, respectively).

Table 2. Examples of effective NYS/statin combinations.

Isolate / Combination [MIC alone (µg/ml)][a]	MIC (µg/ml) of NYS and MIC (µg/ml) of the different statins in combination [effect, IR][b]
C. albicans ATCC 90028	
NYS-LOV [2, 64]	0.031/25 [A, 0.94]
NYS-SIM [2, 8]	0.031/6.25 [A, 0.96]
NYS-FLV [2, 25]	0.063/12.5 [A, 1.06]
C. glabrata CBS 138	
NYS-LOV [1, 128]	0.063/50 [A, 1.31]
NYS-ROS [1, 128]	1/12.5 [A, 0.91]
P. variotii ATCC 36257	
NYS-LOV [1, 64]	0.5/12.5 [A, 1.11]
NYS-SIM [1, 8]	0.5/0.391 [A, 0.56]
NYS-FLV [1, 25]	0.5/12.5 [A, 0.84]
A. flavus SZMC 2521	
NYS-PRA [16, >128]	4/1.563 [A, 1.27]
R. oryzae CBS 109939	
NYS-LOV [>16, 128]	8/50 [A, 1.23]
NYS-FLV [>16, 2-3.125]	16/1.563 [A, 1.08]
NYS-ATO [>16, 32]	4/12.5 [A, 1.43], 1/25 [A, 1.47]

[a] In brackets, MICs of NYS and the given statin are presented, respectively.
[b] Effective drug combinations are presented as the lowest concentrations of the combined drugs that caused total growth inhibition together; the first number indicates the concentration of NYS, and the second is the concentration of the given statin. In brackets, the type of the interaction (A, additive; S, synergistic) and IR values are presented, respectively.

In contrast to the co-administration of azoles and statins, polyene antifungal/statin combinations could be used without serious drug interactions (Herman 1999; Schachter 2004). Therefore, they are potential agents for the treatment of fungal infections (Galgóczy 2009b). Based on the accumulating data on these potential, Kontoyiannis (2007) hypothesized that the widespread use of statins has led to the decreasing number of reported cases of zygomycosis in patients with diabetes mellitus in developed countries since the 1990s, despite the increase in the prevalence of diabetes in those populations.

Acknowledgements

This investigation was financially supported by RET-08/2005 (OMFB-00846/2005) and NKTH IPARJOG-08-1-2009-0026.

References

Afeltra J, Verweij PE (2003) Antifungal activity of nonantifungal drugs. Eur J Clin Microbiol Infect Dis 22:397-407.

Baddley JW, Pappas PG (2005) Antifungal combination therapy: clinical potential. Drugs 65:1461-80.

Chamilos G, Lewis RE, Kontoyiannis DP (2006) Lovastatin has significant activity against Zygomycetes and interacts synergistically with voriconazole. Antimicrob Agents Chemother 50:96-103.

Chin NX, Weitzman I, Della-Latta P (1997) In vitro activity of fluvastatin, a cholesterol-lowering agent, and synergy with fluconazole and itraconazole against *Candida* species and *Cryptococcus neoformans*. Antimicrob Agents Chemother 41:850-852.

Galgóczy L, Ördögh L, Virágh M, Papp T, Vágvölgyi Cs (2009a) *In vitro* susceptibility of clinically important Zygomycetes to combinations of

amphotericin B and suramin. J Mycol Med 19:241-247.

Galgóczy L, Nyilasi I, Papp T, Vágvölgyi Cs (2009b) Are statins applicable for prevention and treatment of zygomycosis? Clin Infect Dis 49:483-484.

Gallagher CG, Ashley ESD, Drew RH, Perfect JR (2003) Antifungal pharmacotherapy for invasive mould infections. Expt Opin Pharmacother 4:147-64.

Gisi U (1996) Synergistic interaction of fungicides in mixtures. Phytopathology 86:1273-1279.

Groll AH (2009) Update on invasive opportunistic mycoses: Clinical trials review, 2008–2009. Curr Infect Dis Rep 11:417-419.

Herman RJ (1999) Drug interactions and the statins. CMAJ 161:1281-1286.

Kontoyiannis DP (2007) Decrease in the number of reported cases of zygomycosis among patients with diabetes mellitus: a hypothesis. Clin Infect Dis 44:1089-1090.

Liao JK, Laufs U (2005) Pleiotropic effects of statins. Annu Rev Pharmacol Toxicol 45:89-118.

Lorenz RT, Parks LW (1990) Effects of Lovastatin (Mevinolin) on sterol levels and on activity of azoles in *Saccharomyces cerevisiae*. Antimicrob Agents Chemother 34:1660-1665.

Lukács Gy, Papp T, Nyilasi I, Nagy E, Vágvölgyi Cs (2004) Differentiation of *Rhizomucor* species on the basis of their different sensitivities to lovastatin. J Clin Microbiol 42:5400-5402.

Macreadie IG, Johnson G, Schlosser T, Macreadie PI (2006) Growth inhibition of *Candida* species and *Aspergillus fumigatus* by statins. FEMS Microbiol Lett 262:9-13.

Moen MD, Lyseng-Williamson KA, Scott LJ (2009) Liposomal amphotericin B: a review of its use as empirical therapy in febrile neutropenia and in the treatment of invasive fungal infections. Drugs 69:361-392.

Nash JD, Burgess DS, Talbert RL (2002) Effect of fluvastatin and pravastatin, HMG-CoA reductase inhibitors, on fluconazole activity against *Candida albicans*. J Med Microbiol 51:105-109.

Natesan SK, Chandrasekar PH, Alangaden GJ, Manavathu EK (2008) Fluvastatin potentiates the activity of caspofungin against *Aspergillus fumigatus* in vitro. Diagn Microbiol Infect Dis 60:369-73.

NCCLS (1997) Reference method for broth dilution antifungal susceptibility testing of yeasts. Approved standard. NCCLS document M27-A, Villanova, Pa, National Committee for Clinical Laboratory Standards, Wayne, PA.

NCCLS (2002) Reference method for broth dilution antifungal susceptibility testing of filamentous fungi. Approved standard. NCCLS document M38-A, National Committee for Clinical Laboratory Standards, Wayne, PA.

Nosanchuk JD (2006) Current status and future of antifungal therapy for systemic mycoses. Recent Patents Anti-Infect. Drug Disc 1:75-84.

Nyilasi I, Kocsubé S, Pesti M, Lukács Gy, Papp T, Vágvölgyi Cs (2010) *In vitro* interactions between primycin and different statins in their effects against some clinically important fungi. J Med Microbiol 59:200-205.

Roze LV, Linz JE (1998) Lovastatin triggers an apoptosis-like cell death process in the fungus *Mucor racemosus*. Fungal Genet Biol 25:119-133.

Schachter M (2004) Chemical, pharmacokinetic and pharmacodynamic properties of statins: an update. Fundam Clin Pharmacol 19:117-125.

Singh N (2001) Trends in the epidemiology of opportunistic fungal infections: predisposing factors and the impact of antimicrobial use practices. Clin Infect Dis 33:1692-1696.

Sun H-Y, Singh N (2009) Antimicrobial and immunomodulatory attributes of statins: relevance in solid-organ transplant recipients. Clin Infect Dis 48:745–755.

Tiphine M, Letscer-Bru V, Herbrecht R (1999). Amphotericin B and its new formulations: pharmacologic characteristics, clinical efficacy, and tolerability. Transpl Infect Dis 1:273-283.

Vazquez JA (2007) Combination antifungal therapy: the new frontier. Future Microbiol 2:115-139.

Volume 54(1):37-43, 2010
Acta Biologica Szegediensis
http://www.sci.u-szeged.hu/ABS

ARTICLE

Contrastive response of *Phlomis tuberosa* to salinity and UV radiation stresses

Ghader Habibi[1], Roghieh Hajiboland[1,2]*, Gholamreza Dehghan[1]

[1]Plant Science Department, University of Tabriz, Tabriz, Iran, [2]Excellent Center of Biodiversity, University of Tabriz, Tabriz, Iran

ABSTRACT Growth, photosynthetic characteristics and antioxidant defense system were investigated under salinity stress and UV radiation in *Phlomis tuberosa* (Lamiaceae) grown under environmentally controlled conditions for two weeks. Salinity at 40 mM results in significant reduction of shoot growth up to 20%, while UV radiation at 10 kJ m^{-2} d^{-1} did not affect plants dry matter production. Salinity did not influnce PSII photochemistry, while UVA+B radiation caused a significant reduction of maximum quantum yield of PSII. The net photosynthesis rate was inhibited by both salinity and UV stress following reduced stomatal conductance. Leaf osmotic and water potential were decreased by salinity but not UV radiation. Activity of antioxidant enzymes increased under both salinity and UV radiation stress, however, membrane damage was occurred only under UV stress. Our data implied that, high salinity sensitivity in this species was mainly attributable to the salt-induced disturbance in water relations and reduced assimilation rate rather than to other factors such as damage to PSII, oxidative stress or membrane damage. However, PSII photoinhibition, membrane damage and significant reduction of net assimilation rate were not able to affect negatively plants performance under UV stress implying involvement of other factors in high UV stress tolerance in *Phlomis tuberosa*.

Acta Biol Szeged 54(1):37-43 (2010)

KEY WORDS

Antioxidant defense system
leaf photochemistry
gas exchange
water relations
salinity
UV stress

Plants, in their natural habitats, are often subjected to various stress conditions such as high light intensity, UV radiation, temperature extremes, drought and salinity. Native vegetations consist of most adapted plant species to their local environmental conditions. A wide spectrum of biochemical and metabolic adaptations are found in plants under these stress conditions.

Environmental stress conditions enhance generation of reactive oxygen species (ROS) and cause imbalance between production of ROS and quenching activity of the antioxidants, resulting in oxidative damage (Mano 2002). ROS causes lipid peroxidation, membrane destruction, protein denaturation and DNA damage (Creissen and Mullineaux 2002). Activity of antioxidant enzymes such as superoxide dismutase (SOD), catalase (CAT), ascorbate peroxidase (APX) and peroxidases (POD) as the most important components in scavenging and prevention of ROS damage are increased under stress conditions (Dat et al. 2000). Considering multiple roles that ROS play in plant metabolism, it is plausible that protective pathways in the plant are indeed shared, than separate pathways. Thus, tolerance mechanisms to several kinds of stress such as drought, salinity and UV radiation are interconnected and partially overlapping. Physiological studies found correlations between levels of antioxidants and the level of stress tolerance among plant species (Perl-Treves and Perl 2002).

The general response of plants to increasing salt concentration includes osmotic stress, specific ion toxicity and nutrient deficits that affect a range of physiological processes involved in cell metabolism (Ashraf and Harris 2004). An increase in salinity causes reduction of water and osmotic potential, leaf area and stomatal density (Parida and Das 2005). Similar with other abiotic stresses, salinity is known to negatively influence CO_2 assimilation via affecting both stomatal and non-stomatal components of photosynthesis (Kao et al. 2003). Moreover, a correlation exists between activity of antioxidant enzymes and salt tolerance of plants (Parida and Das 2005).

Elevated UV radiation at high altitudes in mountain areas causes distinct effects on plants growing at high elevations (Filella and Penuelas 1999). Deleterious effects of UV radiation on the growth, productivity and photosynthesis of higher plants have been extensively studied (Germ et al. 2005; Xu et al. 2008; Surabhi et al. 2009). Evidences suggest that ROS are involved in the damages caused by UV radiation. Like the antioxidant pools, the activity of several key enzymes involved in ROS metabolism such as CAT and APX is altered by UV radiation (Yannarelli et al. 2006). UV radiation impairs all major processes of photosynthesis including photochemical reactions and stomatal conductance (Allen et al. 1998).

Accepted May 20, 2010
*Corresponding author. E-mail: ehsan@tabrizu.ac.ir

However, UVB inhibits maximum net photosynthesis rate in a variety of plants without direct correlation with chlorophyll fluorescence or PSII activity, suggesting that photodamage to PSII is not the primary reason for reduced rates of net assimilation rate (Allen et al. 1998; Fedina et al. 2003).

The Mediterranean climate regions of the world occupy less than 5% of the Earth's surface, but harbor about 20% of the world total known vascular plant species (Cowling et al. 1996). The genus *Phlomis* L. comprises over 100 species including herbs, shrubs and sub-shrubs of the family Lamiaceae (Albaladejo et al. 2005) and is distributed mainly in the Mediterranean region of Anatolia (Turkey) and Iran (Azizian and Moore 1982). *P. tuberosa* is a summer perennial herb growing in an altitudinal gradient of increasing UV radiation of mountains in NW of Iran. Considering conditions of natural habitat, this species is expected to be adapted well with high UV radiation, however, is likely sensitive to salinity similar with other species from Lamiaceae.

The present work was aimed to study the effect of salinity and UV radiation stresses on growth, photosynthesis and antioxidant defense capacity of *P. tuberosa*. Involvement of stomatal and non-stomatal factors in the response of plants photosynthesis to salinity and UV radiation was studied. In addition, functional significance of antioxidant defense system in plants adaptation to UV radiation in comparison with that to salinity was investigated.

Materials and Methods

Plant materials and treatments

Seeds of *Phlomis tuberosa* were collected from Mishoudagh, near the city of Marand, 65 km south of Tabriz (45°38' E, 38°22' N) at an elevation of 1800 m, East-Azarbaijan Province (NW of Iran). Seeds were surface sterilized and germinated on filter paper moistened with distilled water and $CaSO_4$ at 0.05 mM. Ten-day-old seedlings were transferred to Hoagland nutrient solution (Johnson et al. 1957) and were pre-cultured for 45 days prior to the start of treatments. Thereafter, plants with uniform size were selected and subjected to either salinity or UV radiation treatments. Salinity treatment consisted of control, 20 mM and 40 mM NaCl. For UV radiation treatments, in addition to the photosynthetic active radiation (PAR, 400-700 nm) supplied by cool white fluorescent lamps throughout the day time, UVAB fluorescent lamps (30 W, Hagen, Japan) was used without filter for UVA+B, with transparent Plexiglass filter cutting wavelength under 320 nm for UVA and with yellow colored Plexiglass filter for cutting wavelength under 400 nm for control plants with 6 h irradiance periods centered midway through the photoperiod. The spectral outputs of the three lighting conditions were measured with a calibrated spectrophotometer (Shimadzu, UV-2450) and biologically effective UV doses employed were 10 kJ m^{-2} d^{-1} calculated based on Caldwell's generalized plant damage action spectrum normalized to 300 nm (Caldwell 1971).

Plants were grown in a growth chamber under environmentally controlled conditions at about 150 µmol m^{-2} s^{-1} light intensity, 18/6 h light/dark photoperiod, 25/17°C day/night temperature and relative humidity of 60/70%.

Harvest

Two weeks after treatment, plants were harvested. Leaf samples were washed with distilled water, blotted dry on filter paper and dried for 48 h at 70°C for determination of dry weight.

Determination of chlorophyll fluorescence and gas exchange parameters

Chlorophyll fluorescence parameters were recorded using a portable fluorometer (OSF1, ADC Bioscientific Ltd., UK) for both dark adapted and light adapted leaves. Measurements were carried out on the second youngest, fully expanded and attached leaf. An average of 4 records from different parts of each individual leaf was considered for each replicates. Leaves were acclimated to dark for 30 min using leaf clips before measurements were taken. Initial (F_0), maximum (F_m), variable ($F_v=F_m-F_0$) fluorescence as well as maximum quantum yield of PSII (F_v/F_m) and F_v/F_0 ratios were recorded. Light adapted leaves (400 µmol $m^{-2}s^{-1}$) were used for measurement of steady-state (F_s) and maximum (F'_m) fluorescence. Calculations were made for F'_0 ($F'_0=F_0/[(F_v/F_m)+(F_0/F'_m)]$), photochemical quenching, qP $[(F'_m- F_s)/(F'_m-F'_0)]$, non-photochemical quenching, qN $(1-[(F'_m-F'_0)/(F_m-F_0)])$ and effective quantum yield of PSII, Φ_{PSII} $[(F'_m-F_s)/F'_m]$ (Krall and Edwards 1992).

Leaf gas exchange parameters were determined in parallel with Chl fluorescence measurements in the same leaf with a calibrated portable gas exchange system (LCA-4, ADC Bioscientific Ltd., UK) between 10:00 A.M. and 13:00 P.M at harvest. The measurements were conducted with PPFD at the leaf surface of 350 µmol $m^{-2}s^{-1}$ measured by a quantum sensor attached to the leaf chamber of the gas exchange unit. The net photosynthesis rate by unit of leaf area (A, µmol CO_2 $m^{-2}s^{-1}$), transpiration rate (E, mmol H_2O $m^{-2}s^{-1}$) and stomatal conductance to water vapor (g_s, mol $m^{-2}s^{-1}$) were measured by the infrared gas analyzer of the portable photosynthesis system. Water use efficiency was calculated using the values of A and E ($WUE=A/E$, µmol $mmol^{-1}$).

Leaf water and osmotic potential

Leaf osmotic potential (ψ_s) and water potential (ψ_w) was determined in the second youngest leaf harvested at 1 h after light on in the growth chamber. Leaves were homogenized in pre-chilled mortar and pestle and centrifuged at 4000 g for 20 min at 4°C. The osmotic pressure of samples was measured

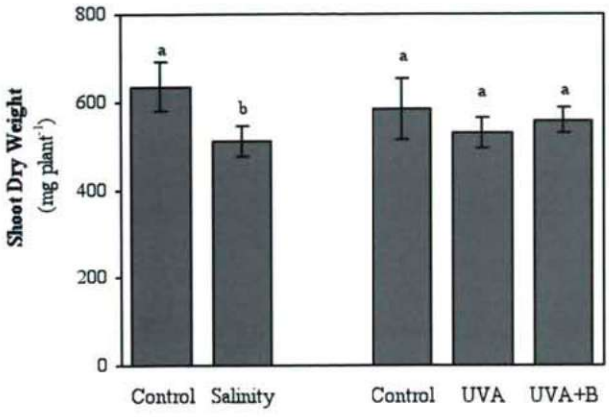

Figure 1. Shoot dry weight (mg plant-1) of Phlomis tuberosa grown for two weeks in nutrient solution with 40 mM NaCl salinity or under UV radiation at 10 kJ m-2 d-1. Values are the mean ± SD (n=4). Bars indicated by the same letters are not significantly different (P<0.05).

by an osmometer (Micro-Osmometer, Heman Roebling MESSTECHNIK, Germany), and the miliosmol data were recalculated to MPa. Water potential was measured using a pressure chamber (DTK-7000, Japan).

Assay of antioxidant enzymes and related metabolites

Determination of the activity of antioxidant enzymes and concentration of related metabolites were undertaken according to optimized protocols described elsewhere (Hajiboland and Hasani 2007). Fresh samples were ground in the presence of liquid nitrogen and measurements were undertaken using spectrophotometer (Specord 200, Analytical Jena, Germany). The activity of ascorbate peroxidase (APX, EC 1.11.1.11) was measured by determining ascorbic acid oxidation, one unit of APX oxidizes ascorbic acid at the rate of 1 μmol min^{-1} at 25°C. Catalase (CAT, EC 1.11.1.6) activity was assayed by monitoring the decrease in absorbance of H_2O_2 at 240 nm, unit activity was taken as the amount of enzyme, which decomposes 1 μmol of H_2O_2 min^{-1}. Peroxidase (POD, EC 1.11.1.7) activity was assayed using the guaiacol test, the enzyme unit was calculated as enzyme protein required for the formation of 1 μmol tetraguaiacol min^{-1}. Total superoxide dismutase (SOD, EC 1.15.1.1) activity was determined using monoformazan formation test. One unit of SOD was defined as the amount of enzyme required to induce a 50% inhibition of NBT reduction as measured at 560 nm, compared with control samples without enzyme aliquot. Lipid peroxidation was estimated from the amount of malondialdehyde (MDA) formed in a reaction mixture containing thiobarbituric acid (Sigma) at 532 nm. MDA levels were calculated from a 1,1,3,3-tetraethoxypropane (Sigma) standard curve. The concentration of H_2O_2 was determined using potassium titanium-oxalate at 508 nm. Proline was extracted with 3% sulfosalicylic acid, after centrifugation the supernatant was treated with acetic acid and acid ninhydrin, boiled for 1 h, and then absorbance at 520 nm was determined. Proline (Sigma) was used for production of standard curve. Soluble proteins were determined using a commercial Bradford reagent (Sigma) and BSA (Merck) as standard (Hajiboland and Hasani 2007).

Experiments were under taken in complete randomized block design with 4 replications. Statistical analyses were carried out using sigma stat (3.02) with Tukey test (P<0.05).

Table 1. Leaf photochemical parameters including photochemical efficiency of PSII (F_v/F_m), ratio of variable to initial fluorescence (F_v/F_0), photochemical quenching (q_P), non-photochemical quenching (q_N) and quantum yield of PSII (Φ_{PSII}) and gas exchange parameters including net photosynthetic rate (*A*, μmol m^{-2} s^{-1}), transpiration rate (*E*, mmol m^{-2} s^{-1}), stomatal conductance to water vapor (g_s, mol m^{-2} s^{-1}) and water use efficiency (*WUE*, μmol $mmol^{-1}$) in *Phlomis tuberosa* grown for two weeks in nutrient solution with 0, 20 and 40 mM NaCl salinity. Values are the mean ± SD (n=4). Data of each row indicated by the same letters are not significantly different (P<0.05).

	Treatment		
Photochemistry	Control	20 mM NaCl	40 mM NaCl
F_v/F_m	0.84 ± 0.01[a]	0.82 ± 0.02[a]	0.80 ± 0.04[a]
F_v/F_0	5.17 ± 0.07[a]	4.61 ± 0.67[a]	4.17 ± 1.00[a]
qP	0.898 ± 0.004[a]	0.936 ± 0.027[a]	0.962 ± 0.057[a]
qN	0.080 ± 0.019[a]	0.146 ± 0.077[a]	0.160 ± 0.087[a]
Φ_{PSII}	0.746 ± 0.004[a]	0.748 ± 0.010[a]	0.748 ± 0.015[a]
Gas exchange			
A	4.74 ± 0.72[a]	4.60 ± 0.26[a]	2.97 ± 0.51[b]
E	0.90 ± 0.44[a]	0.73 ± 0.20[a]	0.54 ± 0.03[a]
g_s	1.33 ± 0.898[a]	0.293 ± 0.126[b]	0.160 ± 0.010[b]
WUE	6.16 ± 2.81[a]	6.67 ± 2.26[a]	5.48 ± 0.76[a]

Results

Shoot dry weight was inhibited by salinity at 40 mM NaCl up to 20% in *Phlomis tuberosa* plant. In contrast, UV radiation did not affect dry matter production of plants significantly (Fig. 1).

Under saline conditions, chlorophyll fluorescence parameters were not influenced significantly (Table 1). However, slight reduction of maximal efficiency of PSII in dark-adapted leaves (F_v/F_m) and the proportion of active Chl associated with the reaction centers (RCs) of PSII (F_v/F_0) as well as increase in photochemical quenching (*qP*), non-photochemical quenching (*qN*) and quantum yield of PSII (Φ_{PSII}) were detectable in leaves of salt-stressed plants. Net assimilation rate (*A*) was not influenced by 20 mM salinity stress, but reduced up to 37% by 40 mM salt concentration (Table 1). Although a slight reduction was detected in the transpiration rate (*E*), it was not affected significantly by the used NaCl concentrations, while the stomatal conductance to water vapor (g_s) was reduced strongly by both salt stresses (about 88%).

Table 2. Leaf photochemical parameters including photochemical efficiency of PSII (F_v/F_m), ratio of variable to initial fluorescence (F_v/F_0), photochemical quenching (q_P), non-photochemical quenching (q_N) and quantum yield of PSII (Φ_{PSII}) and gas exchange parameters including net photosynthetic rate (*A*, μmol m^{-2} s^{-1}), transpiration rate (*E*, mmol m^{-2} s^{-1}), stomatal conductance to water vapor (g_s, mol m^{-2} s^{-1}) and water use efficiency (*WUE*, μmol $mmol^{-1}$) in *Phlomis tuberosa* grown for two weeks under UV radiation at 10 kJ m^{-2} d^{-1}. Values are the mean ± SD (n=4). Data of each row indicated by the same letters are not significantly different (P<0.05).

	Treatment		
Photochemistry	Control	UVA	UVA+B
F_v/F_m	0.84 ± 0.01^a	0.81 ± 0.04^a	0.75 ± 0.06^b
F_v/F_0	4.82 ± 0.66^a	4.55 ± 1.04^a	3.27 ± 0.59^a
qP	0.968 ± 0.011^a	0.950 ± 0.071^a	0.994 ± 0.023^a
qN	0.073 ± 0.070^a	0.097 ± 0.059^a	0.201 ± 0.112^a
Φ_{PSII}	0.786 ± 0.002^a	0.759 ± 0.025^a	0.766 ± 0.001^a
Gas exchange			
A	4.84 ± 0.52^a	4.36 ± 0.33^{ab}	3.65 ± 0.70^b
E	1.21 ± 0.25^a	0.80 ± 0.23^b	0.61 ± 0.11^b
g_s	1.22 ± 0.742^a	0.327 ± 0.144^b	0.217 ± 0.081^b
WUE	4.18 ± 1.42^a	5.76 ± 1.51^a	5.97 ± 0.67^a

Table 3. Water potential (ψ_w) and osmotic potential (ψ_s) (MPa) in the leaves of *Phlomis tuberosa* grown for two weeks in nutrient solution with 0, 20 and 40 mM NaCl salinity or under UV radiation at 10 kJ m^{-2} d^{-1}. Values are the mean ± SD (n=4). Data of each column within each treatment indicated by the same letters are not significantly different (P<0.05).

Treatment	ψ_s	ψ_w
Control	−0.640 ± 0.086^a	−0.737 ± 0.097^a
20 mM	n.d.	n.d.
40 mM	−0.933 ± 0.043^b	−1.34 ± 0.108^b
Control	−0.711 ± 0.054^a	−0.777 ± 0.205^a
UVA	−0.668 ± 0.052^a	−0.812 ± 0.185^a
UVA+B	−0.708 ± 0.031^a	−0.837 ± 0.254^a

Water use efficiency (*WUE*) showed only a slight reduction by salinity.

In plants grown under UV radiation treatments, the maximal efficiency of PSII in dark adapted leaves (F_v/F_m) was not affected by UVA, while UVA+B treatment caused a significant reduction up to 11% in the F_v/F_m ratio (Table 2). UVA+B affected F_v/F_0 ratio only slightly. In light adapted leaves, *qP*, *qN* and Φ_{PSII} remained unchanged under UV treatments. Net assimilation rate (*A*) was reduced by UVA treatment slightly. In contrast, effect of UVA+B treatment on *A* was significant and reached up to 24% compared with control plants without UV treatment. Simultaneous with reduction of *A*, transpiration rate (*E*) and stomatal conductance (g_s) were reduced strongly by both UVA and UVA+B treatments. Effect of UVA+B was more pronounced than UVA. *WUE* was not affected by UV treatment significantly (Table 2).

Table 4. Leaf content of MDA (nmol g^{-1} FW) and H_2O_2 (nmol g^{-1} FW) in *Phlomis tuberosa* grown for two weeks in nutrient solution with 0, 20 and 40 mM NaCl salinity or under UV radiation at 10 kJ m^{-2} d^{-1}. Values are the mean ± SD (n=4). Data of each column within each treatment indicated by the same letters are not significantly different (P<0.05).

Treatment	MDA	H_2O_2
Control	12.67 ± 1.37^a	494 ± 49^b
20 mM	16.37 ± 1.48^a	501 ± 39^b
40 mM	14.20 ± 3.73^a	680 ± 66^a
Control	12.84 ± 0.51^b	467 ± 16^a
UVA	12.98 ± 1.42^b	545 ± 27^a
UVA+B	17.91 ± 3.39^a	507 ± 94^a

Leaf water potential (ψ_w) was lowered by about 45% with 40 mM salinity, similarly, leaf osmotic potential (ψ_s) decreased up to 31% (Table 3). In contrast, UV treatments did not affect significantly ψ_w and ψ_s. However, a slight reduction of ψ_w and ψ_s was detected in leaves of *Phlomis tuberosa* particularly under UVA+B treatment compared with control (Table 3).

Specific activity of all studied enzymes was increased by both applied salinity levels (Fig. 2). Activity of APX was influenced by salinity (up to 70%), more than other enzymes. SOD, CAT and POD activities increased by 40 mM salinity with similar extent (by about 40%). Concentration of MDA remained unchanged under salinity, while H_2O_2 concentration increased under 40 mM NaCl salinity significantly (Table 4).

Under UV treatments, only activity of CAT and APX was influenced significantly. Activity of APX was increased by UV stress up to 53% and CAT by 30% (Fig. 2). UVA+B treatment, in contrast to salinity, caused a significant increase of MDA content of leaves, while did not influence H_2O_2 concentration (Table 4).

Discussion

Contrastive response of *Phlomis tuberosa* to salinity and UV radiation

Phlomis tuberosa showed a high sensitivity to salinity. Studies on various Lamiaceae species often demonstrated a high to moderate salt sensitivity in these species (Tabatabaie and Nazari 2007). However, these works have mainly focused on the effects of salinity on the quality and quantity of secondary metabolites (Karray-Bouraoui et al. 2009; Ben Taarit et al. 2009). Data regarding the effect of salinity on photosynthesis and water relations are rare and little attention has been paid on the mechanisms of high salt susceptibility in these species.

In contrast, UV radiation stress did not affect dry matter production of plants, a response characteristic for plants growing at high elevations (Filella and Penuelas 1999).

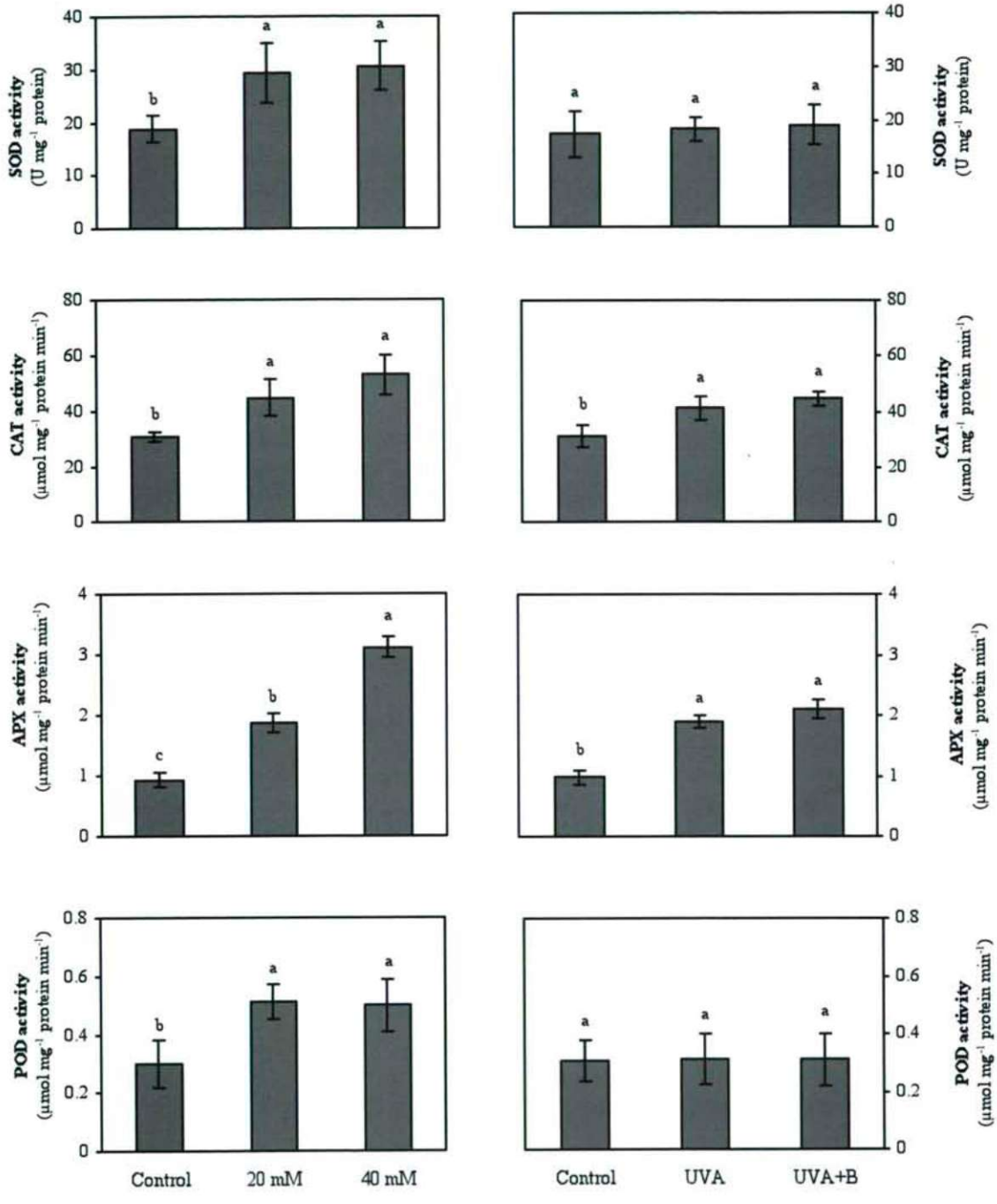

Figure 2. Specific activity of superoxide dismutase (SOD), catalase (CAT), ascorbate peroxidase (APX) and peroxidase (POD) in the leaves of *Phlomis tuberosa* grown for two weeks in nutrient solution with 0, 20 and 40 mM NaCl salinity or under UV radiation at 10 kJ m^{-2} d^{-1}. Values are the mean ± SD (n=4). Bars indicated by the same letters are not significantly different (P<0.05).

Leaf photochemistry and gas exchange under salinity and UV radiation stress

Though a high sensitivity to salt as judged by changes in plants dry matter production, PSII photochemistry was not affected under these conditions. Significant change in leaf photochemical parameters such as F_v/F_m due to salinity was reported for some salt sensitive (Wang et al. 2007) but not salt tolerant (Megdiche et al. 2008) species. Many authors suggested application of chlorophyll a fluorescence analysis as a reliable method to assess the changes in the function of

PSII under stress conditions (Maxwell and Johnson 2000). Fluorescence parameters have been used to screen for salinity tolerance in some plant species (Jiang et al. 2006). Lack of change in photochemical parameters in *Phlomis tuberosa* under growth-inhibiting salinity levels in this work demonstrated that PSII was highly resistant to salinity stress in this species and damage to PSII was not involved in plants response to salinity. In contrast to leaf photochemistry, gas exchange parameters were influenced strongly by salinity. Net assimilation rate (*A*) is an important photosynthetic parameter that represents the maximal photon utilization capacity of plants and thus, reflects the net primary productivity (Surabhi et al. 2009). Reduction of net assimilation rate (*A*) under salinity was correlated well with elevated stomatal resistance in our work as was reported by other authors (Jiang et al. 2006; Wang et al. 2007). Salinity-induced partial closure of stomata may improve the efficiency of plants for an economical use of water for growth. Accordingly, an improvement of water use efficiency (*WUE*) has been reported in plants subjected to salinity (Parida and Das 2005). In this work, however, concomitant with only a slight reduction of transpiration rate, *WUE* remained unchanged under salinity. In addition, significant reduction of leaf osmotic potential and water potential revealed a serious salt-induced disturbance in water relations (Romeroaranda et al. 2001) that was correlated with reduction of leaf growth under salinity.

UV radiation stress did not cause any change in leaf photochemistry with the exception of reduction of F_v/F_m, an indicator of photoinhibitory damage (Maxwell and Johnson 2000) caused by light or other environmental stresses under UVA+B stress. This change revealed higher sensitivity of PSII to UVA+B radiation in *Phlomis tuberosa*. UVB radiation can impair all major processes of photosynthesis including photochemical reactions in thylakoid membranes as well as stomatal conductance (Surabhi et al. 2009). A remarkable drop in *A* especially in the UVA+B treatment in this work was associated with significant reduction of stomatal conductance.

Responses of antioxidant defense system to salinity and UV radiation

A large number of studies on various species indicated that salt stress alters the amount of the enzymes involved in scavenging ROS (Parida and Das 2005). SOD is reported to play an important role in cellular defense against oxidative stress, as its activity directly modulates the amount of H_2O_2 (Sudhakar et al. 2001). In the present work, a pronounced increase was observed in the activity of all antioxidant enzymes studied even at salinity as low as 20 mM NaCl. As expected, H_2O_2 was accumulated under salinity likely following an imbalance between production and scavenging of H_2O_2. In contrast, leaf MDA content remained unchanged under salinity presumably due to the increased activity of antioxidant enzymes which was sufficient to avoid a substantial elevation in lipid peroxidation. Accordingly, salinity did not cause membrane damage and lipid peroxidation in leaves of *Phlomis tuberosa* consistent with the unaffected leaf photochemistry in the leaves of salinized plants.

Under UV radiation, in contrast, activity of CAT and APX but not SOD or POD was enhanced. Under similar doses of UVB radiation applied in our work, activity of SOD was reported to be increased, decreased or remained unaffected depending on plant species (Xu et al. 2008). Increased APX activity in our work due to UV radiation is consistent with the results of several other studies and may suggest an important role for this enzyme in the response and adaptation of plants to UV stress (Xu et al. 2008 and refs therein). Accordingly, leaf concentration of H_2O_2 did not change by UV stress likely because of an efficient scavenging by APX and CAT under these conditions. Some studies report an increase (Kalbina and Strid 2006) while others report no change (Xu et al. 2008) of tissue content of H_2O_2 due to UVB stress. In contrast to H_2O_2, a significant increase of leaf MDA content was observed under UVA+B stress. It implied that an oxidative damage has been occurred under UVA+B stress likely by ROS other than H_2O_2 e.g. superoxide anions ($O_2^{\cdot-}$), the dominant ROS in UV-irradiated leaves (Hideg et al. 2002). Although the $O_2^{\cdot-}$ was not determined in this work, it is likely that elevated production without an accompanying increase in the ability to scavenge the formed $O_2^{\cdot-}$ results in accumulation of this radical in UVA+B affected leaves.

Conclusion

Phlomis tuberosa was shown to be highly sensitive to salinity but relatively resistant to UV radiation stress as judged by dry weight data of plants. Information from leaf photochemistry and gas exchange as well as antioxidant defense system of plants revealed that, the cause of high salinity sensitivity of *Phlomis tuberosa* is not damage to PSII or membrane destruction. Indeed, salinity induced stomatal limitation and strong reduction of net assimilation rate, without efficient limitation of water loss from salt affected leaves. Accordingly, disturbance in water relations rather than the effect of other factors such as oxidative stress, inhibited leaf photochemistry or membrane damage was involved in determination of responses of *Phlomis tuberosa* to salinity.

In contrast, UV stress, which caused PSII damage, increased MDA content and significant reduction of net assimilation rate, did not significantly influence plants growth. This implies that these factors were not able to affect negatively plants performance under UV stress at least during the short period of exposure in this work.

There are few published works on the effect of UV radiation in Lamiaceae species (Chang et al. 2009). Plants are known to react to UV radiation by radical scavenging and pigmentation (Jacobs et al. 2007). Screening out UV-B radia-

tion by accumulation of flavonoids in the leaf epidermis was suggested as mechanisms for resistance to UV-B radiation (Jacobs et al. 2007). Members of Lamiaceae are well known to produce flavonoids (Tomás-Barberán and Wollenweber 1990) and accumulate these compounds in the leaf surface (Jamzad et al. 2003). Our results suggested that since antioxidant defense system is obviously inefficient in protection of plants against UV radiation, biochemical defense plays presumably a determinant role in high resistance to UV stress in *Phlomis tuberosa*.

References

Albaladejo RG, Aguilar JF, Aparicio A, Feliner GN (2005) Contrasting nuclear-plastidial phylogenetic patterns in the recently diverged Iberian *Phlomis crinita* and *P. lychnitis* lineages (Lamiaceae). Taxon 54:987-998.

Allen DJ, Nogues S, Baker NR (1998) Ozone depletion and increased UV-B radiation: is there a real threat to photosynthesis? J Exp Bot 49:1775-1788.

Ashraf M, Harris PJC (2004) Potential biochemical indicators of salinity tolerance in plants. Plant Sci 166:3-16.

Azizan D, Moore DM (1982) Morphological and palynological studies in *Phlomis* L. and *Eremostachys* Bunge (Labiatae). Bot J Linn Soc 85:249-281.

Ben Taarit M, Msaada K, Hosni K, Hammami M, Kchouk ME, Marzouk M (2009) Plant growth, essential oil yield and composition of sage (*Salvia officinalis* L.) fruits cultivated under salt stress conditions. Ind Crop Prod 30:333-337.

Caldwell MM (1971) Solar UV irradiation and the growth and development of higher plants. In Giese AC, ed., Photophysiology. Academic Press, New York, NY, USA, 131-137.

Chang X, Alderson PG, Wright CJ (2009) Enhanced UV-B radiation alters basil (*Ocimum basilicum* L.) growth and stimulates the synthesis of volatile oils. J Hort Forest 1:27-31.

Cowling RM, Rundel PW, Lamont BB, Arroyo MK, Arianoutsou M (1996) Plant diversity in Mediterranean-climate regions. Trees 11:362-366.

Creissen GP, Mullineaux PM (2002) The molecular biology of the ascorbate-glutathione cycle in higher plants. In Inzé D, Montganu MV, ed., Oxidative Stress in Plants. Taylor & Francis, UK, 247–270.

Dat J, Vandenabeele S, Vranova´ E, van Montagu M, Inze´ D, van Breusegem F (2000) Dual action of active oxygen species during plant stress responses. Cell Mol Life Sci 57:779-795

Fedina IS, Grigorova IT, Georgieva K (*2003*) Response of barley seedlings to UV-B radiation as affected by NaCl. J Plant Physiol 160:205-208.

Filella I, Penuelas J (1999) Altitudinal differences in UV absorbance, UV reflectance and related morphological traits of *Quercus ilex* and *Rhododendron ferrugineum* in the Mediterranean region. Plant Ecol 145:157-165.

Germ M, Kreft I, Osvald J (2005) Influence of UV-B exclusion and selenium treatment on photochemical efficiency of photosystem II, yield and respiratory potential in pumpkins (*Cucurbita pepo* L.). Plant Physiol Biochem 43:445-448.

Hajiboland R, Hasani BD (2007) Responses of antioxidant defense capacity and photosynthesis of bean (*Phaseolus vulgaris* L.) plants to copper and manganese toxicity under different light intensities. Acta Biol Szeged 51:93-106

Hideg É, Barta C, Kálai T, Vass I, Hideg K, Asada K (2002) Detection of singlet oxygen and superoxide with fluorescent sensors in leaves under stress by photoinhibition or UV radiation. Plant Cell Physiol 43:1154-1164

Jacobs JF, Koper GJM, Ursemb WNJ (2007) UV protective coatings: A botanical approach. Prog Org Coat 58:166–171

Jamzad Z, Grayer RJ, Kite GC, Simmonds MSJ, Ingrouille M, Jalili A (2003) Leaf surface flavonoids in Iranian species of *Nepeta* (Lamiaceae) and some related genera. Biochem Syst Ecol 31:587-600.

Jiang Q, Roche D, Monaco TA, Durham S (2006) Gas exchange, chlorophyll fluorescence parameters and carbon isotope discrimination of 14 barley genetic lines in response to salinity. Field Crop Res 96:269-278.

Johnson CM, Stout PR, Broyer TC, Carlton AB (1957) Comparative chlorine reguirements of different plant species. Plant Soil 8:337-353.

Kalbina I, Strid A (2006) Supplementary ultraviolet-B irradiation reveals differences in stress responses between *Arabidopsis thaliana* ecotypes. Plant Cell Environ 29:754-763.

Kao WY, Tsai TT, Shih CN (2003) Photosynthetic gas exchange and chlorophyll a fluorescence of three wild soybean species in response to NaCl treatments. Photosynthetica 41:415-419.

Karray-Bouraoui M, Rabhi M, Neffati M, Baldan B, Ranieri A, Marzouk B, Lachaâl M, Smaoui A (2009) Salt effect on yield and composition of shoot essential oil and trichome morphology and density on leaves of *Mentha pulegium*. Ind Crop Prod 30:338–343

Krall JP, Edwards GE (1992) Relationship between photosystem II activity and CO_2 fixation in leaves. Physiol Plant 86:180-187.

Mano J (2002) Early events in environmental sresses in plants induction mechanisms of oxidative stress. In Inzé D, Montganu MV, ed., Oxidative Stress in Plants. Taylor & Francis, UK, 217–246.

Maxwell K, Johnson GN (2000) Chlorophyll fluorescence–a practical guide. J Exp Bot 51:659-668.

Megdiche W, Hessini K, Gharbi F, Jaleel CA, Ksouri R, Abdelly C (2008) Photosynthesis and photosystem 2 efficeincy of two salt-adapted halophytic seashore *Cakile maritime* ecotypes. Photosynthetica 46:410-419.

Parida AK, Das AB (2005) Salt tolerance and salinity effects on plants: a review. Ecotoxicol Environ Saf 60:324-349.

Perl-Treves R, Perl A (2002) Oxidative stress: an introduction. In Inzé D, Montganu MV, ed., Oxidative Stress in Plants. Taylor & Francis, UK, 1–32.

Romeroaranda R, Soria T, Cuartero J (2001) Tomato plant-water relationships under saline growth conditions. Plant Sci 160:265-272.

Sudhakar C, Lakshmi A, Giridarakumar S (2001) Changes in the antioxidant enzymes efficacy in two high yielding genotypes of mulberry (Morus alba L.) under NaCl salinity. Plant Sci 161:613-619.

Surabhi GK, Reddy KR, Singh SK (2009) Photosynthesis, fluorescence, shoot biomass and seed weight response of three cowpea (*Vigna unguiculata* L. Walp.) cultivars with contrasting sensitivity to UV-B radiation. Environ Exp Bot 66:160-171.

Tabatabaie SJ, Nazari J (2007) Influence of nutrient concentrations and NaCl salinity on the growth, photosynthesis, and essential oil content of peppermint and lemon verbena. Turk J Agr Forest 31:245-253.

Tomás-Barberán FA, Wollenweber E (1990) Flavonoid aglycones from the leaf surfaces of some Labiatae species. Plant Syst Evol 173:109-118.

Wang R, Chen S, Deng L, Fritz E, Hüttermann A, Polle A (2007) Leaf photosynthesis, fluorescence response to salinity and the relevance to chloroplast salt compartmentation and anti-oxidative stress in two poplars. Trees 21:581-591

Xu C, Natarajan S, Sullivan JH (2008) Impact of solar ultraviolet-B radiation on the antioxidant defense system in soybean lines differing in flavonoid contents. Environ Exp Bot 63:39-48.

Yannarelli GG, Gallego SM, Tomaro ML (2006) Effect of UV-B radiation on the activity and isoforms of enzymes with peroxidase activity in sunflower cotyledons. Environ Exp Bot 56:174-181.

Volume 54(1):45-49, 2010
Acta Biologica Szegediensis
http://www.sci.u-szeged.hu/ABS

ARTICLE

Antioxidant and antimicrobial activities of fruit juices and pomace extracts against acne-inducing bacteria

Lilla Ördögh[1], László Galgóczy[1], Judit Krisch[2]*, Tamás Papp[1], Csaba Vágvölgyi[1]

[1]Department of Microbiology, Faculty of Science and Informatics, University of Szeged, Szeged, Hungary, [2]Institute of Food Engineering, Faculty of Engineering, University of Szeged, Szeged, Hungary

ABSTRACT Acne vulgaris is the most common skin disease in the world, and the number of antibiotic resistant acne-inducing bacterial strains has been increasing in the past years. Natural substances from plants are promising candidates to treat this disease. In the present study, *in vitro* biological activity of the juice, as well as water and methanol extracts of the pomace, of 20 cultivated and wild fruits was investigated on 4 acne-inducing bacteria (*Propionibacterium acnes, Staphylococcus aureus, Staphylococcus epidermidis, Streptococcus pyogenes*). The MIC values of juices and pomace extracts (water and methanol) were determined by broth microdilution assays at pH 7 and at skin neutral pH 5.5. Total phenol content and radical scavenging capacity of the active juices and extracts was also determined. Red and purple berries revealed a substantial antibacterial and antioxidant effect but there was no strong correlation between the antioxidant and antimicrobial properties. *Staphylococcus* strains were the most sensitive to the juices, and *S. pyogenes*, to the methanol extracts. Among the bacteria tested, *P. acnes* proved to be the most insensitive species in this study. The growth inhibition effect of *Ribes uva-crispa* (gooseberry) juice was stronger at acidic pH (MIC 0.40 mg/ml) than at neutral pH (MIC 5.30 mg/ml). The antibacterial effect of the other fruits and berries showed no significant difference at the different pH values.
Acta Biol Szeged 54(1):45-49 (2010)

KEY WORDS

acne vulgaris
Propionibacterium
Staphylococcus
Streptococcus
pomace extract

Acne vulgaris is a common skin disease of humans caused by bacteria inducing non-inflammatory and inflammatory skin lesions (Leyden 1997; 2003). It is not a serious disease but often involves both physical scarring and social embarrassment (Lehmann et al. 2002; Harper 2004). *Propionibacterium acnes*, *Staphylococcus aureus*, *Staphylococcus epidermidis* and *Streptococcus pyogenes* have been recognized as acne-inducing bacteria (Harper 2004) with staphylococci and *P. acnes* being the most prevalent causes of the disease (Hassanzadeh et al. 2008). Numerous topical and oral drugs are available to treat acne vulgaris, but the number of strains resistant to common antibiotics such as erythromycin, kanamycin, neomycin or tetracycline has been increasing in the past years (Hassanzadeh et al. 2008; Swanson 2003). There is therefore a substantial demand for new compounds with antibacterial activity against acne-inducing bacteria. Natural substances promising such biological activity have been extensively studied, especially during the last decade (Gnan and Demello 1999; Rabanal et al. 2002; Chomnawang et al. 2005, 2007; Kumar et al. 2007).

In this study, *in vitro* biological activity of the juice, as well as water and methanol extract of the pomace (peels, seeds, and flesh remaining after juice pressing), of 20 cultivated and wild fruits was investigated on acne-inducing bacteria by broth dilution method.

Accepted May 11, 2010
*Corresponding author. E-mail: krisch@mk.u-szeged.hu

Materials and Methods

Bacterial isolates and their maintenance

Clinical isolates of *Staphylococcus aureus* (Szeged Microbial Collection, University of Szeged, Szeged, Hungary; SZMC 900), *Staphylococcus epidermidis* (SZMC 901) and *Streptococcus pyogenes* (SZMC 902) was maintained on T1 medium (4% beef extract, 4% peptone, 1% glucose, 1% yeast extract). *Propionibacterium acnes* (American Type Culture Collection, USA; ATCC 11827) was maintained on PA medium (1.5 % tryptone, 0.5% yeast extract, 0.5% NaCl, 0.5% beef extract, 0.3% glucose, 0.2% KH_2PO_4).

Plant material

The fruits and berries used were as follows. *Crataegus monogyna* Jacq., *Fragaria ananassa* Duch., *Prunus armeniaca* L., *P. avium* L., *P. avium* Gold, *P. cerasus* L., *P. persica* L., *Rubus fruticosus* L., *R. idaeus* L. from the family Rosaceae. *Ribes x nidigrolaria* Bauer, *R. nigrum* L., *R. rubrum* L., *R. uva-crispa* L. from the family Grossulariaceae. *Morus alba* L., *M. nigra* L. (Moraceae), *Berberis thunbergii* DC. cv. *atropurpurea* , *Mahonia aquifolium* (Pursh.) Nutt. (Berberi-

Table 1. Minimal Inhibitory Concentration (MIC, mg dry matter content / ml) of juices, water and methanol extracts at pH 7 and pH 5.5 after 48h incubation (J, juice; W, water extract; M, methanol extract).

		S. aureus		*S. epidermidis*		*S. pyogenes*		*P. acnes*	
		pH 7	pH 5.5	pH 7	pH 5.5	pH 7	pH 5.5	pH 7	pH 5.5
Berberidaceae									
Berberis thunbergii DC.	J	-[a]	-	-	-	-	-	-	-
	W	-	-	-	-	-	-	-	-
	M	-	-	14.73	14.73	0.83	0.83	15.73	15.73
Caprifoliaceae									
	J	-	-	-	-	5.45	5.45	-	-
Sambucus nigra L.	W	-	-	-	-	-	-	-	-
	M	-	-	-	-	-	-	-	-
Cornaceae									
	J	-	-	-	-	-	-	-	-
Cornus mas L.	W	-	-	-	-	-	-	-	-
	M	-	-	-	-	1.9	1.9	-	-
Grossulariaceae									
	J	-	-	13.49	11.09	-	-	-	-
Ribes rubrum L.	W	-	-	5.13	5.13	-	-	-	-
	M	-	-	-	-	-	-	-	-
	J	-	-	14.29	14.29	-	-	-	-
Ribes x nidigrolaria Bauer	W	-	-	-	-	-	-	-	-
	M	-	-	-	-	-	-	-	-
	J	5.43	5.43	5.03	0.40	-	-	-	-
Ribes uva-crispa L.	W	-	-	-	-	-	-	-	-
	M	-	-	-	-	-	-	-	-
Rosaceae									
	J	-	-	-	-	-	-	-	-
Fragaria ananassa Duch.	W	-	-	-	-	-	-	-	
	M	-	-	-	-	6.06	6.06	-	-
	J	4.83	7.42	-	-	-	-	-	-
Prunus armeniaca L.	W	-	-	-	-	-	-	-	-
	M	-	-	-	-	-	-	-	-
	J	-	-	-	-	15.6	15.6	13.87	14.65
Prunus avium L.	W	-	-	-	-	-	-	-	-
	M	-	-	-	-	6.13	6.13	-	-
	J	3.32	3.32	3.52	3.52	-	-	-	-
Rubus fruticosus L	W	-	-	-	-	-	-	-	-
	M	-	-	-	-	-	-	-	-
	J	-	-	12.35	9.18	-	-	-	-
Rubus idaeus L.	W	-	-	-	-	-	-	-	-
	M	-	-	-	-	-	-	-	-
Gentamycin		16[b]		8		2.0		1.0	
Ampicillin		> 64		> 64		0.5		1.0	

[a]No inhibition effect at the highest concentration. [b] MIC for control antibiotics (µg /ml).

daceae), *Sambucus nigra* L., *S. alba* Raf. (Caprifoliaceae), and *Cornus mas* L. (Cornaceae).

Commercial fresh fruits were purchased on a local market (Szeged, Hungary), *M. alba, M. nigra, B. thunbergii, M. aquifolium, S. nigra, S. alba* were harvested in the neighbourhood of Szeged, and *C. mas* in the Mátra mountains. Harvested plants were identified using the Plant Identification Manual of Hungarian Vascular Plants (Simon 2004) or by the kind help of Dr. E. Mihalik (University Botanical Garden, Szeged).

Extraction methods

Fruit juices were freshly pressed and stored at -20°C. The remaining pomace was dried overnight at 60°C in an oven and then ground to powder. One gram of each powdered pomace was extracted 3 times with 10 ml of distilled water or methanol per cycle. The extracts were combined and evaporated to dryness at 100°C in an oven (water extracts) or at 35-40°C in a water bath (methanol extracts). The dry material was re-dissolved in 4 ml of distilled water (water extracts) or of 10% methanol-water solution (methanol extracts), and frozen in 1 ml aliquots. One aliquot from each extract was dried again and weighed for dry matter content calculation. The juices and extracts were diluted in the appropriate media for the tests.

Table 2. Total phenol content, radical scavenging capacity (of the tenfold dilution) and RC_{50} for DPPH of the juices and extracts with antibacterial activity. (J, juice; W, water extract; M, methanol extract.)

Plant species		Total phenol[a] (mg g^{-1})	Radical scavenging capacity (%)	RC_{50} (mg ml^{-1})[b]
B. thunbergii	M	171.29 ± 1.05	81.5 ± 8.4	0.17 ± 0.02
S. nigra	J	70.52 ± 4.24	79.9 ± 3.4	0.35 ± 0.01
C. mas	M	28.07 ± 0.04	80.4 ± 0.50	1.11 ± 0.08
R. rubrum	J	14.81 ± 0.47	82.3 ± 9.8	1.51 ± 0.22
	W	14.20 ± 0.04	59.2 ± 6.7	1.11 ± 0.09
R. x nidigrolaria	J	18.87 ± 0.08	84.3 ± 3.0	3.5 ± 0.87
R. uva-crispa	J	28.91 ± 0.78	91.0 ± 5.9	1.02 ± 0.01
F. x ananassa	M	51.03 ± 0.98	89.7 ± 8.9	1.01 ± 0.45
P. armeniaca	J	9.43 ± 0.22	37.8 ± 3.1	4.52 ± 0.35
P. avium	J	6.95 ± 0.06	17.8 ± 3.1	2.04 ± 0.69
	M	6.29 ± 0.12	28.7 ± 4.4	3.83 ± 0.24
R. fruticosus	J	61.24 ± 0.27	83.8 ± 8.7	0.85 ± 0.17
R. idaeus	J	21.52 ± 0.21	87.5 ± 6.6	0.88 ± 0.21

[a] Total phenol content is expressed as mg gallic acid equivalent per g dry mater content of juices or pomace extracts.
[b] RC_{50} is given as mg dry matter content per ml of juices or pomace extracts.

Determination of antibacterial effect by broth microdilution method

The *in vitro* antibacterial activities were determined by microdilution plate assay. Juice or extract dilutions were applied in a range of ten- to eighty-fold dilution, buffered to pH 7 or 5.5 with 0.165 M morpholino-propane sulfonic acid. In each well, 100 µl of diluted and sterile-filtered (0.45 µm, Millipore) juice or extract dilution was mixed with 100 µl bacterium cell suspension (10^5 cells/ml in the appropriate medium). The absorbance of the bacterial cultures was measured at 620 nm. Each test plate contained an uninoculated control (100 µl juice or extracts + 100 µl medium) the absorbance of which was subtracted from the absorbance of bacterial cultures containing the same juice or extract; a positive growth control, a medium-free sterility control for the juices or extracts, and a drug-free sterility control for the medium. The samples were tested in triplicate and the results were recorded after 48 h.

Determination of total phenolics

Total soluble phenolics were determined by the Folin-Ciocalteu method (Singleton and Rossi 1965). Before adding to the reagent solution, juices and extracts were diluted 1:10 or 1:100 with the appropriate medium (DW or 10% (v/v) methanol). Absorption was measured at 725 nm. Total phenolics were expressed as mg gallic acid equivalent per g dry matter content of juices or extracts.

Determination of radical scavenging capacity with DPPH (1,1-diphenyl-2-picrylhydrazil)

Radical scavenging capacity was measured spectrophotometrically at 515 nm. Tenfold dilutions of the juices and water and methanol extracts of pomace (0.2 ml) were added to a 1.2 ml solution of DPPH (100 µM in methanol). Control was prepared by adding 0.2 ml methanol instead of sample. After 30 min, the absorbance was measured at 515 nm. Radical scavenging capacity was determined by the following equation:

$$(A_{control} - A_{sample})/A_{control} \times 100.$$

Determination of RC_{50} values

RC_{50} was defined as the dry matter content of the sample, in milligrams per ml, required for decreasing the initial DPPH concentration by 50%, and was extrapolated from a dose-response curve (Valavanidis et al. 2004). Different dilutions (10, 50, 100, 150, 200x) of the juices and water and methanol extracts of pomace were added to a DPPH solution, and absorbance was measured as described above. Experiments were carried out in triplicate, and results were expressed as mean values ± standard deviation (SD).

Results

Approximately half of the tested juices or extracts had inhibitory potential against the investigated species (Table 1). The following plants had no effect on any of the bacteria: *C. monogyna, P. avium* Gold, *P. cerasus, P. persica, S. nigra, R. nigrum, M. aquifolium, M. alba* and *M. nigra*. Generally, the juices showed the broadest antimicrobial activity.

Staphylococci were inhibited by the juices of *Ribes* and *Rubus* species and *P. armeniaca*. *S. epidermidis* was sensitive to the methanol extract of *B. thunbergii* and to the water extract of *R. rubrum* pomace. It is worth to mention that this was the only case when an aqueous extract of pomace had any effect on the bacterial growth. *S. pyogenes* was more sensitive to methanol extracts than to juices; and especially to *B. thunbergii* and *C. mas* pomace with MIC values of 0.83 and 1.9 mg/ml, respectively. *P. acnes* was the most insensitive bacterium, its growth was inhibited only by the methanol extract of *B. thunbergii* and the juice of *P. avium*. Changes in pH had no or slight effect on the MIC values of the tested fruits; except for *R. uva-crispa* where acidic pH decreased the MIC value to less than one tenth of the value measured at neutral pH, suggesting the presence of undissociated antimicrobial phenolic and organic acids at pH 5.5.

Radical scavenging capacity of the juices and pomace extracts showing antibacterial activity had a broad range from 15.6% (*P. avium* juice) to 91% (*R. uva-crispa* juice) (Table 2.). There was no real correlation between antioxidant capacity and MIC values, suggesting that not only phenolic antioxidants are responsible for the antimicrobial effect.

Discussion

Antibacterial activity of berry juices has been demonstrated

against both Gram-positive and Gram-negative bacteria (Puupponen-Pimiä et al. 2001; Ryan et al. 2001; Cavanagh et al. 2003; Lee et al. 2003). Both cultivated and wild berries are rich in bioactive substances such as phenolic compounds including flavonoids, tannins, and phenolic acids, and have an important role in the maintenance of the human health. Berries of the *Ribes* genus contain benzoic acid, the flavonoid quercetin, and anthocyanins, all of which can have antibacterial action. The fruits in the genus *Rubus* are rich in ellagitannins which can permeabilize the outer cell membrane of Gram-negative bacteria (Puupponen-Pimiä et al. 2004). In the literature, no data were found on the antibacterial effect of the investigated *Ribes* and *Rubus* species on acne-inducing bacteria. In our experiments, however, berry juice and extracts had good antibacterial effect against the two staphylococci tested. On *S. epidermidis* (and on *Klebsiella pneumoniae*), *P. avium* fruit extracts exerted growth inhibition (Lee et al. 2003). In our study, juice and/or methanol extract of *P. avium* inhibited the growth of *S. pyogenes* and *P. acnes* but not *S. epidermidis*. For butanolic extract of *P. armeniaca*, inhibitory effect on the growth of Gram-negative and -positive bacteria was reported (Rashid et al. 2007). In our experiments, apricot juice had good antibacterial activity against *S. aureus*.

The difference in the antibacterial activity of juices and extracts may be due to their different components; soluble in aqueous and alcoholic media. Water extract contains the majority of anthocyanins, tannins, starches, saponins, polypeptides and lectins, while methanol extracts also contain polyphenols, lactones, flavones, and phenons (Cowan 1999). For example, the major alkaloid of *B. thunbergii*, berberine, has a proven antibacterial effect (Amign et al. 1969) and is rather non-polar. Accordingly, only the methanol extract of *Berberis* pomace showed antibacterial effect. In case of the other efficient methanol extracts (*P. avium, C. mas, F. ananassa*) the non-polar active compound is, as yet, unknown.

The effect of pH is very important in case of microbicidal acids of the fruits. These are membrane-active substances which damage the inner cell membrane in their undissociated form. They alter the membrane permeability of the microbial cell and acidify the cytoplasm (Puupponen-Pimiä et al. 2004). In our experiments, the antibacterial effect of juices and extracts was more or less independent from pH changes, suggesting that other, non-dissociable compounds were responsible for the growth inhibition.

The majority of reports on natural components against acne-inducing bacteria refer to medicinal plants. The effect of Thai (Chomnawang et al. 2005, 2007) and Indian (Kumar et al. 2007) herbal extracts against *P. acne* and *S. aureus* was investigated. Seven Indian and 13 Thai medical plants inhibited the growth of the bacteria, achieving best MIC values with *Garcinia mangostana* (0.039 mg/ml) and *Coscinium fenestratum* (0.049 mg/ml). There is also a study about the antimicrobial effect of *Hypericum* spp. on *S. aureus*, and *S. epidermidis* (Rabanal et al. 2002), where, similar to our results, only methanol and chloroform extracts but not aqueous extracts had antibacterial activity. Guava (*Psidium sp.*) aqueous leaf extract with MIC of 5.6 mg/ml inhibited the growth of *S. aureus* (Gnan and Demello 1999). In our study, the antimicrobial effect of commercial and wild fruits was investigated against these bacteria, and MIC values ranging from 0.40 to 15.73 mg/ml were found. Medicinal plants have lower values but by extraction of the active compounds from fruit juices or from the by-products of juice making the minimal inhibitory concentration could be decreased. Active ingredients from foodstuffs have the advantage being non-toxic and familiar to the human body. Their inhibitory potential on bacterial growth may be utilized in the development of natural drugs or cosmetics to treat acne vulgaris.

Acknowledgments

This work was supported in part by the grant ETT 214/2006.

References

Amign AH, Subbiah TV, Abbasi KM (1969) Berberine sulphate. Antimicrobial activity, bioassay, and mode of action. Can J Microbiol 15:1067-1076.

Cavanagh HMA, Hipwell M, Wilkinson JM (2003) Antibacterial activity of berry fruits used for culinary purposes. J Med Food 6:57-61.

Chomnawang MT, Surassmo S, Nukoolkarn VS, Gritsanapan W (2005) Antimicrobial effects of Thai medicinal plants against acne-inducing bacteria. J Ethnopharmacol 101:330–333.

Chomnawang MT, Surassmo S, Nukoolkarn VS, Gritsanapan W (2007) Effect of *Garcinia mangostana* on inflammation caused by *Propionibacterium acnes*. Fitoterapia 78:401–408.

Cowan MM (1999) Plant products as antimicrobial agents. Clin Microbiol Rev 12:564-582.

Gnan SO, Demello MT (1999) Inhibition of *Staphylococcus aureus* by aqueous Goiaba extracts. J Ethnopharmacol 68:103–108.

Harper JC (2004) An update on the pathogenesis and management of acne vulgaris. J Am Acad Dermatol 51:S36-38.

Hassanzadeh P, Bahmani M, Mehrabani D (2008) Bacterial resistance to antibiotics in acne vulgaris: An in vitro study. Ind J Dermatol 53:122-124.

Kumar GS, Jayaveera KN, Ashok Kumar CKA, Sanjay UP, Swamy BMV, Kumar DVK (2007) Antimicrobial effects of Indian medicinal plants against acne-inducing bacteria. Trop J Pharm Res 6:717-723.

Lee YL, Cesario T, Wang Y, Shanbrom E, Thrupp L (2003) Antibacterial activity of vegetables and juices. Nutrition 19:994-996.

Lehmann HP, Robinson KA, Andrews JS, Holloway V, Goodman SN (2002) Acne therapy: A methodological review. J Amer Acad Dermatol 47:231-240.

Leyden JJ (1997) Therapy for acne vulgaris. New Engl J Med 336:1156–1162.

Leyden JJ (2003) A review of the use of combination therapies for the treatment of acne vulgaris. J Amer Acad Dermatol 49:200-210.

Puupponen-Pimiä R, Nohynek L, Alakomi HL, Oksman-Caldentey KM (2004). Bioactive berry compounds - novel tools against human pathogens. Appl Microbiol Biotechnol 67:8-18.

Puupponen-Pimiä R, Nohynek L, Meier C, Kahkonen M, Heinonen M, Hopia A, Oksman-Caldentey KM (2001) Antimicrobial properties of phenolic compounds from berries. J Appl Microbiol 90:494–507.

Rabanal RM, Arias A, Prado B, Hernández-Pérez M, Sánchez-Mateo, CC (2002) Antimicrobial studies on three species of *Hypericum* from the

Canary Islands. J Ethnopharmacol 81:287-292.

Rashid F, Ahmed R, Mahmood A, Ahmad Z, Bibi N, Kazmi SU (2007) Flavonoid glycosides from *Prunus armeniaca* and the antibacterial activity of a crude extract. Arch Pharm Res 30:932-937.

Ryan T, Wilkinson JM, Cavanagh HMA (2001) Antibacterial activity of raspberry cordial in vitro. Res Vet Sci 71:155-159.

Simon H (2004) Plant identification manual of Hungarian vascular plants (in Hungarian). Nemzeti Tankönyvkiadó, Budapest.

Singleton VL, Rossi JA Jr. (1965) Colorimetry of total phenolics with phosphomolybdic-phosphotungstic acid reagents. Am J Enol Viticult 16:144-158.

Swanson IK (2003) Antibiotic resistance of *Propionibacterium acnes* in acne vulgaris. Dermatol Nurs 5:359–361.

Valavanidis A, Nisiotou C, Papageorgiou Y, Kremli I, Satravelas N, Zinieris N, and Zygalaki H (2004) Comparison of the radical scavenging potential of polar and lipidic fractions of olive oil and other vegetable oils under normal conditions and after thermal treatment. J Agric Food Chem 52(8):2358–2365.

Volume 54(1):51-56, 2010
Acta Biologica Szegediensis
http://www.sci.u-szeged.hu/ABS

ARTICLE

Pollen morphology of the genus Pyrus (*Rosaceae*) in Iran

Zamani A[1]*, Attar F[1], Maroofi H[2]

[1]Central Herbarium of University of Tehran, School of Biology, Faculty College of Science, University of Tehran, Tehran, Iran,
[2]Research Center of Agriculture and Natural Resources, Kurdistan Province, Sanandaj, Iran

ABSTRACT In this study, pollen morphological characters of nine species of the genus *Pyrus* L. belonging to four sections, *Argyromalon*, *Pashia*, *Pyrus* and *Xeropyrenia* were examined by light (LM) and scanning electron (SEM) microscope. Regarding pollen shape, two forms can be recognized in the same specimen: the first form ranges from prolate- spheroidal, subprolate to prolate, while the second form includes triangular, trilobate and circular shapes, the apertures structure usually consists of three ectocolpi and three endopores. colpi occupy 85- 91% of length of pollen, often arranged meridionally but also parallel pattern can be recognized, endopore is located in the middle of colpi. Regarding sculpturing of the exine in proximal face, striate sculpturing is observed that according to some characters such as degree of slope of ridges, percentage of ridges and perforations, diameter of perforations is subdivided to four main types. Results of pollen grain fertility studies in the genus showed high percentage of fertility among studied species except in one species. **Acta Biol Szeged 54(1):51-56 (2010)**

KEY WORDS

Iran
Pollen grain
Pyrus
Rosaceae

The genus *Pyrus* L. (Pear) that initially was defined by Linnaeus (1753) covering not only pear- trees but also apple-trees in that time, is a tree member of subtribe Pyrinae (formerly subfamily Maloideae), family Rosaceae (Campbell et al. 2007). *Pyrus* probably originated in the mountainous regions of western and southwestern China in Tertiary or, possibly, even more ancient time and evolved and spread eastward and westward (Rubtsov 1944), and nowadays consists of 41 species in the temperate zones of Northern Hemisphere (except for North America) and exceptionally enters the most northwestern tip of Africa (Browicz 1993; Zamani et al. 2009; Zamani and Attar 2010). The highest number of taxa is found in Caucasus (specifically in Armenia) where more or less half of the species occur (Browicz 1993). Iran comprises of 7 (Schönbeck-Temesy 1969), 12 (Khatamsaz 1992) to 18 species (Zamani 2009; Zamani et al. 2009a, b; Zamani and Attar 2010) species that eight of them are endemic. The genus consists of two main centers of distribution in Iran, namely Alborz (N Iran) and Zagros (NW to S Iran) Mts.; however a few locations are reported from east and south (Browicz 1982) of Iran. The most important studies on the genus were those of Schönbeck-Temesy (1969), Browicz (1972a, 1972b, 1973, 1993) and Maleev (1971) that are mainly based on morphology and distribution of the genus. Pollen morphology has been proved to be useful in systematic of the Rosaceae (Hebda and Chinnappa 1990) as well as some of its particular genera and species (Reitsma 1966; Ueda and Tomita 1989; Arzani et al. 2005; Bednorz et al. 2005; Wronska- Pilarek and Boratynska 2005; Wronska- Pilarek and Lira 2006; Polyakova and Gataulina 2008). However it has been emphasized (Moore et al. 1991) that pollen morphological characters of the family are variable, even among several populations of the same species. Regarding *Pyrus*, there are only a few works dealing with pollen morphology of *Pyrus* (Westwood and Challice 1978; Fang and Yi-Xuan 1990). For this reason and also lacking any study in Iran, this survey aims to: (1) present detailed quantative and qualitative data on pollen morphology of the genus and (2) evaluate taxonomical value of these data.

Materials and Methods

Pollen of 16 populations belonging to nine species of *Pyrus* was studied by light microscope (LM) and scanning electron microscope (SEM). These species include 1- *P. boissieriana* Buhse, 2- *P. longipedicellata* Zamani and Attar, 3- *P. pashia* Hamilton ex D. Don. from sect. *Pashia*, 4- *P. hyrcana* Fed., 5- *P. grossheimii* Fed., 6- *P. farsistanica* Browicz from sect. *Pyrus* , 7- *P. mazanderanica* Schönbeck-Temesy, 8- *P. syriaca* Boiss. from sect. *Xeropyrenia* and 9- *P. salicifolia* Pall. from sect. *Argyromalon*. Voucher specimens were deposited in TUH (acronym according to Holmgren et al. 1990) and Herbarium of research institute of forests and rangelands of Orumieh. Pollen obtained from flower buds at anthesis was prepared for light microscope (LM) using methods described in Harley (1992) with some modifications and mounted in glycerol jelly on glass slides and sealed. Because the surface of the pollen grains was not adequately cleaned which made an exact study of sculpturing patterns difficult, the time of acetolysis was set at 7–8 min. For LM measurements, at least

Accepted May 4, 2010
*Corresponding author. E-mail: asgharzamani1362@gmail.com

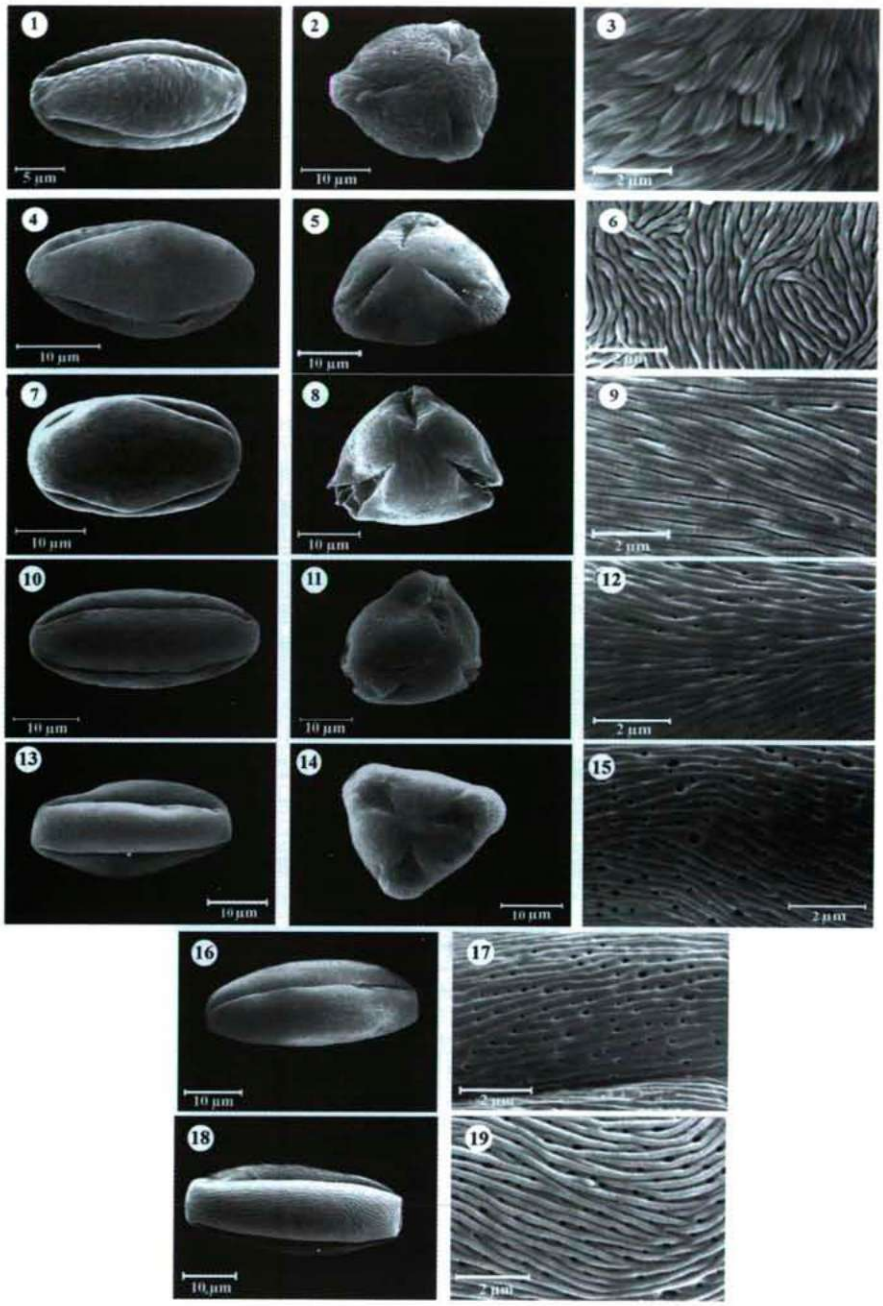

Figures 1-19. SEM micrographs of pollen grains in *Pyrus* spp. Type I: (1-3) *P. syriaca* 37098, (4-6) *P. grossheimii*, (7-9) *P. hyrcana* 38144, Type II: (10-12) *P. syriaca* 37106, (13-15) *P. pashia*, (16-17) *P. salicifolia*, (18-19) *P. farsistanica*.

20–25 pollen grains were measured by Nikon light microscope model 200 M with aid of a ×100 eyepiece. For SEM, after acetolysis, the specimens were mounted on 12.5mm diameter aluminum stubs and then coated in a sputter coater with approximately 25 nm of gold-palladium. The specimens were examined and photographed with Philips scanning electron microscope model XL30 at an accelerating voltage of 20 kV. The terminology follows mainly that of Ertdman (1952) and Halbritter et al. (2007). For detailed examination of sculpturing, we used the classification presented in Ueda and Tomita (1989). For estimation of pollen fertility, the pollen from fresh collected herbarium material was stained by acetocarmin in glycerine jelly, as described by Radford et al. (1974). In total, 11 populations belonging to nine species were analyzed.

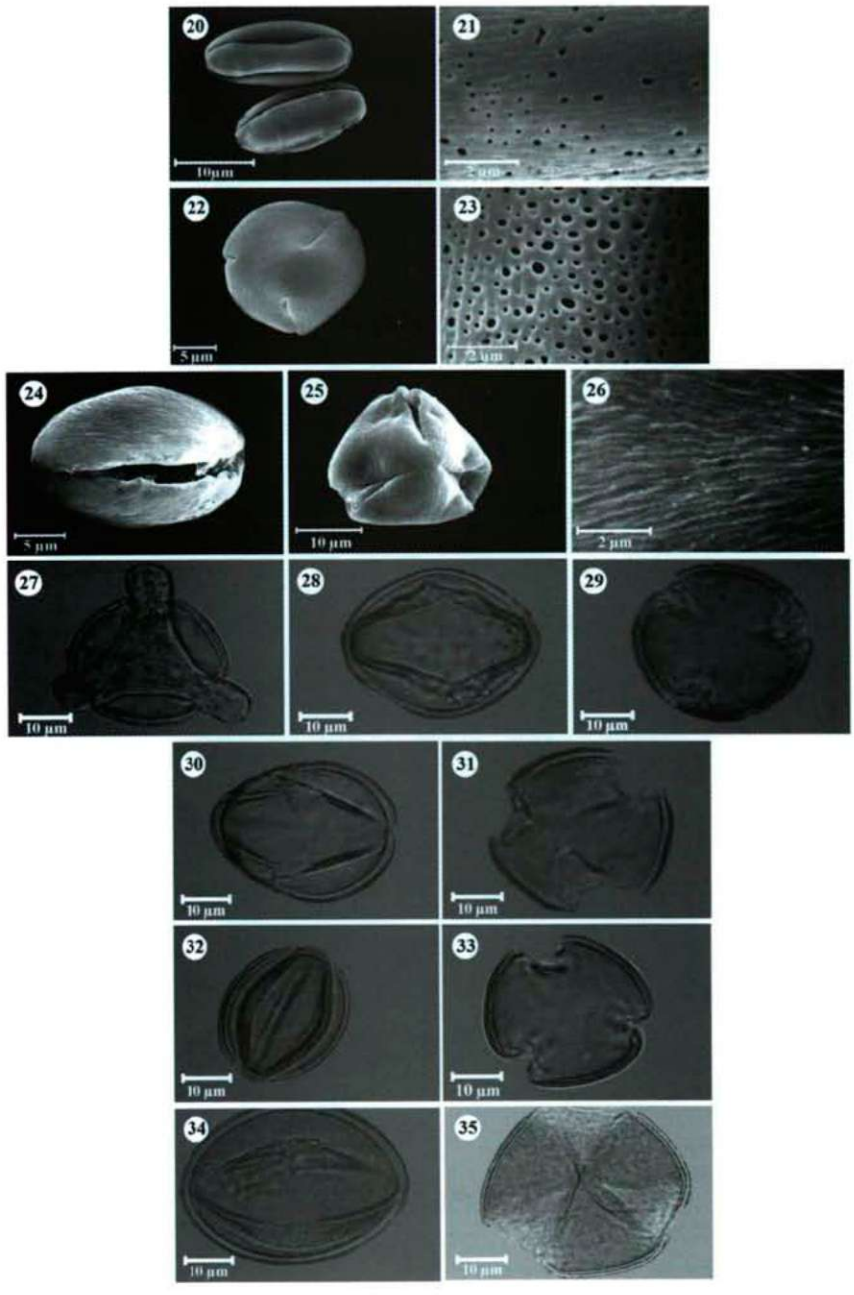

Figures 20-35. SEM and LM micrographs of pollen grains in *Pyrus* spp. Type III: (20-21) *P. mazanderanica*, (22- 23) *P. boissieriana*, Type IV (24-26) *P. longipedicellata*, (27-29) *P. hyrcana*, (30- 31) *P.longipedicellata*, (32-33) *P.salicifolia*, (34-35) *P.farsistanica*.

Results and Discussion

The main features of the investigated pollen grains are summarized in Table 1. Selected SEM and LM micrographs of examined pollen grains are presented in Figures 1-35.

General pollen morphological features

Main pollen characters vary even in different populations of the same species (see Figs. 1-3, 10-12, Table 1). Pollen grains are shed as monad, medium-sized (P= 30.62-34.05 µm), trizonocolporate, isopolar. Regarding shape of pollen, equatorial view includes prolate- spheroidal (Figs. 7, 24), subprolate (Figs. 1, 4) to prolate (Figs. 10, 13, 16, 18) shapes, while polar view includes triangular (Figs. 5, 8, 25) and trilobate shapes (Figs. 2, 11). Ectocolpi converge close to the polar ends, arranged meridionally (Figs. 1, 4, 7, 10) or parallel (Fig. 13, 18). In the middle of ectocolpi, there is endopore that consists of distinct (Figs. 2, 11, 27, 28) or indistinct (Fig. 5) projec-

Table 1. Details of examined characters of *Pyrus* species in this study.

Species	P	E	P/E	C	C/P	M	A	ET	ECTE	ENDE
P. Sect. *Argyromalon*										
P. salicifolia	28.00 (31.45± 1.93) 36.00	26.00 (27.35± 1.37) 31.00	1.15	24.00 (28.75± 3.04) 36.00	0.91	19.00 (22.05± 1.50) 25.00	6.00 (8.05± 1.76) 12.00	1.00 (1.46± 0.36) 2.00	0.77 (1.06± 0.11) 1.25	0.73 (0.96± 0.13) 1.29
P. Sect. *Pashia*										
P. boissieriana	29.00 (33.10± 2.24) 38.00	24.00 (27.55± 1.4) 30.00	1.20	24.00 (28.25± 2.71) 34.00	0.85	14.00 (19.95± 2.60) 25.00	5.00 (6.30± 1.13) 8.00	1.00(1.21± 0.27) 2.00	0.58 (0.82± 0.13) 1.02	0.66 (0.90± 0.14) 1.18
P. longipedicellata	25.00 (30.62± 2.27) 34.00	18.00 (27.34± 3.76) 32.00	1.12	16.00 (26.85± 3.62) 31.00	0.88	11.00 (17.90± 3.71) 23.00	4.00 (5.67± 1.85) 11.00	1.00 (1.63± 0.51) 3.00	0.74 (0.86± 0.067) 1.02	0.78 (1.04± 0.14) 1.30
P. pashia	26.00 (31.23± 2.05) 34.00	20.00 (28.35±2.67) 32.00	1.10	22.00 (28.26± 2.56) 33.00	0.90	17.00 (21.13± 2.45) 25.00	4.00 (6.73± 1.24) 10.00	1.00 (1.34± 0.45) 2.00	0.76 (0.85±0.10) 1.20	0.80 (1.10±0.15) 1.35
*P.*Sect. *Pyrus*										
P. farsistanica	30.00 (34.05± 2.84) 40.00	26.00 (30.50± 2.76) 36.00	1.14	24.00 (29.65± 3.01) 35.00	0.87	16.00 (21.50± 3.15) 27.00	4.00 (5.90 ± 1.52) 9.00	1.00 (1.48± 0.32) 2.00	0.75 (0.93± 0.12) 1.23	1.22 (1.38± 0.11) 1.58
P. grossheimii	29.00 (31.50± 1.82) 36.00	26.00 (27.88± 1.54) 32.00	1.13	24.00 (27.00± 1.72) 31.00	0.86	18.00 (21.20± 2.14) 27.0	5.00 (11.00± 3.80) 19.00	1.00 (1.53± 0.36) 2.00	0.76 (0.89± 0.10) 1.13	0.92 (1.01± 0.10) 1.30
P. hyrcana	30.50 (34.78± 2.93) 41.50	25.00 (30.62± 2.76) 35.50	1.15	26.50 (29.79± 2.40) 35.00	0.86	19.00 (22.86± 2.57) 27.50	4.50 (6.42± 1.28) 9.50	0.95 (1.39± 0.50) 2.50	0.84 (0.98± 0.11) 1.22	0.83 (1.05± 0.09) 1.22
P. sect. *Xeropyrenia*										
P. mazanderanica	26.50 (31.27± 2.26) 34.50	24.00 (28.00± 2.10) 31.50	1.13	22.00 (26.95± 2.33) 30.50	0.86	16.50 (20.85± 2.45) 26.50	4.50 (6.05± 1.28) 9.00	1.00 (1.50± 0.37) 2.10	0.80 (0.97± 0.11) 1.17	0.84 (1.09± 0.15) 1.35
P. syriaca	29.57 (33.51± 2.00) 37.43	23.57 (29.21± 2.66) 33.57	1.17	25.43 (29.02± 2.00) 33.00	0.87	14.86 (21.23± 3.15) 26.71	5.71 (7.18± 1.10) 9.57	0.97 (1.40± 0.32) 2.03	0.84 (1.03± 0.27) 1.26	0.72 (1.04± 0.12) 1.29

tion. Regarding exine, exine thickness (column ET in Table 1) ranges from thin (ET= 1.21-1.40 µm) to medium (ET= 1.46-1.63 µm), clearly consists of two layers (Figs. 27–35); ectexine and endexine. In most species, thickness of endexine is more than ectexine (column ECTE/ENDE<1), except in *P. salicifolia* (ECTE/ENDE= 1.11). On the basis of arrangement of ridges to the colpus, parallel (Figs. 4, 7, 10, 16, 18) and perpendicular (Fig. 1) patterns are recognized. Moreover according to arrangement of ridges to each other, intersecting (Figs. 3, 6) and semi-parallel (Figs. 9, 12, 15, 17, 19) patterns were recognized. The most variable character in this study belongs to sculpturing of the exine so that on the basis of the exine sculpturing in proximal face, striate ornamentation can be recognized; however on the basis of differences in surface structure such as diameter and slope of ridges, interval between ridges, presence, number and size of perforations four main types can be recognized as following:

Type I

This type is recognized by having merely deep and fingerprint like ridges and lacking any perforations on the surface of the exine (Figs. 3, 6, 9). Thickness and slope of ridge in this type is clearly more than other types (Figs. 3, 6, 9; see also column TR in Table 1). This type can also be subdivided according to interval between ridges; type I-A and type I-B with short (*P. syriaca*, Fig. 1) and long (*P. grossheimii* and *P. hyrcana*, Figs. 6, 9) intervals, respectively.

Type II

This type is recognized by having perforations between ridges (Figs.12, 15, 17, 19). This type is subdivided according to density and diameter of perforations; type II-A with sparse and small (*P. syriaca*; Fig. 12) and II-B with dense and large perforations (*P. salicifolia*, *P. farsistanica*, *P. pashia*; Figs. 15, 17, 19).

Table 1. continued.

Species	ECTE/ ENDE	FP	PN	DP	DR	TR	S	Sc	RP
P. Sect. *Argyromalon*									
P. salicifolia	1.11	%96.8	0.00(2.33± 1.80) 5.00	0.089(0.13± 0.037) 0.26	0.12(0.20± 0.042) 0.28	0.13(0.17± 0.021) 0.21	Subprolate, Triangular-Circular	Type II-B	Parallel
P. Sect. *Pashia*									
P. boissieriana	0.91	%97.1	2.00 (4.10± 1.02) 5.00	0.090(0.22± 0.093) 0.45	-	-	Subprolate, Trilobate- Circular	Type III	-
P. longipedicellata	0.83	%96.34	-	-	0.085(0.12± 0.017) 0.15	0.090(0.13± 0.030) 0.20	Prolate-Spheroidal, Triangular	Type IV	Parallel
P. pashia	0.77	%94.3	1.20 (1.98± 1.73) 4.50	0.10 (0.17± 0.045) 0.36	0.092 (0.15± 0.018) 0.16	0.097 (0.14± 0.026) 0.28	Prolate-Spheroidal, Triangular	Type III	Parallel
*P.*Sect. *Pyrus*									
P. farsistanica	0.68	%88.5	1.00 (2.95± 1.07) 5.00	0.13(0.20± 0.053) 0.35	0.092(0.13± 0.025) 0.20	0.14(0.20± 0.028) 0.24	Prolate-Spheroidal	Type II -B	Parallel
P. grossheimii	0.88	%52	-	-	0.076(0.097± 0.017) 0.14	0.18(0.24± 0.045) 0.34	Prolate-Spheroidal, Triangular	Type I-B	Intersecting
P. hyrcana	0.93	%97.57	-	-	0.060(0.087± 0.014) 0.12	0.19(0.23± 0.032) 0.33	Subprolate, Triangular-Circular	Type I -B	Parallel
P. sect. *Xeropyrenia*									
P. mazanderanica	0.89	%90.39	0.00(1.60± 1.34) 4.50	0.10(0.18± 0.071) 0.35	0.090(0.17± 0.070) 0.36	0.16(0.21± 0.047) 0.35	Prolate-Spheroidal, Circular	Type III	Parallel
P. syriaca	0.99	%92.79	0.00(0.75± 0.96) 3.00	0.07(0.11± 0.043) 0.25	0.082(0.11± 0.019) 0.15	0.14(0.21± 0.033) 0.27	Subprolate, Trilobate	Type I-A, II	Parallel, intersecting

Abbreviations: P, polar axis length; E, equatorial axis length; P/E, ratio of polar axis to equatorial axis; C, colpus length; C/P, ratio of colpus length to polar axis length; M, mesocolpium length; A, apocolpium length; ET, exine thickness; ECTE, ectexine thickness; ENDE, endexine thickness; ECTE/ENDE, ratio of ectexine thickness to endexine thickness; PN, perforations number in one square of micrometer; FP, fertility percentage; S, shape of pollen; Sc, pattern of sculpturing of pollen; RP, ridge arrangement's pattern; DP, diameter of perforation; DR, distance between ridges; TR, thickness of ridge; -, there is not the mentioned character; ?, is not observed the mentioned character.

Type III

This type is recognized by having dense (PN ranges from 1.92 to 4.10, Table 1) and large perforations (mean of perforations equals 0.20 µm) and also with obscure ridges (*P. boissieriana*, *P. mazanderanica*; Figs. 21, 23).

Type V

This type is recognized by having obscure ridges due to moderate slope of ridges and lacking of any perforations (*P. longipedicellata*, Fig. 26).

The delimitation of the genus *Pyrus* L. in subgeneric and species level is difficult (Browicz 1993), so that the number of species has been increased to more than 80 (Browicz 1993). In the other hand, several authors have divided the genus to different subgeneric levels (race, section, subsection) (Browicz 1993). The main cause of this problem is the ease of hybridization among different species and different individuals of the same species (Rubtsov 1944; Browicz 1993), however some other reasons such as distributional differences among several individuals of the same species play role in this problem. Moore et al. (1991) have emphasized that Pollen morphology in taxa of Rosaceae is very variable, even among the populations within the same species that is related it to the comparatively frequent occurrence of hybridization in this family. This problem is remarkable in this study in the case of shape and sculpturing, even in different specimens of the same species; specifically in *P. syriaca* (Figs. 1-3, 10-12). On the basis of Fang and Yi-Xuan (1990), exine sculpturing provides useful index for identifying different species of the genus. According to Flora Iranica (Schönbeck-Temesy 1969), the genus includes four sections, *Xeropyrenia*, *Pyrus*, *Pashia*

and *Argyromalon*. In spite of morphologically similarities of the members of these sections (Schönbeck-Temesy 1969), in most cases any remarkable resemblance is not observed among species of these sections (Table 1). As it is clear in Table 1, percentage of fertility in all species is more than 90%, except *P. grossheimii*. In conclusion, pollen morphological features of the genus *Pyrus* can be a descriptive and not diagnostic evidence of the species, specifically in the widespread species.

Acknowledgements

We are grateful N. Fatemi (University of Tehran) for her assistance in preparation of LM samples, N. Raei Niaki (University of Tehran) for his assistance in measurement of quantative data with light microscope, Y. Nejaty (University of California- Davis) for his assistance in collecting some data, Hashemi (University of Tehran) for coating of samples and Rezayi (University of Tarbiat- Modarres) for his kind assistance in taking photos by electron microscope.

References

Arzani K, Nejatian MA, Karimzadeh G (2005) Apricot (*Prunus armeniaca*) pollen morphological characterization through scanning electron microscopy, using multivariate analysis. New Zeland J Crop Hort Sc 33:381-388.

Bednorz L, Maciejewska-Rutkowska I, Wronska-Pilarek D, Fujiki T (2005) Pollen morphology of the Polish species of the genus *Sorbus* L. Acta Soc Bot Pol 74:315-322.

Browicz K (1972a) *Pyrus* L. In Flora of Turkey, ed., Davis PH, Vol. 4., pp. 160-168. Edinburgh University Press.

Browicz K (1972b) Distribution of woody Rosaceae in W. Asia X. Arbor Kornick 17:19-33.

Browicz K (1973) Distribution of woody Rosaceae in W. Asia XII. Arbor Kornick 18:23-33.

Browicz K (1982) *Pyrus farsistanica* Browicz- a new species of pear from southern Iran. Arbor Kornick 27:27-30.

Browicz K (1993) Conspect and chorology of the genus *Pyrus* L. Arbor Kornick 38:17-33.

Campbell CS, Evans RC, Morgan DR, Dickinson TA, Arsenault MP (2007) Phylogeny of subtribe Pyrinae (formerly the Maloideae, Rosaceae): limited resolution of a complex evolutionary history. Pl Syst Evol 266:119-145.

Eide F (1981) Key to the northwest European Rosaceae Pollen. Grana 20:101-118.

Erdtman G (1952) Pollen morphology and plant taxonomy. Almqvist & Wiksell, Stockholm.

Fang X, Yi-Xuan Y (1990) Observation on pollen morphology and exine ultrastructure of *Pyrus* in China. Chin J Bot 3:33-41.

Halbritter H, Werber M, Zetter R, Frosch-Radivo A, Buchner R, Hesse M (2007) Ilustrated Handbook on pollen terminology. < http://www.paldat.org/paldat-Terminology- large.pdf >.

Harley MM (1992) The potential value of pollen morphology as an additional taxonomic character in subtribe Ociminae (Ocimeae: Nepetoideae: Labiatae). In Harley RM, Reynolds T eds., Advances in Labiatae Science: pp. 125-138. Royal Botanic Gardens. Kew, Richmond, Surrey, UK.

Hebda RJ, Chinnappa CC (1990) Studies on pollen morphology of Rosaceae in Canada. Rev Paleobot Palynol 64:103-108.

Holmgren PK, Holmgren NH, Barnett LC (1990) Index Herbariorum I: The Herbaria of the world. 8th ed., Regnum Veg. 20.

Khatamsaz M (1992) *Pyrus* L. In Flora of Iran, NO. 6., pp. 181-200, Research institute of forests and rangelands, Tehran (In Persian).

Linnaeus C (1753) Species plantarum, Vol. 1:479-480, London.

Maleev PV (1971) *Pyrus* L. In Flora of U.S.S.R. ed., Komarov V.L., Vol. 9., pp. 259-274. Academy of Science of the U.S.S.R.

Moore PD, Webb JA, Collinson ME (1991) Pollen Analysis, 2nd ed., Blackwell scientific publications.

Polyakova TA, Gataulina GN (2008) Morphology and variability of pollen of the genus *Spiraea* L. (Rosaceae) in Siberia and the far east. Siberian J Ecol 15:545-551.

Radford AE, Dickison WC, Massey JR, Bell CR (1974) Vascular Plant Systematics. Harper & Row Publishers, New York.

Reitsma T (1967) Some aspects of the pollen morphology of the genus *Sanguisorba* L. (Rosaceae). Rev Paleobot Palynol 4:305-310.

Rubtsov GA (1944) Geographical distribution of the genus *Pyrus* and trends and factors in its evolution. The Amer Natur 78:358-366.

Schönbeck-Temesy E (1969) *Pyrus* L. In Flora Iranica, ed., Rechinger KH, NO. 66., pp 27-36. Graz- Austria.

Ueda Y, Tomita H (1989) Morphometric analysis of pollen exine patterns in Roses. J Jap Soc Hort Sc 58:211-220.

Westwood M, Challice JS (1978) Morphology and surface topography of pollen and anthers of *Pyrus* species. J Amer Soc Hort Sc 103(1):28-37.

Wronska-Pilarek D, Boratynska K (2005) Pollen morphology of *Rosa gallica* L. (Rosaceae) from southern Poland. Acta Soc Bot Pol 74:297-304.

Wronska-Pilarek D, Lira J (20060) Pollen morphology of Polish species of the genus *Rosa*- I. *Rosa pendulina*. Dendrobiology 55:65-73.

Wronska-Pilarek D, Malinski T, Lira J (2006) Pollen morphology of Polish species of genus *Rubus* – part I. *Rubus gracilis*. Dendrobiology 56:69-77.

Zamani A, Attar F, Joharchi MR (2009a) *Pyrus pashia* (Rosaceae), a new record for the flora of Iran. Ir J Bot 15(1):72-75.

Zamani A, Attar F, Joharchi MR (2009b) *Pyrus ghahremanii* Spec. nova and P. giffanica Spec. nova (*Rosaceae-Maloideae*) from Iran. Phyton 49 (1):105:115.

Zamani A (2009) Taxonomic studies on the genus *Pyrus* L. (Rosaceae) in Iran. Ms.C. thesis. University of Tehran, Tehran (In Persian).

Zamani A, Attar F (2010) *Pyrus longipedicellata* sp. nov. (Rosaceae) from Central Alborz, Iran. Nord J Bot 28:484-486.

Volume 54(1):57, 2010
Acta Biologica Szegediensis
http://www.sci.u-szeged.hu/ABS-

OBITUARY

Dr. György Bodrogközi (1924-2010)

Dr. György Bodrogközi was born on the 12th April 1924 in the village of Vid, Veszprém County. He started his school years in the same place, later continuing his studies in the Benedictine Secondary School in Pápa and the Piarist Secondary School in Szeged. In 1943 he matriculated to the natural history-geography course of the Szegedi Miklós Horthy University of Szeged. In his sophomore year he started to work as an unpaid assistant in the Institute of Plant Biology being his only employer until his retirement in 1989. Gradually, he rose to eminence in the university hierarchy, and was appointed associate professor in 1980. Meanwhile in 1962 he defended his thesis as a university doctor and in 1979 as a candidate. After his retirement in 1989 he continued his research of the Tisza Valley for 7 years in the Department of Ecology. In 2005 he was appointed honorary professor.

He was a passionate researcher of plant communities of the Great Hungarian Plain and the floodplains of the river Tisza.

He was mainly attached to his students through his educational work. He must have mastered the art of teaching from his pedagogue parents. Beside the vegetation of the Great Hungarian Plain and the floodplains of the river Tisza he also had profound knowledge of plant communities of the Mecsek Mountains, the Balaton Highlands and the Bükk Mountains. He organized his memorable field practicals to these highland destinations where he expected serious and thorough scientific work, but after working hours he also joined his students in modest amusement. His accuracy manifested itself during these practicals too. He was a teacher of determined character hereby making his students respectful personalities.

From 1966 to 1982 he served as executive editor of Acta Biologica Szegediensis. His merits were honored with the Remarkable Achievement Award, the Attila József commemorative plaquette of the University of Szeged and the Sándor Jávorka commemorative plaquette of the Hungarian Biology Association.

On the 25th April 2010 came the moment of farewell in the course of nature, when we had to say goodbye to our old teacher. From now on he will show heavenly fields to our fellow students. As former students of his we keep his memory in our hearts.

dr. Gyula Farkas L.

Volume 54(1):59-73, 2010
Acta Biologica Szegediensis
http://www.sci.u-szeged.hu/ABS

DISSERTATION SUMMARIES

Monitoring the biogas producing microbes

Norbert Ács

Department of Biotechnology, University of Szeged, Szeged, Hungary, Institute of Biophysics, Biological Research Center, Hungarian Academy of Sciences, Szeged, Hungary

Nowadays, biogas is one of the most important renewable energy carrier. It is produced in many countries and many facilities to treat biological wastes and to produce heat, biofuel and electricity from it. There is significant potential in replacing fossil fuels with biogas in various areas of our energy consumption, particularly as it combines the benefits of organic waste treatment with renewable energy production.

Biogas is produced by a special microbial population, which can be classified into three groups. The first one is the hydrolyzing bacteria; they cut the long biopolymers into smaller pieces. The acetogenic bacteria comprise the second group. They use mono- or oligosaccharides, lipids and amino acids to produce volatile fatty acids and hydrogen. Finally, the methanogenic archeabacteria utilize the volatile fatty acids and the product is biogas, *i.e.*, a mixture of CH_4 and CO_2. In order to increase biogas production and to improve the economical viability of this technology, it is very important to understand the relationship between these microbial populations and the rate limiting molecular events. This information can be collected via molecular biological techniques. Several approaches are employed. First, we developed a method for quantitative identification of a single bacterium in the biogas generating microbial population that invokes Real-Time PCR. The target microbe was the thermophilic bacterium, *Caldicellulosiruptor saccharolyticus*. Two unique genes, which code for proteins characteristic of this organism were selected. These were Ech (similar to *Escherichia coli* hydrogenase-3), and the Cel (cellulase). Successful experiments were carried out with both targeted genes from samples, originated from biogas fermentors. The other bacterium for our studies was the mesophilic eubacterium, *Enterobacter cloacae*. In this case the target gene was coding for one of the large subunit hydrogenase of this microbe, HycE. The detection of this bacterium was also possible, using whole extracted DNA from the liquid samples.

We have also shown that T-RFLP in capillary gel electrophoresis, combined with the conventional cloning-sequencing is a promising way for quantitative and qualitative monitoring of the biogas producing consortia.

Metagenomic methods are used for the identification of novel genes and pathways implicated in biomass degradation and biogas formation. In order to achieve a high yield of prokaryotic DNA, bacteria are extracted from the anaerobic fermentation using methods already available. The DNA samples are independently pooled and used for DNA sequencing and for the construction of metagenomic libraries. DNA sequences are used to identify the biodiversity of genes involved in organic substrate degradation. Metagenomic mass sequencing also lowers the amount of sequencing of clones isolated from metagenomic libraries. For sequencing we use a strategy based on pyrosequencing in order to obtain long (average 400-500) nucleotides, combined with sequencing using SOLiD and Solexa platforms that yield a huge number of short high-quality sequences. Beside the sequence based searches, we will also perform functional screening. Metagenomic sequencing will result in a large database that will include genes and pathways interesting for other biotechnological application. These databases will be screened to search for genes encoding esterases, lipases, proteases, phytases, cellulases, lignolytic enzymes involved in the decomposition of organic waste streams.

Bagi Z, Ács N, Bálint B, Horváth L, Dobó K, Perei K, Rákhely G, Kovács KL (2007) Biotechnological intensification of biogas production. Appl Microbiol Biotechnol 76:473-482.

Bagi Z, Perei K, Rákhely G, Kovács KL (2004) Biotechnological procedure for the intensification of biogas production in a thermophilic system. Hungary. Patent number: P0402444/2004.

Kovács KL, Bagi Z, Ács N, Perei RK, Imre E, Telekes G, Bartha I (2009) Biotechnological methods to increase landfill gas production and degradation of organic waste. Proc. 3rd Int. Workshop "Hydro-Physico-Mechanics of Landfills". Braunschweig, Germany, March 10-13 (2009)

Supervisor: Kornél L. Kovács
E-mail: acsn@brc.hu

Expression analyis of the *hup* genes encoded a NiFe hydrogenase in *Thiocapsa roseopersicina*

Tímea Balogh

Department of Biotechnology, University of Szeged, Szeged, Hungary

Thiocapsa roseopersicina is Gram-negative, phototrophic purple sulphur bacterium, which belongs to the family of Chromatiaceae. There are four active [NiFe] hydrogenases in the cells, which differ in their function, localization and stability. Two of them are membrane-associated [NiFe] hydrogenases (Hyn and Hup), while the other two are soluble hydrogenases (Hox1, Hox2). HynSL shows extraordinary stability and it catalyzes either H_2 uptake or H_2 evolution. The other membrane-associated hydrogenase (Hup) plays a role in hydrogen uptake (hup=hydrogen uptake) exclusively. The soluble hydrogenases of *Thiocapsa roseopersicina*, Hox1 and Hox2 are bidirectional NAD^+

reducing hydrogenases (Kovács et al. 2005; Maróti et al. – in press). Furthermore the bacterium possesses nitrogenase activity, and the atmospheric N_2 fixing is accompanied by H_2 evolution.

The *hup* locus consists of seven genes (*hupSLCDHIR*). Some of these genes are well characterized, *hupC* encodes a cytochrome b-type protein involved in electron transfer (Palágyi-Mészáros et al. 2009), while *hupD* codes for an endopeptidase which plays a role in the maturation of the large subunit (HupL). HupR is a regulatory protein, a part of a transcriptional regulatory system. However little is known about the transcriptional organization and regulation of *hup* gene, function of *hupH* and *hupI* gene products.

According to the literature, HupH protein is required for the translocation of the H_2ase stuctural protein to the membrane by bonding to the small subunit, while HupI is a rubredoxin-type protein plays a role in the electron transfer (Manyani et al. 2005).

In order to investigate the role of *hupH* and *hupI* genes in frame deletion mutants were created and the phenotypical effects of the mutations were analyzed by measuring *in vivo* and *in vitro* hydrogenase enzyme activity. Results showed that the absence neither of HupI nor HupH cause a significant decrease in Hup uptake activity.

The transcription of *hup* genes was investigated by reverse transcription coupled PCR, the results showed that *hupSLCDHIR* genes transcribe as a whole transcript.

Expression level of the *hup* genes was measured by quantitative real-time PCR in cells grown on various medium. Under nitrogen fixing conditions an enhanced *hup* mRNA level was observed, which indicates that the physiological function of Hup is somehow linked to the activity of nitrogenase enzyme complex. In standard non-nitrogen fixing growth conditions the *hupSL* transcription downregulated by both thiosulfate and succinate and upregulated by the inactivation of HupC. Therefore it was hypothesized that the redox status of the membrane/quinone pool controls the expression level of Hup hydrogenase.

To identify regulatory proteins which control the *hup* expression, mini Tn5 transposon based mutagenesis was carried out. A screening procedure was developed for identification of strains having Hup hydrogenase activity when the quinone pool is overreduced. *In vitro* hydrogenase uptake activity measurments were showed an appreciably increased Hup activity in the mutant and this points to the fact that the insertion of the transposon inactivated a gene which encodes a protein likely involved in the redox control of the expression of Hup hydrogenase.

Kovács KL, Kovács ÁT, Maróti G, Mészáros LS, Balogh J, Latinovics D, Fülöp A, Dávid R, Dorogházi E, Rákhely G (2005) The hydrogenases of *Thiocapsa roseopersicina*. Biochem Soc Trans 33(1):61-3.

Palágyi-Mészáros LS, Maróti J, Latinovics D, Balogh T, Klement E, Medzihradszky KF, Rákhely G, Kovács KL (2009) Electron-transfer subunits of the NiFe hydrogenases in *Thiocapsa roseopersicina* BBS. FEBS J. 276:164-74.

Manyani H, Rey L, Palacios JM, Imperial J, Ruiz-Argüeso T (2005) Gene products of the *hupGHIJ* operon are involved in maturation of the iron-sulfur subunite of the NiFe hydrogenase from *Rhizobium leguminosarum* bv. Viciae. J Bacteriol 187(20):7018-7026.

Maróti J, Farkas A, Nagy IK, Maróti G, Kondorosi É, Rákhely G, Kovács KL (2010) Second soluble Hox-type NiFe enzyme completes the hydrogenase set in *Thiocapsa roseopersicina* BBS. Appl Environ Microbiol – in press

Supervisor: Gábor Rákhely, Kornél L. Kovács
E-mail: btimea@brc.hu

Clarifying the mechanism of T-cell apoptosis induced by cell-derived or low and high concentration of soluble recombinant galectin-1

Andrea Blaskó

Lymphocyte Signal Transduction Laboratory, Institute of Genetics, Biological Research Center, Hungarian Academy of Sciences, Szeged, Hungary

Galectin-1 (Gal-1) is a mammalian lectin with β-galactoside binding activity. It is expressed by numerous cell types and binds to cells and extracellular matrix components presenting glycoconjugates of N-acetyl-lactosamine. The most prominent biological function of Gal-1 is its anti-inflammatory effect which is predominantly exerted by induction of apoptosis of Th1 cells (1). Many studies have emerged analyzing Gal-1 signal transduction mechanism during T-cell apoptosis. However these data have resulted confusing knowledge due to using soluble recombinant protein although Gal-1 exerts its physiological function bound to the producing or neighboring cells or extracellular matrix components.

We have aimed to resolve this controversy by comparing cell death induced by low (1.8 μM, lowGal-1) and high (18 μM, highGal-1) concentration of soluble Gal-1. We show that lowGal-1 and highGal-1 trigger phosphatidylserine exposure, generation of rafts and mitochondrial membrane depolarization. In contrast, lowGal-1 but not highGal-1 are dependent on the presence of p56lck and ZAP70 and activates caspase cascade. The results allow the conclusion that the cell-death mechanism strictly depends on the concentration of Gal-1 (2).

Recombinant Gal-1 is always manipulated during purification and in apoptosis assays since it has to be in reduced form for functional conformation. To avoid this process we analyzed the role and mechanism of cell-derived Gal-1 in the apoptotic process. In co-culture system Gal-1 remains as a native, functional protein without any chemical modification and the apoptosis assay also avoids addition of reducing agent. We applied co-cultures of various cell lines producing Gal-1 as effectors and T-cells (activated peripheral blood cells or

Jurkat lymphoblasts) as targets. Both Jurkat and activated peripheral T-cells died when co-cultured with various Gal-1 expressing cells, but HeLa, a Gal-1 non-expressing cervix carcinoma cell line did not affect T-cell viability. Removing cell surface Gal-1 with lactose or knocking down Gal-1 expression in Gal-1 producing tumor cells resulted in the diminution of the cytotoxic effect of these cell lines. Moreover, transgenic expression of Gal-1 in HeLa cells or treating HeLa cells with recombinant Gal-1 (rGal-1) converted these cells cytotoxic. T-cell apoptosis required intimate interaction between the effector tumor and target T-cells since neither conditioned supernatant harvested from the tumor cells, nor physical separation of tumor and T-cells in the same medium triggered T-cell death. Mechanism of apoptosis by cell-bound Gal-1 was comparable to that of low concentration of soluble recombinant Gal-1. Requirement for p56lck and ZAP70 has been proved and both the decrease of mitochondrial membrane potential and caspase activation was detected in T-cell apoptosis triggered by tumor cell-derived Gal-1 (3).

Our results show that cell-derived Gal-1 and low concentration of the soluble lectin triggers identical pathway of T-cell apoptosis in contrast to high concentration soluble Gal-1 which act on a different fashion.

Blaskó A, Fajka-Boja R, Ion G, Monostori E (2010) How does it act when soluble? Critical evaluation of mechanism of galectin-1 induced T-cell apoptosis. Acta Biol Hung (in press)

Kovács-Sólyom F, Blaskó A, Fajka-Boja R, Katona RL, Végh L, Novák J, Szebeni GJ, Krenács L, Uher F, Tubak V, Kiss R, Monostori E (2010) Mechanism of tumor cell-induced T-cell apoptosis mediated by galectin-1. Immunol Lett 127(2):108-18.

Rabinovich GA, Ilarregui JM (2009) Conveying glycan information into T-cell homeostatic programs: a challenging role for galectin-1 in inflammatory and tumor microenvironments. Immunol Rev 230(1):144-59.

Supervisor: Éva Monostori
Email: blaskoa@brc.hu

Evolutionary and functional analysis of *Medicago truncatula* symbiotic genes on nodulating and non-nodulating plant species

Zoltán Bozsóki

Medicago Genetics Group, Institute of Genetics, Biological Research Center, Hungarian Academy of Sciences, Szeged, Hungary

The availability of soil nutrients for plants is a major limiting factor regarding growth and productivity at many agronomically important areas. For this demand an evolutionary solution is the existence of symbiotic associations between plants and soil microbes that provide valuable macronutrients (e.g. P or N) for photosynthates as an exchange material from the plant. An ancient type of coexistence is the symbiosis with arbuscular mycorrhiza fungi. It is originated back to the appearance of the first land plants and present in the majority of land plant families. However, another, more recent type of symbiosis exists between nitrogen fixing soil bacteria and a narrow range of plants consisting of phylogenetically closely related species. During this symbiosis a new organ, the root nodule is formed that is specific for nitrogen fixation. Research on genes involved in the formation of these types of symbiotic associations showed that the two systems share genes supporting the idea that already existing elements of the more ancient program were recruited during the evolution of root nodule symbioses.

The mutual recognition of partners is a key process during the establishment of the symbiotic association. Specific molecules have been identified on both sides that are essential for triggering the symbiotic process, e.g. flavonoids secreted by the plants and the so-called Nod factors produced by the symbiotic bacteria. Due to the intensive ongoing research on symbiotic nitrogen fixation there is a rapid increase in the number of identified plant genes involved in these signaling events. LysM type receptor kinases (*MtLYK3*, *MtNFP*) together with the LRR receptor like kinase *MtDMI2* are needed to promote the most characteristic phenomenon of the early symbiotic signaling process: the perinuclear calcium level oscillation via nuclear pore complex elements (*LjNUP85*, *LjNUP133*) and a putative potassium ion channel *LjCASTOR* and *LjPOLLUX*/ *MtDMI1*. The signature of this so called calcium spiking is decoded and forwarded by a calcium-calmodulin dependent protein kinase (*MtDMI3*) via its phosphorylation substrate (*MtIPD3*) towards transcription factors (*MtNSP1*, *MtNSP2*, *MtERN*, *MtNIN*). Moreover, *NIN* and a cytokinin receptor needed for symbiotic nitrogen fixation (*MtCRE1*) are elements of the pathway that allows crosstalk between Nod factors of the symbiotic bacteria and plant cytokinins during nodulation. Living the days of the genomic era more and more `whole genome sequences' are accessible in the databases including plant genomes as well. Searching these databases makes possible to identify genes homologous to known symbiotic genes with high significance not only from legume genomes but also from non-nodulating plants. However, there are only a few papers published so far on evolutionary relationships of particular symbiotic genes and their homologues in different plant species (most recently Chen et al. 2009 on *LjCASTOR*/ *LjPOLLUX*/ *MtDMI1*). We have done systematic searches using the protein sequences of *M. truncatula* symbiotic genes as query and could identify new homologous genes from non nodulating plants highlighting some interesting aspects of their evolutionarily recruited functions. We have selected a few homologous proteins to explore for their possible function, with special regard on their possible ability of fulfilling symbiotic function as well.

Supervisor: Gabriella Endre
E-mail: bozsokiz@brc.hu

Volume 54(1):59-73, 2010
Acta Biologica Szegediensis
http://www.sci.u-szeged.hu/ABS

EcoTILLING analysis of candidate genes for drought tolerance in barley

András Cseri

Hungarian - German Stress Genomics Laboratory, Institute of Plant Biology, Biological Research Center, Hungarian Academy of Sciences, Szeged, Hungary

The development of new barley varieties with improved drought tolerance is one of the main breeding objectives in Hungary, because drought is a main factor limiting the yield of cereals including barley. The development of stress-tolerant varieties with yield stability will help to reduce the risk in barley cultivation. The probability of a successful breeding for drought tolerance is largely dependent on the understanding and knowing of the genetical factors that regulate this highly quantitative trait.

In this project drought tolerance related candidate genes were analyzed by using the EcoTILLING (Comai et al. 2004) technology. EcoTILLING is a high throughput, low cost technique for rapid discovery of polymorphisms in natural populations. It is a variant of TILLING (Targeting Induced Local Lesions IN Genomes), (Colbert et al. 2001) is based on certain PCR steps, such as the formation of heteroduplexes and a nuclease cutting DNA mismatches. It allows both SNP discovery and haplotyping through the sequencing of unique haplotypes.

We have established the EcoTILLING technology in order to identify putative SNPs and small INDELs in a set of 96 barley cultivars and wild germplasm containing drought tolerant and sensitive genotypes (cultivars and landraces and wild relatives) collected worldwide. Target genes were selected based on studies dealing with drought tolerance. Candidate genes are dedicated as potentially involved in the variation of key agronomic traits. The identification/determination of natural genetic variation in candidate genes can provide valuable information about gene function.

In this pilot study 7 drought related barley candidate genes were screened. In the case of 4 genes overlapping amplicons were designed, trying to cover the whole gene in the genetic diversity screens. For these 4 genes also more easily detectable markers were created after the evaluation of the obtained haplotypes sequences allowing distinguishing the main haplotypes. In the case of 3 candidate genes only one primer pair was planned based on the available mRNA sequences.

EcoTILLING reactions were performed in one-well format using fluorescently labeled nucleotides and after heteroduplex formation ENDO-1 and Cel-1 treated products were visualized on an ABI PRISM 377 sequencer.

Untill now more than one hundred unique haplotypes identified for 9 genes (HvARH1, HvDREB1, HvDRF1, HVA1, HvNHX1, HVP1, HvPPD-H1, HvNUD and HvPRPX) in 18 EcoTILLING screens. It's including more than 1.5 million base pairs sequence. The number of haplotypes identified for screened amplicons ranged from 2 to 9. Overall, 185 single nucleotide polymorphisms and 46 insertions/deletions were finded with a mean of 1SNP/92 bp and 1INDEL/372 bp genomic sequence.

In four candidate genes (HvARH1, HVA1, HvDRF1, HvSRG6) a set of informative polymorphisms were converted into easily detectable genetic markers, which are useful for marker assisted selection.

The obtained sequence/haplotype information will be used for development of further easily detectable genetic markers (potential „within gene marker") useful for linkage mapping and Marker Assisted Selection. Functional alleles can be directly integrated in barley breeding programs for improvement of drought tolerance.

Colbert, T, Till BJ, Tompa R, Reynolds S, Steine MN, Yeung AT, McCallum CM, Comai L, Henikoff S (2001) High-throughput screening for induced point mutations. Plant physiology 26:480-484.

Comai L, Young K, Reynolds SH, Codomo C, Enns L, Johnson J, Burtner C, Henikoff JG, Greene EA, Till BJ, Henikoff S (2004) Efficient discovery of nucleotide polymorphisms in populations by EcoTILLING. Plant Journal 37:778-786.

Supervisor: Dénes Dudits
E-mail: cseria@brc.hu

Application of synthetic antisense oligodeoxynucleotides in higher plants

Emine Dinc

Institute of Plant Biology, Biological Research Center, Hungarian Academy of Science, Szeged, Hungary

Antisense oligonucleotides *i.e.* short, synthetic strands of DNA or analogs that are complementary to a target DNA or RNA along with short interfering RNAs (siRNAs), 21-25 bp dsRNA with dinucleotide 3' overhangs became a powerful tool for the functional genetics. These structures are designed to interfere with nucleic acid metabolism, most preferentially with transcription, translation or splicing. Sequence-selective inhibition of gene expression is applied extensively for elucidation of complex gene expression patterns or validation of results gained from high throughput genomic experiments such as DNA-arrays. Common and attracting features of both antisense oligo and siRNA are that they act in a dose-dependent reversible manner, while no genetic transformation is required.

Though the sequence-selective gene-silencing by these synthetic oligonucleotides is quite general phenomenon for all organisms, only few applications are described for plant systems. We elaborated several methods for the introduction of oligonucleotides into monocot and dicot plants. By fluorescent labeling, we examined the uptake efficiency and inner traffic of these molecules, and determined the optimal conditions of treatment.

To demonstrate the antisense inhibition, we chose phytoene desaturase (pds) as a model gene which is a key-enzyme of the carotenoid biosynthesis in Triticum aestivum and Nicotiana benthamiana. Selection of the antisense target sites was made by a multistep optimization process which raises the targeting efficiency significantly. By means of quantitative RT-PCR method, we demonstrated sequence-specific knock-down of pds mRNA level. We followed the phenotypical changes of the plants by chlorophyll fluorometry and carotenoid content measurement, thus significant loss PDS function was demonstrated. at a significant level. Our experiences open the way for applying the antisense oligonucleotide technique for elucidation of real genetic problems.

Jens Kurreck (2003) Antisense technologies. Improvement through novel chemical modifications. Eur j Biochem 270(8):1628-1644.
Min Wang, Gang Wang, Jing Ji, Jiehua Wang (2009) The effect of pds gene silencing on chloroplast pigment composition, thylakoid membrane structure and photosynthesis efficiency in tobacco plants. Plant Sci 177:222-226
Min Wang, Gang Wang, Jing Ji, (2010) Suppression of the phytoene desaturase gene influence on the organization and function of photosystem II (PSII) and antioxidant enzyme activities in tobacco. Environ Exp Bot 67:460-466

Supervisor: Sandor Bottka
Email: emine@brc.hu

Epigenetic changes in tumor-associated myofibroblast

Ildikó Huliák

Department of Biochemistry and Molecular Biology, University of Szeged, Szeged, Hungary

The tumor microenvironment is an important factor in cancer development and progression.

In the stroma of various epithelial tumors the predominant cell types are myofibroblasts. These spindle-shaped cells were originally described in skin wounds where they facilitate wound healing. Myofibroblasts are differenciated fibroblasts expressing specific markers like alpha smooth muscle actin, vimentin and secreting several extracellular matrix proteins (Desmoulière et al. 2004). Compared to normal tissue, the number of myofibroblasts is increased in the tumor stroma and the shape and distribution of the cells are altered as well. The observed morphological changes are believed to be partially due to epigenetic effects, which cause an altered gene expression profile without influencing the DNA sequence. The epigenetic changes occuring in tumor- associated myofibroblasts are poorly understood (Jiang et al. 2008).

In order to compare epigenetic characteristics and gene expression pattern of tumor-associated myofibroblasts with that of normal myofibroblasts in molecular level, we used primary myofibroblast cultures obtained from the gastrointestinal tract. Cells isolated from tumor stroma or from healthy tissues near the tumor margins were provided by Dr. Peter Hegyi (Dept. of Internal Medicine, Faculty of Medicine, University of Szeged). We studied epigenetic changes such as histone H3 and H4 acetylation and methylation in tumor-associated myofibroblasts by immunocytochemistry. The results indicated lower levels of histone H4 acetylated on lysine 8, 12, 16 and H3 dimethylated on lysine 9 in tumor-associated myofibroblast compared to normal cells. Semi quantitative determination of the level of particular histone modifications by immunoblots using modified histone specific antibodies supported and validated the observed epigenetic alterations. The expression profile of subunits of histone acetyltransferase (HAT) complexes were determined by quantitative RT-PCR. The analysis indicated that the mRNA levels corresponding to the *ada2a, ada3* and *gcn5* genes, which code subunits of several HAT complexes, such as SAGA and ATAC, were lower in tumor-associated samples, then in their wild type counterparts.

The role of myofibroblasts in cancer metastasis is also suspected (De Wever et al. 2008). They can secrete many proteolytic enzymes, which digest extracellular matrix in order to promote cancer cell invasion. Therefore we were interested in studying the expression, secretion and activity of the gelatinase enzymes, matrix metalloproteinase 2 and 9 (MMP-2, 9) in the myofibroblast cultures. Based on quantitative RT-PCR data we performed, we concluded that the expression of MMP-2 was elevated in tumor-associated myofibroblasts, while the messenger of MMP-9 was detectable neither in the tumor-associated nor the control cells. We have also performed a gelatin zymography to detect the activity of MMP-2 and 9. For this protein extracts from tumor associated and normal cells, and as well secreted protein samples obtained from the culture media were loaded onto polyacrylamide gels co-polymerized with gelatin and resolved under nondenaturing conditions. Development of the gels with protein specific stain indicated strong MMP-2 activities in both samples, while the tumor-associated myofibroblasts secreted more MMP-2 enzymes to the extracellular space.

In the forthcoming months we plan to further investigate the differences in the gene expression profile of tumor-associated versus control myofibroblast using microarray. We expect that the results will broaden and refine our understanding on the role of myofibroblasts in tumor formation and invasion.

Desmoulière A, Guyot C, Gabbiani G (2004) The stroma reaction myofibroblast: a key player in the control of tumor cell behavior. Int J Dev Biol 48:509-517.
Jiang L, Gonda TA, Gamble MV, Salas M, Seshan V, Tu S, Twaddell WS, Hegyi P, Lazar G, Steele I, Varro A, Wang TC, Tycko B (2008) Global hypomethylation of genomic DNA in cancer-associated myofibroblasts. Cancer Res 68(23):9900-9908.
De Wever O, Demetter P, Mareel M, Bracke M (2008) Stromal myofibroblasts are drivers of invasive cancer growth. Int J Cancer 123(10):2229-2238.

Supervisor: Imre Boros
e-mail: huliakildiko@gmail.com

Volume 54(1):59-73, 2010
Acta Biologica Szegediensis
http://www.sci.u-szeged.hu/ABS

In memoriam Pál Széchényi. Paleoradiological study of a three-hundred-year-old mummy from Nagycenk

Lilla Alida Kristóf

Department of Anthropology, University of Szeged, Szeged, Hungary

The study of ancient mummies has contributed greatly to the development of paleoradiology. Many results of radiological examinations of human remains have been published since 1896, when the first study was made on an Egyptian mummy (Böni et al. 2004). As there are only few paleoradiological methodological references, it is necessary to develop new methods for X-ray examinations. On the other hand, we have only scanty information about the technical parameters, settings and values or positioning (Aufderheide 2003; Chhem 2008). Since 2001 in co-operation with the researchers of many radiology departments, I have managed to identify define appropriate technical parameters to be used in paleoradiology (Kristóf et al. 2004). Anthropological research of mummies in Hungary has been carried out in multidisciplinary framework (Pap et al. 1997; Pálfi et al. 2009). One of these case-studies, included in my PhD-research, is that of the three-hundred-year-old mummy of Pál Széchényi.

Archbishop Pál Széchényi's name appeared in the Hungarian history several times. The scientific study of Archbishop's mummy to be found in Nagycenk was carried out by our research team composed of the members of several institutions based in Budapest, Győr and Szeged in 2007 (Kristóf et al. 2010). The scientific examinations represented a milestone, since up till now it was unclear whether it was a natural or artificial mummy and the century-old question of whether Pál Széchényi was in fact a victim of arsenic poisoning in 1710 or this story was only a legend could also be answered.

The non-invasive examinations were carried out with multislice CT, traditional X-ray, biopsy, toxicology, energy-dispersive X-ray, X-ray fluorescent analysis, endoscope and 3D rapid-prototyping printing.

17 conventional X-ray radiographs have been made of the skull, trunk and extremities with computerized radiography. The CT examination was carried out by a 16-slices MSCT equipment. 277 and 557 slices of 2,0 and 0,8 mm thickness respectively were taken the skull. In the course of the examination of the whole body 576 and 1440 slices of 5 and 2mm thickness respectively were taken.

Except for his scull and extremities Pál Széchényi's mummy is in poor condition. The corpse was mummified artificially. There is no trace of removal of the brain. The small amount of brain remnants raise several questions. The Archbishop suffered from diffuse idiopathic skeletal hyperostosis (DISH). The small oval ring-like particles of calc density disclosed in muscles have raised suspicion of helminthiasis, e.g. trichinellosis. X-ray-fluorescency (XRF) analysis detected small amount of arsenic only on the surface of skin and buccal mucosa, but it was traceable neither in nails nor hair. The myth about arsenic poisoning of the Archbishop proved to be false. We also got a replica made of the mummy's scull with 3D printing from the MSCT data.

The paleoradiological examinations resulted in important findings about the condition of the mummy. In the future I would like to study more Hungarian mummies from the baroque era, especially of the presumed conservation method of Pauline monks and their burial customs.

Aufderheide AC (2003) The scientific study of mummies. Cambridge University Press, Cambridge. pp. 376-385.

Böni, T, Rhüli, FJ, Chhem, RK (2004) History of paleoradiology: early published literature, 1896-1921. Canadian Association of Radiologistis Journal 4:203-210.

Chhem, RK, Brothwell, DR (2008) Paleoradiology. Imaging Mummies and Fossils. Springer, Berlin

Kristóf LA, Barta HM, Petrik A et al. (2004) Belelátni a múltba. Módszertani lehetőségek a paleoradiológiában. Magyar Radiológia 78/1:24-31.

Kristóf LA, Pohárnok L, Kerényi T et al. (2010) Paleoradiológia és múmiakutatás. A nagycenki múmia interdiszciplináris vizsgálata és 3D koponyamásolatának nyomtatása CT adatok alapján. Magyar Radiológia Online, www.radiologia.hu.

Pálfi Gy, Molnár E, Kristóf LA et al. (2009) Etude paleopathologque de deux sujets partiellement momofies. In Pálfi et al., eds: Des lésions du passé aux diagnostics modernes. Szeged University Press, Szeged, pp. 98-99.

Pap I, Susa, É, Józsa L (1997) Mummies from the 18-19th century Dominican Church of Vác, Hungary. Acta Biol 42:107-112.

Supervisor: György Pálfi
E-mail: kristoflilla@freemail.hu

Characterization of the genus *Bipolaris* based on molecular, morphological and physiological features

Krisztina Krizsán

Department of Microbiology, University of Szeged, Szeged, Hungary

Members of the genus *Bipolaris* (*Ascomycota, Pleosporales, Pleosporaceae*) are imperfect filamentous fungi. Most of them have economical significance as plant pathogens infecting mainly cereals and other graminaceous hosts. However, three species are frequently recorded as human pathogens. *B. australiensis*, *B. hawaiiensis* and *B. spicifera* are agents of phaehyphomycoses (infection caused by melanin

producing filamentous fungi). They cause invasive infections in immunsupressed patients, but they are also able to cause local infections through external injuries (first of all on eye and on skin) in immuncompetent patients (Pfaller et al. 2004). Identification and discrimination of *Bipolaris* species and members of some closely related genera using morphological markers are really difficult, because of the great similarity of their conidia. The present taxonomy, which is based on the morphology of the conidia, is fuzzy, incoherent and it does not fit the real phylogenetical relationships.

Our work had three major aims: (i) phylogenetic analysis of the genus *Bipolaris* to clarify their taxonomical relationships using molecular, physiological and biological methods; (ii) to elaborate a reliable molecular methodology for the detection of the human pathogenic strains; and (iii) to examine the biological activity of the sesterterpene-type secondary metabolites produced by the members of this fungal group.

Twenty-five strains isolated from human keratomycosis and 15 isolates obtained from international strain collections were involved in the study. The ITS region of the ribosomal DNA and fragments of the calmodulin, the β-tubulin and the transcriptional elongation factor-1α genes were sequenced and compared to infer phylogenies and investigate the taxonomic position of the involved strains.

Currently, identification of *Bipolaris* strains isolated from clinical samples is carried out by the examination of the conidial morphology (*i.e.* determining the numbers of the conidial septa). Our preliminary examinations suggested that the three human pathogenic species cannot be distinguished merely on the basis of their conidial septation. In the molecular phylogenies inferred from the analysis of the abovementioned genes and also from RAPD-PCR data, only *B. hawaiiensis* could be clearly distinguished from *B. australiensis* and *B. spicifera*, while these two species formed a more or less uniform group in each resulting trees suggesting that they may belong to the same species. Carbon source assimilation tests (utilization of 68 compounds as a single carbon source was tested in the study) and morphological examinations also confirmed the results of the phylogenetic studies.

Sequence data were analysed to test their applicability as markers for molecular identification. As a result, an effective and rapid PCR-based method was developed to identify the members of the two human pathogenic groups (*i.e. B. hawaiiensis* and *B. australiensis* - *spicifera*).

Sensitivity of the clinical isolates against several generally used antifungal agents was also investigated. Itraconazole, clotrimazole and ketoconazole proved to be the most effective against the *Bipolaris* species. Interestingly, all of the investigated strains were resistant to amphotericin B, one of the most frequently used antifungal agents against filamentous fungi.

Bipolaris species often produce ophiobolins, secondary metabolite compounds of the family of sesterterpens. The phytotoxic, antimicrobial and nematocide effects of these compounds are well-known (Li et al. 1995; Au et al 2000) . In our study, effect of different ophiobolins against opportunistic pathogen Zygomycetes fungi was investigated in a broth microdilution assay. We also started to study the background of this antifungal effect in the case of ophiobolin A. This compound induced apoptotic-like changes in *Mucor* and *Rhizopus* strains presumably through the inhibition of the calmodulin. Further investigations are in progress to prove this hypothesis.

Au TK, Chick SH, Leung PC (2000) The biology of ophiobolins Life Sci 67:733-742.
Li E, Clark AM, Rotella DP, Hufford CD (1995) Microbial metabolites of ophiobolin A and antimicrobial evaluation of ophiobolins J Nat Prod 58:47-81.
Pfaller MA, Diekema DJ (2004) Rare and Emerging Opportunistic Fungal Pathogens: Concern for Resistance beyond *Candida albicans* and *Aspergillus fumigatus* J Clin Microbiol Vol. 42. No 10: 4419-4431.

Supervisor: Tamás Papp PhD.
E-mail: krizsank@gmail.com

Identification of fusarium resistance QTLs in the Ságvári/Nobeoka Bozu//Mini Manó/Sumai3 prebreeded wheat population

Szabolcs Lehoczki-Krsjak

Department of Biotechnology and Resistance, Cereal Research Non-profit Ltd., Szeged, Hungary

Fusarium head blight (FHB) is one of the most serious diseases of wheat worldwide, caused by *Fusarium* species complex. Epidemics of FHB can cause severe yield losses and decreasing quality. During pathogenesis harmful levels of mycotoxins can be accumulated, jeopardizing food and feed safety. The most cost-effective way to control the disease is breeding and cultivation of genetically resistant cultivars.

The FHB resistance in wheat is inherited by quantitative trait locus (QTLs). Many QTLs, with different effectiveness, are found on all wheat chromosomes except 7D from different resistant genotypes (Buerstmayr et al. 2009) Identification, effectiveness, inheritance, usage (marker assisted selection, MAS) and pyramiding of different QTLs is a powerful tool to help breeding varieties with enhanced Fusarium resistance.

105 recombinant inbred lines (RIL) of a double cross population (Ságvári/Nobeoka Bozu//Mini Manó/Sumai3) which contains two resistance sources from Asia – *Nobeoka Bouzu* (NB) a Japanese landrace and *Sumai 3* (Sum3) a Chinese variety - and two Hungarian genotypes - *GK Sagvari* (Sgv) and *GK Mini Mano* (MM) - were tested for *Fusarium* resistance.

Phenotyping was made in field trials during 2008 and 2009. Wheat ears were inoculated artificially with two isolates (one *Fusarium graminearum* and one *F. culmorum*) in 2008 and with four isolates (three *F. graminearum* and one *F. culmorum*) in 2009. Suspension of the

fungus was sprayed directly onto a bunch of ears in full flowering stage. Afterwards 48 hours polyethylene bag coverage was maintained to allow moisture condition for growing fungus. Head blight symptoms were evaluated visually as the percentage of scabby spikelets from 10 days after inoculation (dai) on every 4th day till the 26 dai. Inoculated ears are harvested and trashed so as to evaluate the percentage of Fusarium damaged kernels (FDK) and deoxynivalenol content (DON) by HPLC. Flowering time, plant height, ear type, present of awns, thousand kernel weight (TKW) was evaluated also during the experiment. Analysis of the data was made by two-way ANOVA and Pearson's-correlation.

Genotyping was carried out with microsatellite (SSR) markers, linked to FHB resistance QTLs, collected from literature. At the present time four QTL regions, located on the 2D, 3BS, 5A and the 6B chromosomes was mapped with 40 SSR markers. Since in resistant genotypes Sumai3 alleles dominated the tested regions, alleles were scored as derived from Sumai3 and others non-Sumai3. Linkage analysis and QTL mapping were done with JoinMap and MapQTL. Reduced hegiht (Rht) genes Rht-B1b, Rht-D1b and Rht8 were also detected.

Significant (P = 0,1%) positive correlations were found between FHB, FDK, DON, and TKW data. Plant height was in significant (P = 10%) negative correlation with disease traits. This means that taller plant and plants with lower TKW had lower disease level. Highly effective QTL, originated from Sumai3, found on the 3BS chromosome, explained the 60% of the phenotypic variance (p.v.) of FHB with 21 LOD value and the 45% of p.v. of FDK with 14 LOD value. It is flanked by 3 SSR markers on a 3 cM distance. A Sumai3 originated medium effective QTL found on the 5A (LOD 6-8), and small or medium effective QTL on 2D (LOD 3-7) and 6B (LOD 4-6) chromosomes. The mapped regions had significant effect on TKW also. Sumai3 alleles are linked to lower TKW mainly on 5A and 6B chromosomes which is a negative effect in breeding. The distribution of QTLs according to head type showed significant differences. The ratio of QTL carrying genotypes in the group of tapered and spindle headed plants was larger than in the group of square or semi-butt headed plants.

Fusarium resistance QTLs are identified and their effectiveness and agronomic relation are investigated in this study. However this research program wasn't finished, members of this population with good agronomic characters and Fusarium resistance (supported by known QTLs) are able to start to do marker assisted selection.

Buerstmayr H, Ban T, Anderson JA (2009) QTL mapping and marker-assisted selection for Fusarium head blight resistance in wheat: a review. Plant Breeding 128:1-26.

Supervisor: Ákos Mesterházy
E-mail: lehoczkisz@gabonakutato.hu

The role of the *Drosophila* DAAM in the development of the Indirect Flight Muscle

Imre Molnár

Biological Research Center, Department of Genetics, Szeged, Hungary

In the past few years our group has working on to study of a new *Drosophila* formin protein called DAAM (Dishevelled associated activator of morphogenesis). This protein has many interesting tissue-specific functions. For instance, it regulates the tracheal cuticle pattern (Matusek et al. 2006), plays a role during axon growth (Matusek and Gombos et al. 2008), and participates in the process of genitalia rotation.

In collaboration with a research group from the University of York (UK) we showed that the *Drosophila* DAAM (dDAAM) is localized in the Indirect Flight Muscle (IFM) of both the pupae and adult flies.

In non-muscle cells, generally there are two major actin nucleating-polymerizing systems, the formins and the Arp2/3 complex. Formins are producing long straight actin filaments and the Arp2/3 complex is producing branched actin network (Pollard 2007; Chhabra and Higgs 2007).

Because unbranched straight actin filament is the major form in striated muscle cells, it is possible that a formin family protein serves as the key regulator of actin dynamics in myofibrils (Taniguchi et al. 2009). These straight actin filaments are organized into the contractile unit called sarcomere but little is known about the regulation of actin assembly in muscle cells.

Our aim was to reveal the function of *Drosophila* DAAM insight the striated muscle's sarcomere.

With the use of different approaches, like muscle functional tests, immunohistochemistry, biophysical essays, we confirmed that dDAAM plays role in the nucleation of actin filaments and sarcomere assembly.

In the 6% of the dDAAM loss of function hypomorph mutants, called Ex1, about 16% reduction in the sarcomere length was observed compared to the wild type. These flightless mutants carrying the full length protein construct could rescue the phenotype at 100% both in sarcomere level and functionally as well.

With the overexpression of the tagged full length protein, we found that it is partially localized in the expected region, namely in the M-line of the sarcomere.

The RNA interference-mediated depletion of dDAAM resulted in a marked reduction in sarcomere length and disruption of the sarcomeric structure.

These findings suggested that actin dynamics regulated by dDAAM are critical for sarcomere organization in striated muscle cells.

Chhabra ES, Higgs HN (2007) The many faces of actin: matching assembly factors with cellular structures. Nat Cell Biol 9(10):1110-1121. Review.
Matusek T, Djiane A, Jankovics F, Brunner D, Mlodzik M, Mihály J (2006) The Drosophila formin DAAM regulates the tracheal cuticle pattern through organizing the actin cytoskeleton. Development 133(5):957-966.
Matusek T, Gombos R, Szécsényi A, Sánchez-Soriano N, Czibula A, Pataki C, Gedai A, Prokop A, Raskó I, Mihály J (2008) Formin proteins of the DAAM subfamily play a role during axon growth. J Neurosci 28(49):13310-13319.
Pollard TD (2007) Regulation of actin filament assembly by Arp2/3 complex and formins. Annu Rev Biophys Biomol Struct 36:451-77. Review.
Taniguchi K, Takeya R, Suetsugu S, Kan-O M, Narusawa M, Shiose A, Tominaga R, Sumimoto H (2009) Mammalian formin fhod3 regulates actin assembly and sarcomere organization in striated muscles. J Biol Chem 284(43):29873-81. Epub 2009 Aug 25.

Supervisor: József Mihály
E-mail: molnari@brc.hu

Some neuroprotective approaches in focal and global ischaemia on *in vivo* and *in vitro* rat models

Dávid Nagy

Department of Physiology, Anatomy and Neuroscience, University of Szeged, Szeged, Hungary

Glutamate (Glu) is the major excitatory amino acid neurotransmitter in the central nervous system. It mediates a number of physiological processes, but it is involved in the pathological processes of excitotoxicity too. Traumatic brain injury, focal brain lesion or global hypoperfusion are followed by acute excitotoxicity caused by the presence of abnormally high Glu levels in the cerebrospinal and interstitial fluids.

It has recently been demonstrated that this excess Glu in the brain can be eliminated by the intravenous administration of oxaloacetate (OxAc), which, by scavenging the blood Glu, induces an enhanced and neuroprotective brain-to-blood Glu efflux.

In this study, we subjected rats to a photothrombotic lesion and treated them after the illumination with a single 30-min long administration of OxAc (1.2 mg/100 g, i.v.). Following induction of the lesion, we measured the infarct size by Fluoro-Jade B (FJB)-staining. FJB binds sensitively and specifically to damaged neurons, with increased contrast during acute neuronal stress. Coronal sections (30μm) were cut with a freezing microtome and the sections were stained with FJB. The sections were subsequently analyzed with a fluorescent microscope. The volume of the hemispheric lesion and the number of FJB-positive cells were calculated for each animal. The administration of OxAc resulted in a reduction in the volume of the ischemia-induced cortical damage.

We also examined the functional consequences of the photothrombotic lesion by measuring the amplitudes of the somatosensory evoked potentials (SEPs). SEPs were induced in the contralateral primary somatosensory cortex by electrical stimulation of the right whisker pad and were transcranially recorded. The photothrombotic lesion resulted in appreciably decreased amplitudes of SEPs, but OxAc administration significantly attenuated this reduction.

We suggest that the neuroprotective effects of OxAc are due to its blood Glu scavenging activity, which, by increasing the brain-to-blood Glu efflux, reduces the excess Glu in the brain. This limits the size of the penumbra, improves the tissue perfusion and oxygenation and reduces the ischemia-related functional damage.

Ischemic postconditioning is referred to preventing ischaemia/reperfusion injury in both myocardial and cerebral infarction. The next study was undertaken to evaluate possible neuroprotective effects of kainate postconditioning against delayed neuronal death in hippocampal CA1 neurons if applied two days after hypoperfusion.

Transient global hypoperfusion was induced in male Wistar rats by two-vessel occlusion (2VO) for 30 min. 2VO causes inhibition of protein synthesis in selectively vulnerable brain regions such as CA1 and leads to the decrease of dendritic spine number and resulted in an impaired long-term potentiation (LTP) function in the hippocampal CA1 region.

In order to determine the number of apical dendritic spines we used Golgi-Cox staining. When the impregnation was ready coronal brain sections were cut by vibratome. The clear Golgi sections have been evaluated by light microscopical stereology.

For electrophysiological recordings we prepared coronal slices from the middle part of hippocampi. Field excitatory postsynaptic potencials (fEPSPs) were monitored and after a control period, LTP of the Schaffer collateral-CA1 synaptic response was induced by high-frequency stimulation (HFS). After the HFS the fEPSPs were recorded for at least a further 60 min-long period. If we apply the kainate (5 mg/kg) 48 hours after the 2VO, the loss of hippocampal dendritic spines and dysfunction of LTP could be significantly averted.

These results suggest that a sublethal second post-ischaemic event can be considered as a trigger for the start of protein synthesis activity in post-ischaemic cells. Postconditioning probably causes a re-modulation of protective protein (hsp70, hsp72, Bcl-2) synthesis leading to a switch from pro-apoptotic to anti-apoptotic pathways.

Supervisor: Tamás Farkas, Zsolt Kis
E-mail: david.nagy01@gmail.com

Volume 54(1):59-73, 2010
Acta Biologica Szegediensis
http://www.sci.u-szeged.hu/ABS

Investigation of protein phosphorylation and protein kinases in prokaryotes

Gyula Orosz

Department of Biotechnology, University of Szeged, Szeged, Hungary

Methylococcus capsulatus (Bath) is a Gram-negative, coccoid, methanotrophic bacterium. For the utilization of methane *M. capsulatus* is able to express two methane monooxigenases (MMO): in the presence of copper ions the particulate MMO (pMMO) and its accessory and transport proteins, responsible for copper uptake, are expressed. In the absence of copper the soluble MMO (sMMO) is expressed. sMMO can oxidize a wide range of compounds, from alkanes, alkenes, ethers and haloalkanes to aromatic and even heterocyclic hydrocarbons (Hakemian et al. 2007). Many biodegradation and biotransformation applications for sMMO are currently being investigated.

Although the existence of protein phosphorylation on S, T and Y residues in prokaryotes was first demonstrated in 1978 (Wang et al. 1978), our knowledge about S, T and Y phosphorylation in prokaryotes is very limited. In this recent work the copper regulation of MMO enzymes is studied by comparing the phospoproteome of two cultures grown under distinct conditions and screening for proteins of which's phosphorylation state changes depending on the available copper.

The comparison of the purified phosphoproteomes on 2D ELFO revealed that two subunits of sMMO (smmoB and smmoC) are phosphorylated proteins and unstable elongation factor (EfTU) is only phosphorylated when the media contains no copper. In case of smmoB and EfTU exact phosphorylation sites (smmoB:ser2, EfTU ser144) were determined by mass spectrometry. After changing potential phosphorylation site on smmoB from ser2 to ala by directed mutagenesis the whole enzyme preserved its full activity and smmoB still remained phosphorylated. Furthermore even smmoB heterologously expressed in *E. coli* proved to be phosphorylated by host protein kinases. In order to identify the protein kines(es) that is(are) responsible for the phosphorylation of smmoB a set of kinase deletion mutants were prepared in *E. coli*. After deletion of all known ser/thr and tyr kinases (*yihE, argK, aceK, etk, wzc, hipA, yeaG, yniA*) *E. coli* still preserved its capability to perform protein phosphorylation and smmoB was still phosphorylated, furthermore the deletion of these kinases hardly affected the protein pattern of the whole phosphoproteome of the host bacterium. Although *E. coli* is one of the most studied organisms, its genome is known and well characterized these results suggest that it still may possesses at least one unknown functional protein kinase that is responsible for the phophorylation of the majority of phosphpoproteins including overxpressed smmoB.

During amino acid starvation bacteria activate stringent control elements that result in adaptation to the amino acid shortage by increased amino acid synthesis, restricted protein translation and intensive protein degradation (Chatterji et al. 2001). In *Methylococcus capsulatus* activation of stringent control cascade results in the activation of smmo operon even in copper rich media (unpublished results). Promoting amino acid starvation in *M. capsulatus* grown in copper rich medium also resulted the phosphorylation of EfTU suggesting that phosphorylation of this protein may restrict protein sinthesys *via* direct or indirect inhibition of the translation.

Chatterji, Ojha (2001) Revisiting the stringent response, ppGpp and starvation signaling. Curr Opin Microbiol 4:160–165.
Hakemian, Rosenzweig (2007) The Biochemistry of Methane Oxidation. Annu Rev Biochem 76:223-241.
Wang JY, Koshland DE Jr. (1978) Evidence for protein kinase activities in the prokaryote Salmonella typhimurium. J Biol Chem 253 (21):7605-7608.

Supervisor: Kornél L. Kovács
E-mail: ogyula@gmail.com

A novel genetic approach for Identifying genes involved in abscisic acid regulation

Mary Prathiba Joseph

Institute of Plant Biology, Biological Research Center, Hungarian Academy of Sciences, Szeged, Hungary

Abscisic acid is the main stress response hormone in higher plants. In the past few decades many stress regulatory factors were identified which are involved in ABA dependent stress regulation. In order to understand the complicated regulatory web of ABA signaling the Controlled cDNA Overexpression System have been developed (COS, Papdi et al., 2008). We have transformed the *Arabidopsis* Col-0 wild type plants with the COS library and screened progenies of infiltrated plants for ABA insensitivity in the presence and absence of estradiol in germination assays. Screening one million seeds (aproximately 25,000 transformed seeds), of T1 generation resulted 156 plants, which were selected based on their germination capacity on high concentration ABA supplemented media. By testing of T2 generation, estradiol dependent ABA insensitivity was confirmed in 32 lines. Estradiol dependent ABA insenstitive germination was most notable in A26 and A44 lines, which were able to germinate in the presence of 5μM ABA, which otherwise completely inhibited the germination of wild type seeds. Insertions were identified in both lines and corresponded to full-length cDNA encoding the small heat-shock protein HSP17.6A-cII (A26) and a previously unknown zinc-finger domain containing transcription factor protein (A44). GFP fusion and HA-tagging experiments showed nuclear localization of the A44-derived transcription factor. While constitutive overexpression of this transcription factor reduced

fertility, insertion mutants, where transcription of the corresponding gene was abolished, were hypersensitive to ABA. Our results show, that the COS system is suitable for the identification of novel ABA regulatory factors.

Papdi C, Ábrahám E, Joseph MP, Popescu C, Koncz C, Szabados L (2008) Functional identification of Arabidopsis stress regulatory genes using the Controlled cDNA Overexpression System. Plant Physiol 147:528–542.

Supervisor: Laszlo Szabados
Email: mary.prathiba@gmail.com

Expression and epigenetic studies of MDR1 genes in drug-resistant rat cells

Ádám Sike

Department of Biochemistry and Molecular Biology, University of Szeged, Szeged, Hungary

The overexpression of multidrug resistance 1 protein (MDR1, Abcb1 or P-glycoprotein), a member of the ABC (ATP Binding Cassette) transporter superfamily, can be responsible for the decreased efficiency of chemotherapeutic drugs in tumour cells. MDR1 is an energy-dependent transporter that is able to extrude cytotoxic agents from the cell. In the presence of these drugs MDR1 expression is up-regulated by different mechanisms, though the molecular background of increased MDR expression is mostly unknown. Recent studies suggested that epigenetic modifications (e.g. histone acetylation, methylation) might play an important role in this process.

The aim of our study was to reveal epigenetic modifications responsible for the increased MDR1 level in multidrug resistant cell lines.

We studied the MDR expression in drug resistant rat hepatoma cells kindly provided by A. Venetianer. The cell lines we used in our experiments were a drug sensitive parental rat hepatoma cell line (D12), a medium (col500) and a highly (col1000) drug-resistant variant of it, selected using increasing concentrations of colchicine (Pirity 1996).

In contrast to humans, rodents have two MDR1 isoforms: Abcb1a and Abcb1b. First, we determined the expression of these genes and found that the mRNA levels of both Abcb1a and Abcb1b were increased in the drug resistant cell lines compared to the parental D12. A potential reason for the elevated expression of the Abcb1 genes is gene amplification. Indeed, we observed an increase in the copies of the Abcb1 genes in the col1000 cell line, however our data suggested that gene amplification was not the (only) reason for the overexpression of Abcb1 genes in the resistant cells.

Next we studied the possible role of histone acetylation in the increased expression of Abcb1 genes. For this, we treated the cells with histone deacetylase inhibitors (Na-butirate and trichostatin A) to maintain the acetylated state of histones. As a consequence of the treatment, the acetylation of H3 and H4 histones increased. Surprisingly, Abcb1a and Abcb1b genes responded to the treatment in an opposite way: the expression of Abcb1a was decreased, while the expression of Abcb1b was increased in cells treated with histone deacetylase inhibitors. Since acetylation of histone 3 lysin 9 and 14 (H3K9ac and H3K14ac) have been shown to play key roles in the regulation of chromatin structure and function, and are linked to transcriptional activation, next we focused on these modifications in order to determine whether they play a role in the differential expression of Abc1a and b genes. Using chromatin immunoprecipitation we determined the H3K9ac and H3K14ac levels at the transcriptional start sites and at upstream regulatory regions of both genes. We found elevated H3K9 and H3K14 acetylation in the col500 resistant cell line in all tested Abcb1 regions. In contrast with that, the acetylation levels of these histones were comparable in the parental D12 and in the other resistant (col1000) cell lines. After histone deacetylase inhibitor treatment, H3K9 and H3K14 acetylation increased in all tested regions of both genes, contrary that, their expression changed in opposite directions.

Since HDAC inhibitors changed the expression levels of Abcb1 genes, we wondered whether this treatment affected the drug efflux capacity of the cells. To answer this question we compared the accumulation of a fluorescent cytotoxin, a substrate of MDR1, in treated and untreated cells. As expected, we detected an increased efflux activity in the drug resistant col500 and col1000 cells; however, TSA-treatment did not influence significantly this process.

In conclusion, our data suggest that elevated Abcb1 gene expression is not always coupled to histone acetylation changes and conversely, the H3K9 and H3K14 acetylation levels do not necessarily predict the expression level of the Abcb1 genes. Thus, further histone acetylation sites and other histone modifications need to be examined to understand the complex regulation of MDR by mechanisms affecting chromatin structure.

Pirity M, Hevér-Szabó A, Venetianer A (1996) Overexpression of P-glycoprotein in heat- and/or drug-resistant hepatoma variants. Cytotechnology 19(3):207-14.

Supervisor: Imre Boros
E-mail: sike.adam@gmail.com

Volume 54(1):59-73, 2010
Acta Biologica Szegediensis
http://www.sci.u-szeged.hu/ABS

Involvement of carotenoids in the synthesis and in the assembly of protein subunits of photosynthetic reaction centers of *Synechocystis* sp. PCC 6803

Ozge Sozer

Institute of Plant Biology, Biological Research Center, Hungarian Academy of Sciences, Szeged, Hungary

The *crtB* gene of *Synechocystis* sp. PCC 6803, encoding phytoene synthase, was inactivated in the Δ*crtH* mutant. Thus, a carotenoid-less mutant, Δ*crtH/B*, was produced. Cells of the mutant were light sensitive and could grow only under light-activated heterotrophic growth conditions in the presence of glucose. Carotenoid deficiency did not significantly affect the cellular content of phycobiliproteins while the chlorophyll content of the mutant cells decreased. The mutant cells exhibited no oxygen-evolving activity suggesting the absence of photochemically active PSII complexes. This was confirmed by 2D electrophoresis of photosynthetic membrane complexes. Analyses identified only a small amount of a non-functional PSII core complex lacking CP43, while the monomeric and dimeric PSII core complexes were absent. On the other hand, carotenoid deficiency did not prevent formation of Cyt b_6f complex and PSI, which predominantly accumulated in the monomeric form. Radioactive labeling revealed very limited synthesis of inner PSII antennae, CP47, and especially CP43. Thus, carotenoids are indispensable constituents of the photosynthetic apparatus being essential not only for the anti-oxidative protection, but also for the efficient synthesis and accumulation of photosynthetic proteins and especially that of PSII antenna subunits.

E-mail: ozgebozkurtozge@hotmail.com

The role of bone marrow derived mesenchymal stem cells and their galectin-1 expression in the progression of mouse tumors in models of 4T1 breast carcinoma and B16F10 melanoma

Gábor János Szebeni

Hungarian Academy of Sciences, Biological Research Center, Institute of Genetics, Szeged

Galectin-1 (Gal-1) has a powerful anti-inflammatory effect (Kiss et al. 2007; Veronika et al. 2008) dominantly due to the induction of apoptosis of activated T cells (Ion et al. 2005, 2006). Gal-1 expression or overexpression in a tumor or in the tumor associated stroma must be considered as a sign of a poor prognosis for patients (Camby et al. 2006). Recent literature data report about the role of bone marrow derived mesenchymal stem cells (bmMSCs) in the process of tumorigenesis. It has been shown in these studies that bmMSCs selectively migrate into the tumor sites and are engrafted in the tumor stroma (Berber et al. 2009). Moreover bmMSCs may contribute to the formation of tumor associated stroma supporting the progression of cancerous cells, may regulate the neoangiogenesis and prevent the tumor specific immune response (Lazennec 2008). Several proteomic studies revealed the Gal-1 expression in mesenchymal stem cells (Silva et al. 2003; Panepucci et al. 2004; Kadri 2005; Lepelletier et al. 2009) however its role in MSC has to be elucidated.

Our purpose was to examine the role and influence of bmMSCs and bmMSC derived Gal-1 in the course of primary tumor development and metastasis.

We examined the Gal-1 production in MSCs in Western blot and FACS experiments. Balb/C or C57Bl/6 mice were subcutaneously injected with 4T1 breast carcinoma or B16F10 melanoma cells, respectively with or without bmMSCs. Primary tumor size was regularly measured. After sacrificing the animals, weight of the lung and number of metastatic nodules were analyzed. Histochemical analysis was also carried out on different tissues isolated from treated mice. We established Gal-1 knock-down MSCs in order to investigate their effect in tumor progression, neovascularization and metastasis.

Co-injection of bmMSCs with 4T1 breast carcinoma or B16F10 melanoma tumor cells induced larger primary tumor size and increased necrotic lesions on the 3rd week after treatment compared to these parameters in animals treated with the tumor cells alone. Metastatic phenotype characterized by the lung mass and the number of metastatic nodules is also more pronounced in animals injected with combination of tumor cells and bmMSCs. Histopathology also confirms the participation of bmMSCs in the pathogenesis of cancer, since bmMSCs enhance the number of micrometastasis in lungs and in lymph nodes. Moreover we detected CM-DiI labeled MSCs in the tumor samples on the 3rd week after treatment. Co-transplantation of Gal-1 knock-down MSCs with 4T1 cells slowed down the 4T1 tumor growth and vascularization compared to that of the effect of wild type MSCs.

In this study we show that bmMSCs enhance the growth kinetics of the primary orthotropic 4T1 mouse breast carcinoma and B16F10 melanoma. Also they contribute to progression of metastatic phenotype of the investigated tumor models. Supportive effect of bmMSCs to the tumor progression prevails on the 3rd week of treatment, since co-injection of bmMSCs with tumor cells do not modify the survival period of the animals. MSC derived Gal-1 could play an important role in the tumor promoting effect of MSCs.

Camby I, Le Mercier M, Lefranc F, Kiss R (2006) Galectin-1: a small protein with major functions. Glycobiology 16:137R–157R.

Ion G, Fajka-Boja R, Tóth GK, Caron M, Monostori E (2005) Role of p56lck and ZAP70-mediated tyrosine phosphorylation in galectin-1-induced cell death. Cell Death Differ 12(8):1145-1147.

Ion G, Fajka-Boja R, Kovács F, Szebeni G, Gombos I, Czibula A, Matkó J, Monostori E (2006) Acid sphingomyelinase mediated release of ceramide is essential to trigger the mitochondrial pathway of apoptosis by galectin-1. Cell Signal 18(11):1887-1896

Kadri T(2005) Proteomic Study of Galectin-1 Expression in Human Mesenchymal Stem Cells Stem Cells And Development 14:204–212.

Kiss J, Kunstár A, Fajka-Boja R, Dudics V, Tóvári J, Légrádi A, Monostori E, Uher F (2007) A Novel Anti-Inflammatory Function of Human Galectin-1: Inhibition of Hematopoietic Progenitor Cell Mobilization. Exp Hematol 35:305–313.

Lazennec G (2008) Concise review: adult multipotent stromal cells and cancer: risk or benefit? Stem Cells 26(6):1387-1394.

Lepelletier Y, Lecourt S, Arnulf B, Vanneaux V, Fermand JP, Menasche P, Domet T, Marolleau JP, Hermine O, Larghero J (2010) Galectin-1 and Semaphorin-3A are two soluble factors conferring T cell immunosuppression to bone marrow mesenchymal stem cell. Stem Cells Dev 19(7):1075-1079.

Panepucci RA, Siufi JL, Silva WA Jr, Proto-Siquiera R, Neder L, Orellana M, Rocha V, Covas DT, Zago MA. (2004) Comparison of gene expression of umbilical cord vein and bone marrow-derived mesenchymal stem cells Stem Cells 22(7):1263-1278.

Roorda BD, ter Elst A, Kamps WA, de Bont ES (2009) Bone marrow-derived cells and tumor growth: Contribution of bone marrow-derived cells to tumor micro-environments with special focus on mesenchymal stem cells. Crit Rev Oncol Hematol 69(3):187-198.

Silva WA Jr, Covas DT, Panepucci RA, Proto-Siqueira R, Siufi JL, Zanette DL, Santos AR, Zago MA (2003) The profile of gene expression of human marrow mesenchymal stem cells Stem Cells 21(6):661-669.

Urbán VS, Kiss J, Kovács J, Gócza E, Vas V, Monostori E, Uher F (2008) Mesenchymal Stem Cells Cooperate with Bone Marrow Cells in Therapy of Diabetes. Stem Cells 26:244-253.

Supervisor: Éva Monostori
E-mail: szebenig@brc.hu

Studying the chromatin structure of MDR1 gene in drug-sensitive and drug-resistant human cells

Mónika Tóth

Bay Zoltán Foundation for Applied Research, Institute for Plant Genomics, Human Biotechnology and Bioenergy, Szeged, Hungary

The reason for failure of chemotherapy is often the development of multidrug resistance, which is caused by the elevated level of ABC (ATP binding cassette) type transporters. One of the most often described ABC transporter is encoded by the MDR1 (multidrug resistance 1) gene. It was earlier described that drug induced upregulation of MDR1 is associated with increased H3 acetylation level in discrete region of MDR1 locus. Therefore exploration of the epigenetic mechanisms that contribute to the development of multidrug resistance has great importance. Several human diseases may originate from impaired function of histone acetyl transferases (HATs); therefore, these enzymes will serve as novel molecular targets for therapy in the future.

We aimed to study the changes in specific histone acetylation upon MDR1 gene induction and to analyze the histone acetyl transferase complexes that are responsible for these modifications.

We characterized a drug resistant, MCF7-derived, breast carcinoma cell line named MCF-KCR. It was generated via long term treatment of MCF7 cells with doxorubicin. We examined the level of MDR1 gene and mRNA in these cell lines. We found that the MDR1 gene level is 17 fold while the mRNA level 23000 fold elevated in the drug-resistant cells compared to the parental cells. These data suggest that epigenetic upregulation of MDR1 transcription is more important in developing the drug resistance than gene amplification. Importantly, the level of MRP1 (multidrug resistance protein 1) mRNA was not elevated in the drug resistant cells.

We showed by immunoblotting that the global H3 acetylation is elevated in the MCF-KCR cells. In addition, we examined the histone acetylation pattern in the regulatory regions (two promoters) and the coding region of the MDR1 gene by employing chromatin immunoprecipitation. Our data reveal an interesting acetylation map. With the use of acetylated residue specific antibodies we found that the acetylation level of H3K9 is about 100 fold elevated in the downstream promoter region and in the first exon in the drug resistant subline compared to the drug sensitive cells. H3K4, H3K14 and H4K12 are also slightly increased in the downstream promoter region and in the first exon of the MDR1 gene in those cells that overexpress MDR1 mRNA (Toth et al. 2009).

When we treated the cells with trichostatin A (TSA), a histone deacetylase inhibitor, MDR1 expression increased, while that of the other genes examined did not change in the drug sensitive cells. In contrast, MDR1 mRNA level did not change in the drug resistant cells upon TSA treatment. To try to down-regulate the acetylation and, along with that, the expression of the MDR1 gene, we treated the cells with a novel HAT inhibitor (HATi II) that strongly inhibits p300 and CBP (CREB binding protein) and weakly inhibits PCAF (p300/CBP associated factor) and GCN5 (homolog of yeast general control nonderepressable). Importantly, expression of MDR1 was further increased in the drug resistant MCF-KCR cells, while it did not change in the parental MCF7 cells. Next, we knocked down the level of PCAF, GCN5 and Ada2b (homolog of yeast alteration/deficiency in activation 2b) mRNA by transfecting specific siRNAs. The latter is a component of GCN5 containing multisubunit HAT complexes, such as hTFTC/hSTAGA. Interestingly, PCAF downregulation resulted in a reduction of the MDR1 mRNA level in MCF7 cells but not in the MCF-KCR cells. MDR1 mRNA level did not change in the drug resistant subline and decreased only slightly in drug sensitive cells upon GCN5 or Ada2b knockdown. These data suggest that MDR1 expression can not be easily reduced by simple inhibition of HATs in the drug resistant cells, probably because histone acetylation is highly deregulated in these cells.

Volume 54(1):59-73, 2010
Acta Biologica Szegediensis
http://www.sci.u-szeged.hu/ABS

Toth M, Molnar J, Boros IM, Balint E. Examination of the histone acetylation pattern in the regulatory regions of the human MDR1 gene causing multidrug resistance. EMBO Conference on Chromatin and Epigenetics, 13-17 May, 2009, Heidelberg, Germany. Poster 214.

Supervisor: Éva Bálint
E-mail: tothm@baygen.hu

Functional interplay between factors involved in transcription in *Drosophila melanogaster*

Edith Vamos

Institute of Biochemistry, Biological Research Center, Hungarian Academy of Sciences, Szeged, Hungary

Regulation of transcription, the synthesis of RNA from a DNA template, is one of the most important steps in control of cell growth and differentiation. Gene regulation occurs in the context of chromatin where recruitment of chromatin remodeling complexes such as ATP-dependent remodeling complexes and histone modifying enzymes (HAT, HDAC, HMT, etc.) represents a crucial step in gene transcription (Svejstrup 2004). We are interested in studying the physical and functional interaction between proteins involved in transcription regulation such as the RNA PolII subunit Rpb4, the transcription factor p53, and adaptor proteins of the chromatin modifier complexes.

The RNA polymerase II is composed of a ten-subunit core and a two-subunit dissociable subcomplex comprising the forth and the seventh largest subunits, Rpb4 and Rpb7. In *Drosophila*, Rpb4 is a product of a bicistronic gene together with the ATAC histone acetyltransferase complex constituent ADA2a (Pankotai et al. 2010). The alignment of Ada2a and Rpb4-related sequences indicated that the two proteins share the same transcription unit. Comparison of the related protein and nucleotide sequences revealed that Ada2a and Rpb4 coding region are present in similar organization in 12 *Drosophila* species, other then *D. melanogaster*; however a similar gene organization in other organisms cannot be identified. We investigated the mechanism by which the two mRNAs are generated. From RT-PCR analysis we concluded that the shift between Ada2a and Rpb4 mRNA formation takes place by splice acceptor site selection. Ada2a protein has another distinct homolog in *Drosophila*, Ada2b which is present in the SAGA complex. Although the two proteins contain the same conserved domains and their interacting partners are rather similar, they are part of two distinct HAT complexes. We questioned what confers the complex specificity of the Ada2 adaptors, more precisely which regions are responsible for their interaction with different transcriptional coactivators. Firstly, different Ada2a/Ada2b or Ada2b/Ada2a hybrids proteins were generated by joining PCR fragments corresponding to functional domains of one and the other ADA2. All the hybrid plasmids were generated using the Gateway system and were successfully tested on western blot for their expression in *Drosophila* S2 cells. Since the chimeric structure of the proteins did not disturb their expression in S2 cells, plasmids suitable for embryo injections were generated. Our goal is to see if their expression will restore one or the other ADA2 function. The coding region of hybrid proteins were inserted into a P-element containing vector allowing site specific insertion and injected into *Drosophila* embryos. Two out of six plasmids are ready for *in vivo* analysis in *Ada2a* and *Ada2b* mutant background.

Previous studies have shown that HATs, beside their ability to relax chromatin, can regulate many other factors through acetylation, including transcription factors (Wang et al. 2001). In mammalian system it was shown that the Gcn5-containing acetyltransferase complex (STAGA) plays a role in p53-dependent gene activation. Ada2b and Gcn5L proteins are identified as direct interacting partners of the p53 transcription factor (Gamper and Roeder 2008). According to previous studies *Drosophila* p53 is a functional homolog of mammalian p53 (Ollmann et al. 2000). We investigated whether the adaptor proteins of the HAT complex have any effect on p53 transcriptional activity. A plasmid containing three copies of *rpr* consensus binding site upstream of the luciferase gene was constructed. The reporter plasmid was cotransfected into S2 cells with different constructs expressing Ada2a, Ada2b or Ada3 proteins and performed luciferase assays. There was no significant change in transcriptional activity of the p53 responsive element. Although it was previously described that hAda3 can increase p53 trancriptional activity (Wang et al. 2001), perhaps in *Drosophila* S2 cells the efficiency of this interaction requires additional factors which can promote a significant response. We also tested plasmid vectors containing *Drosophila melanogaster* p53 (Dmp53) and a point mutant form of it ($Dmp53^{K302R}$) in reporter assays. Expression of either the wild type or the mutant variant increased the activity of the reporter gene 20 fold compared to control. No significant change was observed in the level of transcriptional activation ability of the wild type and the mutant variant of Dmp53. Future *in vivo* studies are planned to understand the mechanism by which p53 is activated.

Gamper AM, Roeder RG (2008) Multivalent binding of p53 to the STAGA complex mediates coactivator recruitment after UV damage. Mol Cell Biol 28:2517-27.

Ollmann M, Young LM, Di Como CJ, Karim F, Belvin M, Robertson S, Whittaker K, Demsky M, Fisher WW, Buchman A, Duyk G, Friedman L, Prives C, Kopczynski C (2000) Drosophila p53 is a structural and functional homolog of the tumor suppressor p53. Cell 101(1):91-101.

Pankotai T, Ujfaludi Z, Vamos E, Suri K, Boros IM (2010) The dissociable RPB4 subunit of RNA Pol II has vital functions in Drosophila. Mol Genet Genomics 283:89-97.

Svejstrup JQ (2004) The RNA polymerase II transcription cycle: cycling through chromatin. Biochim Biophys Acta 1677:64-73.

Wang T, Kobayashi T, Takimoto R, Denes AE, Snyder EL, el-Deiry WS, Brachmann RK (2001) hADA3 is required for p53 activity. EMBO J 20:6404-6413.

E-mail: edith@szbk.u-szeged.hu

Volume 54(1):59-73, 2010
Acta Biologica Szegediensis
http://www.sci.u-szeged.hu/ABS

Regulation of the phosphorylation status of rice retinoblastoma-related protein by PP2A phosphatase

Ping Yu

Institute of Plant Biology, Biological Research Center of the Hungarian Academy of Science, Szeged, Hungary

The retinoblastoma protein (pRB), a nuclear phosphoprotein, is a general regulator of cell proliferation. The ability of pRB and pRB-related proteins to inhibit cellular proliferation is counterbalanced by the action of Cdks (Nakagami et al. 2002). Sixteen potential sites for Cdk-mediated phosphorylation (Ser/Thr-Pro motifs) exist in pRB, and twelve of these sites have been shown to be phosphorylated *in vivo* (Nakagami et al. 2002). In quiescent and early G1 cells, pRB exists in a predominantly unphosphorylated state. As cells progress towards S phase, pRB becomes phosphorylated. Inactivation of pRB by phosphorylation leads to the dissociation and activation of E2F, allowing the expression of many genes required for cell cycle progression and S phase entry (Inoue et al. 2007; Poznic 2009). The phosphorylated state of pRB is accumulating till the end of mitosis when pRB is dephosphorylated by protein phosphatases (Nakagami et al. 2002; Poznic 2009).

Two retinoblastoma-related (RBR) genes have been found in rice, OsRBR1 and OsRBR2. OsRBR2 is expressed mainly in differentiated cells, but the function of the OsRBR1 gene may be related to cell division or cell cycle progression (Lendvai et al. 2007).

Protein phosphatase 2A (PP2A) is a family of serine-threonine phosphatases implicated in the control of a diverse array of cellular processes. The PP2A core enzyme consists of a catalytic C subunit and a structural A subunit. The AC dimer recruits a third regulatory B subunit that has been predicted to dictate the substrate specificity and function of the PP2A heterotrimeric complex. Four unrelated families of B subunits have been identified in mammals (Groves et al. 1999; Yan and Mumby1999; Janssens and Goris 2001; Cicchillitti et al. 2003). In plants B subunits are also important for cellular localization and substrate specificity. B subunits are classified into at least three distinct groups: B, B' and B'', based on molecular weight and domains (Janssens and Goris 2001). The PP2A was reported to be implicated in the dephosphorylation of RBRs, particularly upon oxidative stress (Cicchillitti 2003). A PP2A regulatory subunit (PR70) was also shown to associate with hyperphosphorylated pRb and mediate its dephosphorylation (Groves et al. 1999).

Yeast-two hybrid interaction results show that the OsPP2A B'' regulatory subunit is a strong interactor of OsRBR1, but has no detectable association with OsRBR2.

All the proteins in the RB family can be divided into three regions: the N-terminal region, the pocket domain (include A, B domain and the spacer between A and B) and the C-terminal region. OsPP2A B'' interacts strongly with the OsRBR1 protein minus the C-terminal version, even more strongly than with the full length of OsRBR1, but does not interact with any version of the protein which has some part of pocket domain missing. In addition, there was no interaction between OsRBR1 and EF-hand truncated OsPP2A B'' protein. It was demonstrated that the interaction between the OsRBR1 and OsPP2A B'' proteins needs an intact pocket domain of the RBR protein and the presence of the EF-hands domains on the B'' regulator subunit.

We used OsPP2A B'' regulatory subunit as a bait to screen the interactor from rice suspension cells and leaves cDNA libraries, but then switched to the OsPP2A B'' one-EF-hand minus version because of the self-activation of the full length B'' subunit. We got 30 more interesting interactors of B'' subunits by screen, which we will use in following research.

We have constructed clone encoding the His_6 and GST-tagged OsRBR1, OsRBR2 and OsPP2A B'' proteins using pET-28a and pGEX vectors. Recently, we verified the binding of recombinant His-tagged OsRBR1 protein to GST-PP2A B'' demonstrated that this binding increase in the presence of Ca^{2+}.

Cicchillitti L, Fasanaro P, Biglioli P, Capogrossi CM, Martelli F (2003) Oxidative Stress Induces Protein Phosphatase 2A-dependent Dephosphorylation of the Pocket Proteins pRB, p107, and p130. J Biol Chem 278(21):19509-19517.

Groves MR, Hanlon N, Turowski P, Hemmings AB, Barford D (1999) The Structure of the Protein Phosphatase 2A PR65/A Subunit Reveals the Conformation of Its 15 Tandemly Repeated HEAT Motifs. Cell 96:99-110.

Janssens V, Goris J (2001) Protein Phosphatase 2A: a Highly Regulated Family of Serine/Threonine Phosphatases Implicated in Cell Growth and Signaling. Biochem J 353:417-439.

Lendvai A, Pettko-Szandtner A, Csordas-Toth E, Miskolczi P, Horvath VG, Gyorgyey J, Dudits (2007) Dicot and Monocot Plants Differ in Retinoblastoma-Related Protein Subfamilies. J Exp Bot 58(7):1663–1675.

Inoue Y, Kitagawa M, Taya Y (2007) Phosphorylation of pRB at Ser612 by Chk1/2 Leads to a Complex Between pRB and E2F-1 After NA Damage. The European Molecular Biology Organization 26:2083-2093.

Nakagami H, Kawamura K, Sugisaka K, Sekine M, Shinmyo A (2002) Phosphorylation of Retinoblastoma-Related Protein by the Cyclin D/ Cyclin-dependent Kinase Complex is Activated at the G1/S-Phase Transition in Tobacco. Plant Cell 14(8):1847-1857.

Poznic M (2009) Retinoblastoma Protein: a Central Processing Unit. Journal of Bioscience 34(2):305-312.

Yan Y, Mumby CM (1999) Distinct Roles for PP1 and PP2A in Phosphorylation of the Retinoblastoma Protein. J Biol Chem 274 (45):1917-31924.

Supervisor: Gabor V. Horvath
Email: yuping0508@yahoo.com.cn

Instructions to Authors

Submission of manuscripts

Submission of a manuscript to Acta Biologica Szegediensis automatically involves the assurance that it has not been published and will not be published elsewhere in the same form. Manuscripts should be written in English. Since poorly-written material will not be considered for publication, authors are encouraged to have their manuscripts corrected for language and usage by a trusted expert.

There are no explicit length limitations: a normal research article will occupy 4-6 printed pages; reviews might be considerably longer. Authors should submit three sets of the complete manuscript and illustrations, together with a computer disk containing an electronic version of their manuscript. The elctronic file is considered the final material. Both Macintosh and PC versions will be accepted. The disk should be labeled with the date, the first author's name, the file name of the manuscript and the software, disk format and hardware used. Acta Biologica Szegediensis will not return copies of submitted manuscripts and figures. Requests to return original figures will be honored as a courtesy, but cannot be guaranteed. If instructions are not followed, authors will be asked to retype their manuscripts.

Manuscript format

Only good-quality laser printouts will be accepted. All pages should be printed with full double spacing, 2.5 cm margins, and a nonjustified right margin. A standard 12 point typeface (e.g. Times, Helvetica or Courier) should be used throughout the manuscript, with symbol font for Greek letters. Boldface, italics or underlined text should not be used anywhere in the manuscript. Footnotes are not permitted. Each page should be numbered at the bottom as follows:

Page 1. Title page: Complete title, first name, middle initial, last name of each author; where the work was done (authors' initials in parentheses if necessary); mailing address, phone, fax, and e-mail of the corresponding author; a running title of no more than 48 characters and spaces.

Page 2. Abstract: no more than 200 words, followed by 4-6 key words.

Beginning on page 3: Introduction, Materials and Methods, Results, Discussion, Acknowledgments, References, Figure Legends, Tables. Each section should be begun on a new page.

The manufacturer's name and location should be given in parentheses for reagents and instruments. Sources for all antibodies and nucleotide sequences should be indicated. Customary abbreviations in common use need not be defined in the text (e.g. DNA or ATP). Other abbreviations should be defined the first time that they are used. Quantitative results must be presented as graphs or tables and supported by appropriate experimental design and statistical tests. Only SI units may be used. For studies that involve animals or human subjects, the institutional, national or international guidelines that were followed should be indicated.

References

Only work that has been published or is in the press may be referred to. Personal communications should be acknowledged in the text and accompanied by written permission. In the text, references should be cited by name and year, e.g. Bloom (1983) or (Schwarz-Sommer et al. 1990) or (Maxam and Gilbert 1977). In the References, references should be listed alphabetically by first authors (including all co-authors) and chronologically for a given author (beginning with the most recent date of publication). Where the same author has more than one publication in a year, lower case letters should be used (e.g. 1999a, 1999b, etc.). Periods should not be used after authors' initials or abbreviated journal titles (e.g. Acta Biologica Szegediensis should be cited as Acta Biol Szeged). Inclusive page numbers should be used. Examples:

Bloom FE (1983) The endorphins: a growing family of pharmacologically pertinent peptides. Annu Rev Pharmacol Toxicol 23:151-170.

Coons AH (1978) Fluorescent antibody methods. In Danielli JF, ed., General Cytochemical Methods. Academic Press, New York, 399-422.

Maxam AM, Gilbert WA (1977) A new method for sequencing DNA. Proc Natl Acad Sci USA 74:560-564.

Monod J, Changeux J-P, Jacob F (1963) Allosteric proteins and cellular control systems. J Mol Biol 6:306-329.

Schwarz-Sommer Z, Huijser P, Nacken W, Saedler H, Sommer H (1990) Genetic control of flower development by homeotic genes in Antirrhinum majus. Science 250:931-936.

Illustrations

Three complete sets, including a high-quality "original" for publication, must be submitted with the manuscript. The back of each figure or composite plate should be labeled in soft lead pencil, indicating the orientation, the figure number, and the first author's name. The back of the best set should be marked "use for reproduction" or "original". Authors are encouraged to submit digital images of photographs, line drawings or graphs for printing. Most major image editing and drawing/illustrator computer software files (both Macintosh and PC) in TIFF or EPS formats are acceptable. It is particularly important that adequate resolution (at least 300 dpi, preferably 600 dpi) is used in making the original image.

Figure legends

Figures should be numbered consecutively with Arabic numerals. Material in the text should not be duplicated and methods should not be described. The size of scale bars should be indicated when appropriate. The first figure in the text should be referred to as Fig. 1, and so on.

Tables

Tables should be numbered consecutively with Arabic numerals. A brief title should be included above the table. Each table should be printed double spaced, without vertical or horizontal lines, and on a separate sheet. Material in text should not be duplicated and methods should not be described. The first table in the text should be referred to as Table 1, and so on.